Smithsonian

Contributions to Astrophysics

VOLUME 2, NUMBER 5

GEOMAGNETISM AND THE EMISSION-LINE CORONA, 1950–1953

By BARBARA BELL *and* HAROLD GLAZER

SMITHSONIAN INSTITUTION

Washington, D. C.

1957

For sale by the Superintendent of Documents, U. S. Government Printing Office
Washington 25, D. C. - Price 65 cents

Publications of the Astrophysical Observatory

This series, *Smithsonian Contributions to Astrophysics*, was inaugurated in 1956 to provide a proper communication for the results of research conducted at the Astrophysical Observatory of the Smithsonian Institution. Its purpose is the "increase and diffusion of knowledge" in the field of astrophysics, with particular emphasis on problems of the sun, the earth, and the solar system. Its pages are open to a limited number of papers by other investigators with whom we have common interests.

Another series is *Annals of the Astrophysical Observatory*. It was started in 1900 by the Observatory's first director, Samuel P. Langley, and has been published about every 10 years since that date. These quarto volumes, some of which are still available, record the history of the Observatory's researches and activities.

Many technical papers and volumes emanating from the Astrophysica Observatory have appeared in the *Smithsonian Miscellaneous Collections*. Among these are *Smithsonian Physical Tables*, *Smithsonian Meteorological Tables*, and *World Weather Records*.

Additional information concerning these publications may be secured from the Editorial and Publications Division, Smithsonian Institution, Washington, D. C.

FRED L. WHIPPLE, *Director*,
Astrophysical Observatory,
Smithsonian Institution.

Cambridge, Mass.

Contents

Geomagnetism and the Emission-Line Corona, 1950–1953

By Barbara Bell[1] and Harold Glazer[2]

Introduction

In this paper we investigate the relation between the intensity of the coronal emission-lines, λ5303 and λ6374, and the geomagnetic character figure, *Kp*, generally interpreted as a measure of the solar corpuscular radiation. However, a summary of previous research on the general problem of solar-geomagnetic relations may be useful. We are limiting this summary to those effects generally thought to arise from solar corpuscular radiation; and we are not considering geomagnetic phenomena believed to arise from solar ultraviolet radiation.

The displaced and greatly broadened Balmer lines observed independently by Meinel (1951) and Gartlein (1950, 1951) in spectra of aurorae comprise the only direct evidence for streams of corpuscles striking the earth. Spectra obtained by Meinel during the intense aurora of Aug. 18 and 19, 1950, indicated a velocity of impact above 3000 km/sec for the protons. If the corpuscles come directly from the sun, a particle velocity of 3000 km/sec would correspond to a travel time of about 14 hours.

There can be little doubt that disturbances of the earth's magnetic field (geomagnetic storms), as well as aurorae, are caused by streams of corpuscles emitted by the sun, because: (1) many geomagnetic storms are world-wide, affecting the dark and sunlit sides of the earth equally; (2) storms are more pronounced in higher latitudes; (3) storms often follow flares and/or central meridian passage (CMP) of large sunspots with a time lag of 1–4 days; and (4) storms show a 27-day recurrence tendency corresponding very closely to the synodic rotation period of equatorial regions of the sun.

The 27-day recurrence tendency was demonstrated by Maunder (1904) and confirmed by Chree and Stagg (1927). Greaves and Newton (1929), from analysis of Greenwich magnetic records 1874–1927, found that the recurrence tendency was most pronounced for storms of moderate intensity, decreased with increasing storm intensity, and vanished in the case of great storms. Newton (1949) found that superposed epoch analysis of 1907–44 data also indicated this nonrecurrence of great magnetic storms.

On the other hand, Benkova (1942) has studied the 27-day recurrence tendency for storms of different intensities from data recorded at the Sloutzk Observatory, 1878–1939. She found that the extra-great magnetic storms showed a pronounced tendency to occur in a sequence, while the great storms showed less such tendency than either moderate or extra-

[1] Harvard College Observatory, Cambridge, Mass.
[2] Formerly at Harvard College Observatory, Cambridge, Mass.; now at Sylvania Waltham Laboratories, Waltham, Mass.

great storms, results partly contrary to those of Greaves and Newton. All categories, however, showed an appreciable recurrence tendency. Extra-great storms, Sloutzk data indicated, occurred often as members of the longer sequences and tended to be the second member of the sequence.

Chernosky (1951) has found evidence of a systematic variation in the length of the recurrence interval with phase of the spot cycle. Early in the cycle he finds a period of 28½ days, which decreases to 26¾ days near the end of the cycle. Recurrent magnetic storms are most common on the declining branch of the sunspot cycle and scarcest on the rising branch and around maximum. Isolated storms appear to parallel the general solar cycle of activity more closely.

Terrestrial magnetic activity shows a 6-month periodicity (Bartels, 1932) with maximal disturbance in March and October. According to Bartels, the maxima are closer to the equinoxes than to the times of maximal inclination of the solar axis (March 5 and September 7); and they are present about equally in years of high, moderate, and low sunspot activity. The cause of the equinoctial maxima in geomagnetism, which appear also in aurorae, has long been a mystery. Sunspot numbers show no significant seasonal variation.

Bhargava and Naqvi (1954) however have pointed out two very long sequences of recurrent geomagnetic activity in the period 1950–53, each of which appears to show an annual variation in storm intensity. The longest sequence, beginning July 11, 1950, shows maximum activity around September and a minimum around March. The second sequence, beginning Nov. 21, 1951, has its maximum in March and a minimum around September. These authors accordingly suggest that the apparent semiannual period may actually be an annual period, caused by the inclination of the solar axis to the plane of the ecliptic (see also Naqvi and Bhargava, 1954).

Bartels (1932) first investigated the relation between magnetic storms and visible features of the solar disc. Using monthly means, 1928–30, he found no significant correlation of sunspots, bright or dark flocculi, or faculae with the terrestrial magnetic activity figure *u*. The correlations of character figure *C* with solar disc features were negative, because during the period covered by his study general solar activity declined while geomagnetic activity increased. (Large magnetic character figures, whether *C* or *K*, correspond to disturbed conditions, small numbers to quiet conditions.) Bartels found the various solar indices to be highly correlated and concluded that one could not therefore be expected to give significantly better results than another. The hypothetical sources on the sun of the corpuscular streams producing recurrent magnetic storms he named M-regions. M-regions, most numerous and conspicuous in their effects one or two years before sunspot minimum, are longer lived phenomena than sunspots; some M-regions have survived for more than a year. Bartels noted that M-regions often occurred when the visible solar hemisphere was bare of spots, and they tended to be absent when spots were near the central meridian of the sun. He also called attention to long sequences of quiet conditions.

Waldmeier (1946, 1950) has suggested that M-regions may develop in areas empty of spots but where a large spot group recently disappeared.

Allen (1944) has suggested that one should distinguish two fundamentally different types of magnetic storms. He listed the following distinguishing characteristics, but emphasized that exceptions to all of the characteristics listed often make it difficult to classify an individual storm. Storms of the first type are intense, are associated with sunspots, follow flares by about one day, have world-wide sudden commencement (sc) and show no recurrence after 27 days. Storms of the second type are of more moderate intensity, are independent of sunspots, flares and other visible disc features, begin gradually, and show a strong tendency to recur with a period of 27 days. Newton and Milsom (1954) emphasize the "sc" as the distinguishing feature and find that storms of the "sc" type appear to follow the sunspot cycle in frequency of occurrence, whereas storms of the second type reach their maximum development one or two years before sunspot minimum.

A statistical study by E. and O. Thellier (1948) of 688 storms since 1884 supports the validity of the distinction between storms of

sudden and gradual commencement with respect to the recurrence tendency. By the superposed epoch method, with the character figure *C*, they found that storms of sudden commencement showed no recurrence tendency, while those of gradual appearance showed a marked 27-day period. With one exception the 37 most intense storms commenced suddenly, a fact which may help to explain the results of Greaves and Newton. (Benkova did not use the superposed epoch method.)

Allen distinguished between recurrent and isolated storms in his study of the relation of storms to sunspots and flares. Isolated storms showed a moderate rise in frequency after CMP of large (i. e., >400 millionths of visible solar hemisphere) sunspot groups, with a maximum on day +4. M-type storms, on the other hand, showed a marked decrease in frequency of occurrence after CMP of large sunspots, with a minimum on day +3; maxima occurred on days −1 and +8. These maxima, together with the decrease in frequency of M-type storms after CMP of large spots, led Allen to conclude that sunspots tend to interfere with M-regions within about 40° of themselves and to increase the frequency of those just outside this area. The development of a spot in a previously spot-free M-region may end the storm sequence; in other cases the sequence merely may be interrupted, to resume after the disappearance of the spots. While M-regions apparently show a significant tendency to avoid spot areas, this avoidance does not seem to be universal.

Allen suggested that the white light coronal streamers were a probable source of M-region activity. Since white light coronal streamers have not been observed outside of solar eclipse, data to test this hypothesis are inadequate. However, von Klüber (1952) has called attention to a possible connection between an intense streamer seen at the eclipse of Feb. 25, 1952, at 10° N, and the large M-type storm beginning on March 3 (the CMP date of the streamer).

Newton (1949) has used Greenwich data, 1914–44, to study the relation between sunspots and geomagnetic storms. He grouped the spots according to area. A marked increase in geomagnetic activity, centered at about day +2, followed CMP of spots larger than 1500 millionths of a solar hemisphere. This relationship diminished rapidly with decreasing spot size and disappeared below 1000 millionths. Sunspot grouping based on flare incidence greatly improved the relation in the expected sense that spots with frequent flares were more likely to produce storms than were spots deficient in flares.

Newton (1943) also investigated the relation between solar flares and geomagnetic storms. From a study of class 3+ flares, 1859–1942, he found that magnetic storms began within 2 days in 27 out of 37 cases. Eighty percent of the 3+ flares that occurred within 45° of the CM were followed by storms. Two-thirds of the storms associated with flares in this central zone were great storms, whereas no great storms followed flares outside this zone. Some 3+ flares more than 45° from the CM did produce moderate storms. The most common travel time of the corpuscles was 20–25 hours.

Extending his investigation to flares of class 3 and 2, Newton (1944) found that flares of intensity 3 in the central zone were followed by a small maximum in geomagnetic activity on day +2. Flares of intensity 2 produced no significant geomagnetic effect.

Kiepenheuer (1947) found that filament area along the central meridian showed a maximum 3–5 days before geomagnetically disturbed days in the years of low solar activity 1922–24. The increase in filament area appeared in both low (<30°) and high (>30°) latitude filaments. To state the relation conversely, the magnetic character figure *C* showed a (small) maximum 4 days after the CMP of regions with large filament areas. No systematic variation in filament areas appeared around magnetically quiet days. We note that Kiepenheuer's filament areas showed a minimum one day before geomagnetically disturbed days, as conspicuous as the maximum 4 days before the disturbance. Hence it is not clear whether either the maximum, the minimum, neither, or both are significant in the relation between filament areas and geomagnetism. Neither of these phenomena appeared to continue during high solar activity, 1926–28. (For figures illustrating some of the above mentioned results of Bartels, Allen, Newton, and Kiepenheuer, see Kiepenheuer, 1953, pp. 443–448.)

A recent study by Roberts and Trotter

(1955), covering 16 months between May 1951 and June 1954, suggests that the minimum may be the significant feature in Kiepenheuer's curves. They calculated the average prominence area, from limb observations, around zero days defined by the 5 most geomagnetically disturbed and by the 5 least geomagnetically disturbed days in each of 16 months. A minimum in area of prominences between the poles and 20° and between the poles and 30° solar latitude (thus the low latitude prominences are omitted) appears in their curves 0–3 days west of central meridian at the time of the geomagnetically disturbed days. The mean lines shown in their published curves are individual averages of the points plotted in each curve. If Roberts and Trotter had instead drawn for comparison an overall average prominence area for the 16 months, the minimum in prominence areas would appear considerably more impressive; in addition the curves would then suggest that quiet days might be associated with above-average prominence areas around the central meridian.

Becker (1953) has made a superposed epoch analysis for 1946–50 sunspot data. He defined zero days by the presence on the central meridian of two sunspot groups of comparable degrees of evolution and symmetrically located with respect to the solar equator. He found that the magnetic character figure possessed a minimum 2 days after CMP of the pairs of spot groups.

One of the most promising lines of investigation has made use of intensity measures of radio noise in conjunction with visible disc features. Measures of 158 Mc/s radiation have permitted Denisse (1952, 1953) and coworkers (Denisse et al., 1951) to classify the visible active centers occurring in 1948–50 into two groups: type R, producing an increase in 158 Mc radiation; and type Q, producing no change or a slight decrease in 158 Mc radiation. They used the superposed epoch method and defined zero days by CMP of R- and Q-type spots. Type R spots appeared to produce a rise in *C*, with the maximum 1–2 days after CMP, whereas the type Q spots were followed by a decline in *C*, with a minimum 2–3 days after CMP. Denisse noted that the magnetic activity associated with type R spots is of the sudden commencement and nonrecurrent type rather than the M-region type. He concluded that noisy (R) spots appear to be the source of relatively dense corpuscular streams, and that quiet (Q) spots tend to inhibit the normal evaporation of corpuscles from the corona. He attributes the moderate level of geomagnetic activity present outside of storms to this evaporation. Denisse further pointed out that the existence of noisy and quiet spots, having directly opposite geomagnetic effects, would explain the commonly poor "spot versus *C*" correlations obtained when the two groups are not in some way separated.

Becker and Denisse (1954) subsequently combined their methods of defining zero days to study the period 1948–50. They found that CMP of a pair of quiet spots, one north and one south, tends to be followed by a decline in geomagnetic activity—with a minimum on day 3—greater than that following either MPC of a single Q-spot or CMP of a pair of spots without regard to their radio properties. Further, the apparent storm-producing effect of a noisy spot tends to be diminished if it is paired with a quiet spot in the other solar hemisphere.

We come now to the specific problem of the present paper, namely the relation, if any, between coronal emission-line intensity and geomagnetism. So far we have seen that isolated storms tend to be associated with flares and with CMP of some but not all large sunspots, while M-regions tend to avoid such centers. No one-to-one relation has been found between geomagnetism and any visible solar feature. A mere tendency, while significant, is not adequate either for reliable prediction or for understanding the solar mechanism of storm production.

The intensity of the coronal emission line λ5303 follows the same 11-year cycle, both in intensity and in latitude distribution, as do other manifestations of solar activity. Since there exists, furthermore, a general tendency to association among the various active features, a one-to-one relation between 5303 intensity and *Kp* is unlikely. On the other hand, different active features do not always show disturbances in the same area or to the same degree, so that the relation of *Kp* to

5303 intensity could be closer than its relation to other phenomena.

Waldmeier (1939, 1942) was the first to study this problem, shortly after beginning 5303 observations at Arosa. Using necessarily fragmentary 5303 data for 1939–40, he found that the appearance of regions of unusual brightness of the line 5303, which he called C-regions, was correlated with the occurrence of geomagnetic disturbances about 7.4 days later (E limb) and 6.2 days earlier (W limb). Most subsequent studies have not confirmed this result, perhaps because they pertain to a later stage of the solar cycle.

Shapley and Roberts (1946), by the superposed epoch method, explored the relation between the magnetic character figure C_A, and the Climax 5303 intensities for the period Aug. 1942–Aug. 1944. Since sunspot minimum occurred early in 1944, their investigation covers a period of more M-type activity and fewer isolated storms than Waldmeier's period. They took 5303 intensity ≥ 10 on the east limb to define zero days and calculated the average value of $20C_A$ from days -4 through $+14$. They calculated also the frequency of days having $20C_A \geq 9$, and of days having $20C_A \geq 15$; the average value of $20C_A$ for the period was 8.6. Each of these three calculations indicated that the probability of a high C_A was markedly greater when bright 5303 regions were on the eastern half of the sun. As their figures 3–4 show, C_A had a maximum on day east limb passage $+4$ for Aug. 1942–July 1943, and a broader maximum on ELP $+2$ through $+8$ for Aug. 1943–July 1944. By the time the active region passed CM the probability of large C_A was declining and was below average on days 9–12 (i. e., 2–5 days after CMP of the active regions).

Noting that C-regions tend to persist for a number of rotations of the sun, Shapley and Roberts adopted the hypothesis that C-regions and M-regions were coincident. With this hypothesis they then concluded that C-regions are most effective in producing geomagnetic storms when located about 40° east of the solar central meridian.

Shapley (1946) has studied the relation between Ca II plages and $20C_A$ for 1942–44. He defined zero days by CMP of large, long-lived plages. We include this plage study here because the results are so closely similar to the coronal results. The plage study indicated a tendency for high C_A when a large plage was on the eastern half of the sun, and a marked minimum 3–4 days after CMP of the plage. Wolf and Nicholson (1948, 1950) also found that M-regions tended to occur, in 1942–44, when plages were on the eastern half of the sun.

Kiepenheuer (1947) has made a superposed epoch study using Wendelstein 5303 intensities, 1943–45. He defined zero days by "strong" 5303 corona at east and west limbs, and computed mean Potsdam magnetic indices, K, for days ELP $+4$ to $+14$ and WLP -6 to $+4$. The most conspicuous feature is a minimum of K at ELP $+10$ and WLP -3 in 1943. Perhaps there is also a maximum on ELP $+4$ but Kiepenheuer's curves do not extend far enough before CMP to establish this with certainty. The agreement between the observational results of Kiepenheuer and of Shapley and Roberts appears quite satisfactory. Kiepenheuer, however, assumed that the corpuscular radiation must be emitted from the region of the CM and therefore concluded that strong coronal intensities correspond to low geomagnetic character figures. Bright 5303 regions tended to coincide with spots and plages and to have a similar weakening effect on K-indices. The relation apparent between 5303 and K in 1943 virtually disappeared in 1944 and 1945, with the start of the new cycle of solar activity.

Kiepenheuer made a separate calculation for cases of "very strong" 5303 corona, 1943–45. Here he found maxima in K on days ELP $+7$, and WLP -7, in agreement with the results of Waldmeier.

A recent study by Denisse and Simon (1954) covering the period 1946–52 indicates that CMP of active centers showing emission in the λ5694 coronal line tends to be associated with disturbed geomagnetic conditions; whereas CMP of centers where 5694 emission is clearly absent tends to be associated with diminished values of Kp. The study also points out a tendency for enhanced 158 Mc radio noise and 5694 emission to be present or absent together.

Lincoln and Shapley (1948) extended the superposed epoch analysis through 1944–46, using data from Climax, Pic du Midi, and

422953—57——2

Wendelstein combined. The authors stated that "in general one suspects that the variations shown in a superposed epoch diagram are real if (1) the same relationship, or time lag, is observed in each of two or more arbitrarily chosen samples of the data, and (2) the variation curve is more or less smooth . . . The evidence is not conclusive. The relationships for 1942 (second half), 1943, and 1944 are similar, and differ from those for both 1945 and 1946. The curves for 1942, 1943 and 1944 are relatively smooth, and the likelihood of a real relationship thereby enhanced." If the variations from year to year are real, "the time lag between east-limb passage of the selected coronal region and the related magnetic activity varies with the stage of the sunspot cycle." To settle this question, data from at least a complete spot cycle would be needed. The only feature the years 1944–46 have in common is a below-average probability of geomagnetic storm on day ELP +10, a property found also for 1942–44.

A similar analysis for large sunspots, 1890–1936, divided into four groups by phase of the sunspot cycle, showed no resemblance to the coronal results. Lincoln and Shapley concluded, in part from detailed examination of 1944–46 data, that corona and sunspots were more or less independent manifestations of solar activity. "Of the 32 largest sunspots with area greater than ten square degrees, only three were within seven degrees of longitude of the center of a bright coronal region while 14 were within 25°. Observations were incomplete in some of the remaining cases; in others, the largest sunspot was probably associated with a coronal region of minor importance according to the criteria used in this paper. Apparently the size of a sunspot bears little relation to the intensity of the corona above it."

Note that, as we should expect if 5303 intensity measures are reasonably reliable, all studies of the relation between geomagnetic and visible solar features covering the same time interval agree in results if not in interpretation. In 1942–44, magnetic storms tended to occur when active regions were on the eastern hemisphere of the sun; after CMP of the active region the magnetic character figure tended to show a minimum. Since both M-regions and C-regions often persist for several months, and since each has a recurrence period of 27 days, the existence of an apparent relation between the phenomena is inevitable. The appearance of a relationship therefore does not necessarily establish any significant physical connection between the two phenomena. The existence of a physical relationship, of course, will become increasingly probable the greater the number of independent cases in which the same relation appears.

Smyth (1952) has used the average intensity $\pm 30°$, from Climax data, to investigate the period June 1950–Jan. 1951 by the superposed epoch method. He found a tendency for a lower-than-average geomagnetic index 1–5 days after CMP of bright corona. The relation appeared for both 5303 and 6374. The eastern hemisphere effect of Shapley and Roberts was not confirmed. Smyth has also calculated the intensity of 5303 and 6374 around the time of the principle M-region. The intensity of 5303 showed a pronounced minimum on the east limb 8 days before the onset of the M-region.

Bruzek (1952) has studied from Wendelstein data the 5303 intensity around three M-regions—the above mentioned M-region of 1950 and the two prominent M-regions in 1942–44. He found that each of these M-regions appeared to coincide with the presence on the central meridian of a region of unusually weak 5303 corona.

On the other hand, Trotter and Roberts (1952) noted that the eastern hemisphere effect, found by Shapley and Roberts in 1942–44, appeared to be returning in 1952 after being largely absent during maximum solar activity. Müller (1953) found similar results for Feb.–Aug. 1952 from Weldenstein 5303 data. He has suggested that the discordant results of various workers may arise primarily from the different phases of the sunspot cycle they have studied. (This 1952 M-region is the one that von Klüber (1952) has attributed to CMP of the white light coronal streamer seen at the February 1952 eclipse.)

Part I. Single intensity index for each coronal line

The present investigation covers an interval of 45 months, from Feb. 1, 1950—the date when regular observations were begun at Sacramento Peak—through mid-October 1953. This period, well on the descending branch of the recent sunspot cycle, is much richer in M-region activity than was the corresponding phase of the preceding cycle.

As a measure of the solar corpuscular radiation, or geomagnetic activity, we used the daily sums of the 3-hour *Kp* values. The scale for the 3-hour *Kp* values is 0 (very quiet) to 9 (very disturbed), giving a range of 0–72 for the daily sums. This planetary index, derived from data of 11 observatories between geomagnetic latitudes 47 and 63 degrees, was designed by Bartels to measure solar particle-radiation by its magnetic effects.

In the first part of this investigation, we use as a measure of the intensity of the green coronal line, λ5303, the daily mean of its five highest east-limb intensities corrected to a plate threshold of five. This quantity we hereafter designate simply as the daily "5303 intensity"; east-limb values are implied unless we specifically say west-limb 5303 intensity. We obtained both the coronal and the geomagnetic data used in this study from the monthly Central Radio Propagation Laboratories (CRPL) Bulletins.

We corrected the 5303 intensities to a plate threshold of five by the following equations derived from a least squares analysis (Glazer and Bell, 1954):

$$I_s' = I_s + 0.93\ (T_s - 5) \qquad \text{for Sac Peak}$$
$$I_c' = I_c + 0.61\ (T_c - 5) \qquad \text{for Climax,} \tag{1}$$

where I_s and I_c are the respective observed intensities, I_s' and I_c' are the respective corrected intensities, and T_s and T_c are the plate threshold values.

The daily 5303 intensities were obtained from the Sac Peak observations. These were supplemented, however, for days when bad weather prevailed at Sac Peak, by I_c' values adjusted to the Sac Peak scale by the approximate relation

$$I_s' = 1.5\, I_c'. \tag{2}$$

For days when neither station observed, we derived interpolated intensities, primarily by reference to west-limb intensities 14 days before and after and secondarily by reference to east-limb intensities 27 days before and after the day in question. Such interpolations seemed not unreasonable because the intensity of the 5303 line generally changes only slowly with time. In cases where the interpolations were particularly uncertain, we assigned intermediate values to the interpolated intensities; consequently we made little subsequent use of them.

For a few weeks in the spring of 1952, the Sac Peak coronagraph was out of adjustment; and from March 14 through April 28 the Sac Peak 5303 intensities were regularly no stronger than the corresponding Climax observations. Therefore, we increased all Sac Peak intensities in this period to bring them into their usual relation with those of Climax, believing these corrected values to reflect more accurately the 5303 activity on the Sac Peak scale.

As a measure of the daily intensity of the red coronal line, λ6374, in Part I we use the mean of the three highest east-limb intensities. This quantity we define as the daily 6374 intensity. We did not introduce any threshold correction for 6374 because at this stage of the investigation it had not been adequately determined. The 6374 intensities are known to change more rapidly than those of 5303. Therefore we did not consider it proper to make interpolations and have used simply the observed 6374 intensities from both Sac Peak and Climax.

We used the superposed epoch method of analysis (Chree and Stagg, 1927). We were fortunate in having access to IBM equipment for the analysis, and accordingly punched the data on standard 80-column IBM cards. The use of IBM equipment permitted us to investigate a wider variety of possible relationships than would otherwise have been practicable.

Because of the substantial decline in the 5303 intensity over the 46 months under consideration, we divided the data into four time periods: (1) 1 Feb. 1950 to 31 Oct. 1950; (2) 1 Nov. 1950 to 31 Oct. 1951; (3) 1 Nov. 1951 to 31 Oct. 1952; (4) 1 Nov. 1952 to 15 Oct. 1953. Relative intensities within each period, rather than absolute values, define the zero-days of strong and weak coronal intensity. In selecting zero-days for superposed epoch analysis we found it desirable to divide the first period into two equal parts; the decrease in 5303 intensity was sufficiently great during 1950 that we could not use

the same criteria for "strong" and "weak" coronal intensity throughout the period without causing most of the "strong" intensities to fall in the early months and most of the "weak" intensities in the later months of the period. To be consistent we divided the 6374 intensities into the same time intervals.

The green line, λ5303, [*Fe* XIV].—We determined mean *Kp* values for days −4 through +16 around zero days defined by the ELP of the 10 percent, 20–10 percent, and 30–20 percent of the strongest and the weakest 5303 intensities within each of the four time periods. Since we did not wish to include any given intensity in two different categories, the percent limits are necessarily only approximate.

To obtain an over-all result for the 45 months we combined the separate results of the four periods, thus taking account of the decreasing general level of 5303 activity during these years. The geomagnetic activity, *Kp*, increased from 1950 to the spring of 1952 and decreased thereafter. We shall examine the 45-month result first, and then compare the results of the individual periods.

Figure 1*a,b* shows the average values of *Kp* for the 45-month period. The sample size for each of these curves is approximately 125. The average value of *Kp* for the period is 22.65, as indicated on each curve.

In the period studied the standard deviation of a single daily *Kp*-sum is 9.87, so that the ordinary standard error of the mean would be $\sigma=9.87/\sqrt{N}$, where N is the size of the sample. To take account of the positive autocorrelation known to exist between the *Kp*'s for lags of 1, 2, 27, and 54 days, however, the ordinary standard error of the mean must be increased by factors involving the autocorrelation coefficients.

The mathematical definition of the variance (standard deviation squared) of a variable x, in terms of "expected values," is

$$\sigma^2=E[x-E(x)]^2. \tag{3}$$

$E(x)$ is the expected value of x, or the mean m. We call σ^2 the second moment about the mean. To get the variance of $\bar{x}=\Sigma x_i/N$, we replace x by $\bar{x}$ in equation (3). Whence

$$\begin{aligned}\sigma_{\bar{x}}^2&=E[\bar{x}-E(\bar{x})]^2=E\left[\frac{1}{N}\Sigma(x_i-m)\right]^2\\&=E\left[\frac{1}{N^2}\Sigma(x_i-m)^2\right]+E\left[\frac{2}{N^2}\sum_{i<}(x_i-m)(x_j-m)\right].\end{aligned} \tag{4}$$

When we assume independence between x_i and x_j, the second term becomes zero and we have

$$\sigma_{\bar{x}}^2=N\sigma^2/N^2=\frac{\sigma^2}{N}$$

where $\sigma_{\bar{x}}$ is the ordinary standard error of the mean. When x_i is not independent of x_j, we define

$$E(x_i-m)(x_j-m)=\rho_d\sigma^2$$

where ρ_d=the autocorrelation coefficient of lag $|j-i|$.

Shapley (1947), working with the autocorrelation of the magnetic character figure *C*, found correlations of about 0.5 for 1-day lag, 0.2 for 2-day lag, and negligible correlation for a lag of 3 days. He also found strong autocorrelation in the 27-day recurrence tendency, so we consider both the 27-day and the 52-day lag correlations. Accepting his figures as adequately representing the autocorrelations existing in our sample, we have used 0.5 and 0.25 as the correlations for lags of 27 and 54 days respectively. We then listed all values from which we calculated our 10 percent maximum and 10 percent minimum, and determined the frequencies of lag 1, 2, 27, and 54 days in our sample. With this information, we may now proceed to use equation (4).

Let

ρ_d=the autocorrelation coefficient of lag d,

and

n_d=the frequency of occurrence in sample of days with lag d.

Then

$$\sigma'_{\bar{x}}=\frac{\sigma}{\sqrt{N}}\sqrt{1+\frac{2}{N}(n_1\rho_1+n_2\rho_2+n_{27}\rho_{27}+n_{54}\rho_{54})}. \tag{5}$$

From this equation we obtain

$$\sigma' \text{ (maximum 10\%)}=1.28$$

$$\sigma' \text{ (minimum 10\%)}=1.25.$$

These values may be compared with 0.88, the ordinary standard error derived under the assumption of independence of the *Kp*'s from one another.

As a guide to the significance of the variations in the curves in figure 1*a,b*, where relevant, we have drawn dotted lines at a distance of two standard errors (adjusted for autocorrelation, σ') from the mean of 22.65. Although

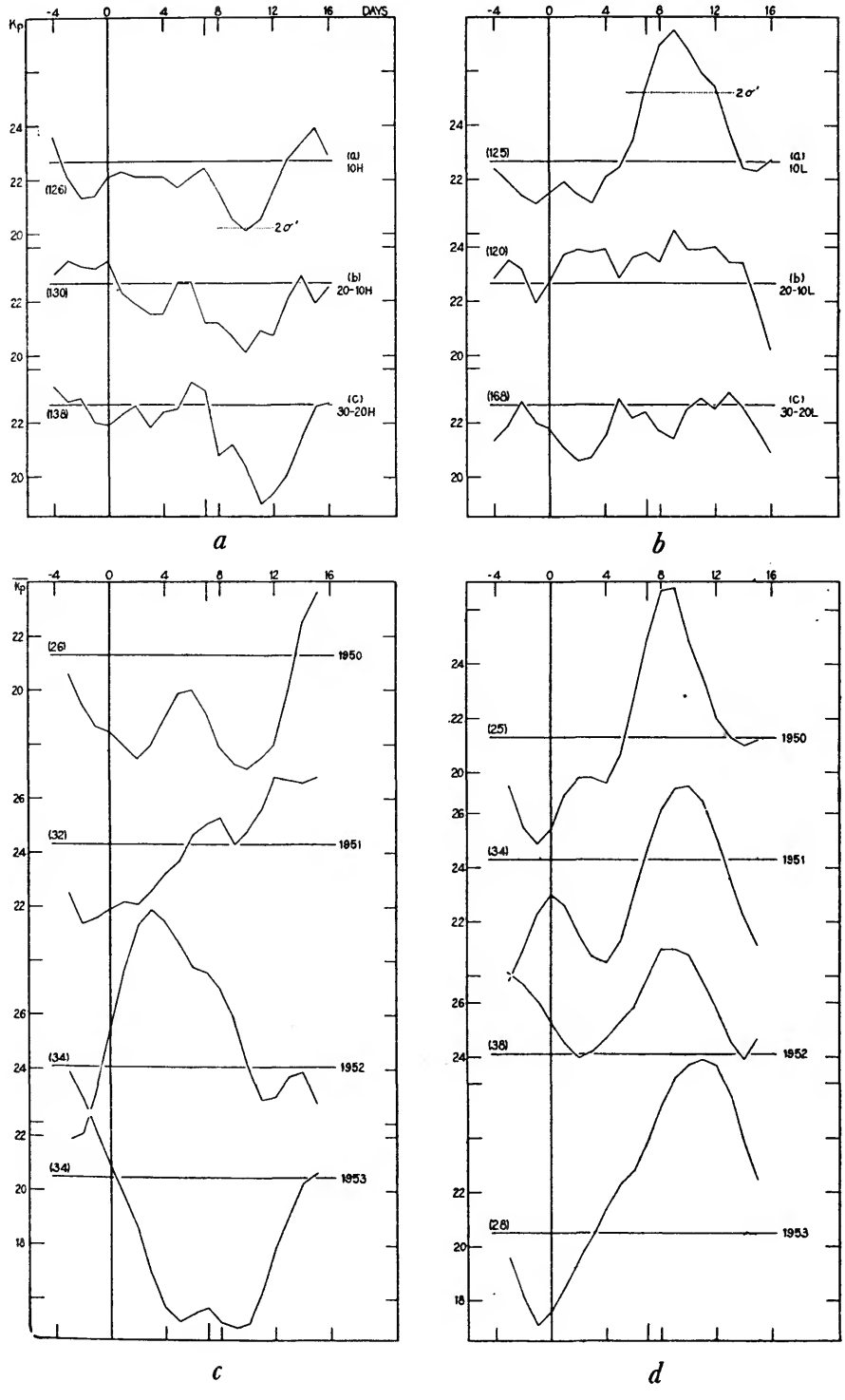

FIGURE 1.—Mean *Kp* for each day following ELP of various coronal conditions. *a*, *Kp* after ELP of the 10 percent strongest (a), the 20—10 percent strong (b), and the 30—20 percent strong (c) intensities of 5303, 1950–53. *b*, *Kp* after ELP of the 10 percent weakest (a), the 20—10 percent weak (b), and the 30—20 percent weak (c) intensities of 5305, 1950–53. *c*, 10 percent brightest 5303 intensities for the individual years (3-day running means). *d*, 10 percent faintest intensities for the individual years (3-day running means). Number of cases shown in parentheses.

this criterion of significance is not exact when applied to the results obtained by the superposed epoch method of analysis, it should provide a fairly reliable guide for judging the results.

Figure 1*a* shows that strong 5303 corona on the east limb is followed on days 8–12 by a *Kp* below the mean, although only *Kp*(+10) falls outside the 2-standard-error band. This minimum in *Kp* after CMP of strong 5303 corona agrees with the result of Kiepenheuer (1947) and appears also in the curves of Shapley and Roberts (1946) for the previous cycle. On the other hand, we find no indication of the maximum around day ELP+4 that showed so prominently in the curves obtained by Shapley and Roberts in the previous cycle. The patterns of *Kp*'s after ELP of strong, very strong, and moderately strong 5303 intensities do not differ significantly from one another. Even the 5 percent strongest intensities failed to produce any significant rise in *Kp* around days +7 to 8, such as that found by Waldmeier (1939, 1942) and by Kiepenheuer (1947) for "very strong" corona.

From line (a) of figure 1*b* we see that weak 5303 corona on the east limb of the sun is followed on days 7–12 by *Kp* significantly above the mean, with a maximum on day +9. *Kp* (+9) is very close to four standard errors (σ') above the mean, while *Kp* (+8) and (+10) are almost three standard errors above the mean, so that this result appears highly significant. The most probable time for a geomagnetic disturbance, in this phase of the solar cycle, is two days after CMP of a weak coronal region, a conclusion in general agreement with the results of Smyth (1952) and of Bruzek (1952). The 5 percent weakest 5303 intensities give a curve very similar to the 10 percent curve shown. The effect, however, rapidly disappears with increasing 5303 intensity, being very slight for the weak 20–10 percent group and disappearing entirely for the weak 30–20 percent group of intensities. Thus the moderately weak corona shows no relation to *Kp* (line (c) of figure 1*b*); while the moderately strong corona shows a relation similar to that of the strong corona.

Comparison of results from two or more independent samples of data provides an important test for the reality of the results of any superposed epoch analysis. With this in mind we examined the results of the four time periods (see p. 57) separately. Because of the smaller samples, these curves are less smooth than the 45-month curves. In order to emphasize the principal trends and minimize the irrelevant minor fluctuations we plotted these results as 3-day running means, $\overline{Kp}$. Figure 1*c* shows the values of $\overline{Kp}$ following ELP of strong (10 percent) 5303 coronal regions for the four periods, and figure 1*d* shows the values of $\overline{Kp}$ following ELP of weak (10 percent) 5303 coronal regions. Mean $\overline{Kp}$'s are shown for each period.

Looking at figure 1*c* we see that the curves of $\overline{Kp}$ following ELP of strong 5303 intensity differ considerably from year to year. The $\overline{Kp}$'s for the first and fourth periods are conspicuously below the means for these periods. The second period curve rises more or less continuously after ELP of the strong corona. The curve for the third period resembles rather closely the results found by Shapley and Roberts in the preceding cycle, and shows a strong maximum in *Kp* on day 3. Period three covers the time for which Trotter and Roberts (1952) and Müller (1953) noted a return of the eastern-hemisphere effect. Because this effect does not appear in our other three periods—and for reasons to be seen in Part II—we are inclined to doubt the existence of any physical connection between the 5303 corona on the eastern hemisphere of the sun and the M-region responsible for the rise in *Kp*. One feature common to all four curves in figure 1*c* is a tendency for a dip in the $\overline{Kp}$ values 9–12 days after ELP of the bright coronal regions. While the tendency is present in each curve, in some cases it is very slight and not particularly convincing.

In figure 1*d* the curves of $\overline{Kp}$ following ELP of weak 5303 intensity are very similar in shape for all four periods, particularly after day 5. A conspicuous maximum occurs in each period 9–11 days after ELP of the faint corona.

The relationship between 5303 intensity and geomagnetism can be approached, alternatively, through a study of the frequency distributions of *Kp* following ELP of various coronal conditions. This approach, as Shapley and Roberts (1946) have pointed out, serves to reduce the possibility that one or two very intense

storms might dominate the shape of the curve, particularly when the sample size is small.

We were particularly interested, of course, in the extremes of 5303 and in the high values of Kp. Because of the tendency to weak Kp on day 10 after ELP of strong corona, the distribution of weak values of Kp is also of interest. We determined, for each time period, the fraction of strong corona on the east limb that is followed by (a) $Kp > 30$ and by (b) $Kp \leq 12$, and the fraction of weak 5303 corona that is followed by (c) $Kp > 30$ and by (d) $Kp \leq 12$. For comparison we computed the fraction of strong and of weak intensities of 5303 which should be followed by strong or weak Kp, if there were no connection between 5303 intensity and Kp. This "expected fraction" is essentially the number of days with $Kp > 30$ (or of days with $Kp \leq 12$) in the period divided by the total number of days in the period.

The results agree well with those found by the previous method. Result (a) is quite similar to figure 1*c*. The four periods do not agree with one another, except that the observed fraction tends to lie below the expected value (or in period 3 to decline toward it) after CMP of strong corona. Group (b) shows, in each of the four periods, a fairly clear tendency for the observed fraction of weak Kp to rise above the expected value 0–4 days after CMP of strong corona. Result (c) is substantially in agreement with figure 1*d*. The observed fraction lies significantly above the expected fraction 1–4 days after CMP of weak corona in each of the four periods; that is, strong Kp follows CMP of weak corona significantly more frequently than would be expected in the absence of any actual relation between these phenomena. Category (d) shows a systematic tendency in each period for the observed fraction of weak Kp to fall below the expected value 0–5 days after CMP of weak corona.

To investigate the effect of the threshold corrections and the interpolations on our results, we calculated mean Kp's for the 10 percent maximum and minimum 5303, using three different sets of data: (a) the Sac Peak observed intensities, uncorrected for plate threshhold, (b) the Sac Peak observed intensities, corrected to plate threshold five, and (c) Sac Peak corrected intensities plus intensities derived from Climax observations and interpolated intensities. Figure 2 shows the results for the 10 percent maximum and 10 percent minimum 5303 intensities. For comparison, the graph includes similar calculations made for the quantity used by Shapley and Roberts (1946), namely the (d) single maximum intensity of 5303 observed at Sac Peak and corrected to plate threshold five.

While the four curves differ in detail and in smoothness, each indicates the same general results, a minimum in Kp 10 days after ELP of strong 5303 and a maximum in Kp 9 days after ELP of weak 5303 regions. We found no statistically significant differences between the four curves for either the strong or the weak 5303 cases.

After ELP of strong 5303 intensities, curves (a), (b), and (d) show a secondary minimum on day 5, followed by a slight rise in Kp around days 7–8. This rise may be a trace of the effect observed by Waldmeier (1939, 1942). We recall

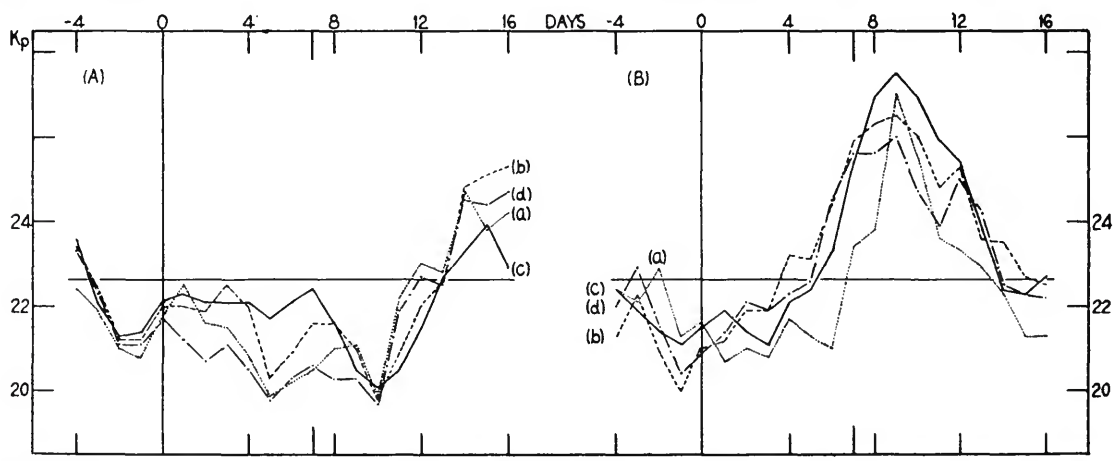

FIGURE 2.—Mean Kp following ELP of strong (A) and weak (B) 5303 intensities. The curves show the results from coronal intensities uncorrected for threshold (a), corrected to plate threshold five (b), corrected and interpolated (c), and the single maximum observed intensity (d).

that Denisse (1952, 1953) found evidence, from radio-noise observations, for two types of solar active centers, those (R) that produce geomagnetic storms and those (Q) that reduce corpuscular radiation. The curves of *Kp* following ELP of strong corona are therefore probably a composite of these two types of active centers. From the behavior of the composite, we infer that Q-type centers were probably more numerous than R-type centers during the interval covered by our study. Note that this rise of *Kp* around CMP is present also in figure 1*a* and more or less in the four curves of figure 1*c*.

Correlation coefficient.—To compute the coefficient of correlation between *Kp* and coronal intensity we divided the data into our usual four time periods. For each period we sorted the cards by 5303 intensity into ten equal groups, and assigned intensities on a new arbitrary scale of 1 to 10. This change in the 5303 scale was made in order to remove the effect of the progressive decline in coronal intensity over the 45 months. In the usual way we then computed the correlation between the 5303 intensities on the 1–10 scale and *Kp* (−2) through *Kp* (+15). Figure 3 shows the correlogram of the average correlation coefficients for the four periods. The correlations are very close to zero except on days 7–13 when they become negative. The largest correlation, −0.18, occurs for *Kp*(10), indicating once again a time lag of about 3 days between CMP of a strong or weak coronal region and its maximum geomagnetic effects.

The red line, λ6374, [*Fe* x].—We determined mean values of *Kp* for days −4 through +16, as shown in figure 4, around zero days defined by ELP of the strongest 10 percent and of the weakest 10 percent of the 6374 values; the data from Sacramento Peak and those from Climax were used separately. As with the green line, the percent limits with the red line are necessarily only approximate. To obtain the over-all result shown in the figure for the 45 months, the separate results of the four periods were combined.

Figure 4 indicates, with a general similarity between the Climax and Sac Peak curves, that ELP of strong (10 percent) 6374 corona tends to be followed on days 8–9 by a *Kp* significantly below the mean. Examination of the years separately supports this conclusion. On the other hand, following ELP of weak 6374 the *Kp* curves are very irregular and lack any significant features; the strong rise in *Kp* following CMP of weak 5303 intensities is entirely absent for 6374. Outside of active

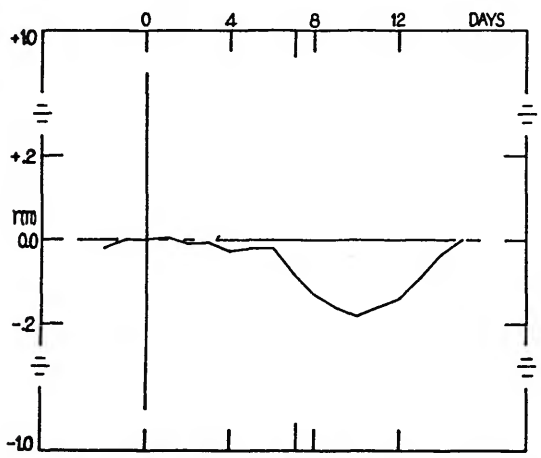

FIGURE 3.—Coefficients of correlation between 5303 intensity and *Kp*, with lags in *Kp* of −2 to +15 days after coronal ELP.

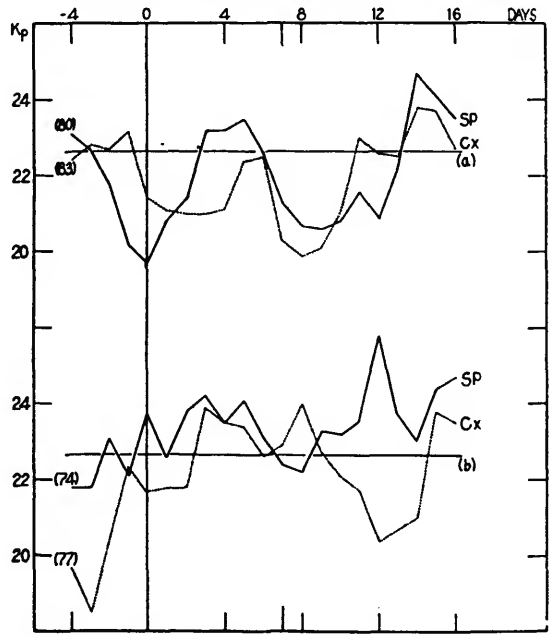

FIGURE 4.—Mean *Kp* following ELP of strong (a) and weak (b) 6374 intensities, from Sacramento Peak (SP) and Climax (Cx) data.

regions the intensity of the 6374 line appears to be more uniformly distributed than that of 5303. Therefore minima are perhaps less precisely defined for 6374 and no relation with *Kp* should be expected.

In general we conclude that *Kp* shows a substantially closer relation to the intensity of the 5303 line than to the intensity of the 6374 line.

Green line and red line, simultaneously.—In investigating the effects of the two lines simultaneously, we used only Sacramento Peak red line intensities and the green line intensities corrected to standard threshold. We determined mean values of *Kp* for days −4 through +16 around zero days defined by various combinations of the two lines, with the results shown in figure 5*a*, *b*.

The top curve of figure 5*a* shows that when both coronal lines are strong, *Kp* declines quite smoothly (heavy line) from day 3 to a minimum on day 10 which is deeper than any of the minima obtained by using only one coronal line. Days 8–10 have *Kp* two or more standard errors (σ') below the mean value of 22.65. The asymmetry of the curve about its minimum probably reflects the tendency of *Kp* to rise more rapidly than it declines. To facilitate comparison we include the mean *Kp* following ELP of strong 5303 corona and of strong 6374 corona, each computed as before without regard to the behavior of the other line. We suggest also comparison with figures 1*a*, 2, and 4. Most noteworthy is the disappearance of the small rise in *Kp* around days 6–8 when both lines are used; this rise we attribute to storm-producing active centers as distinguished from the more common

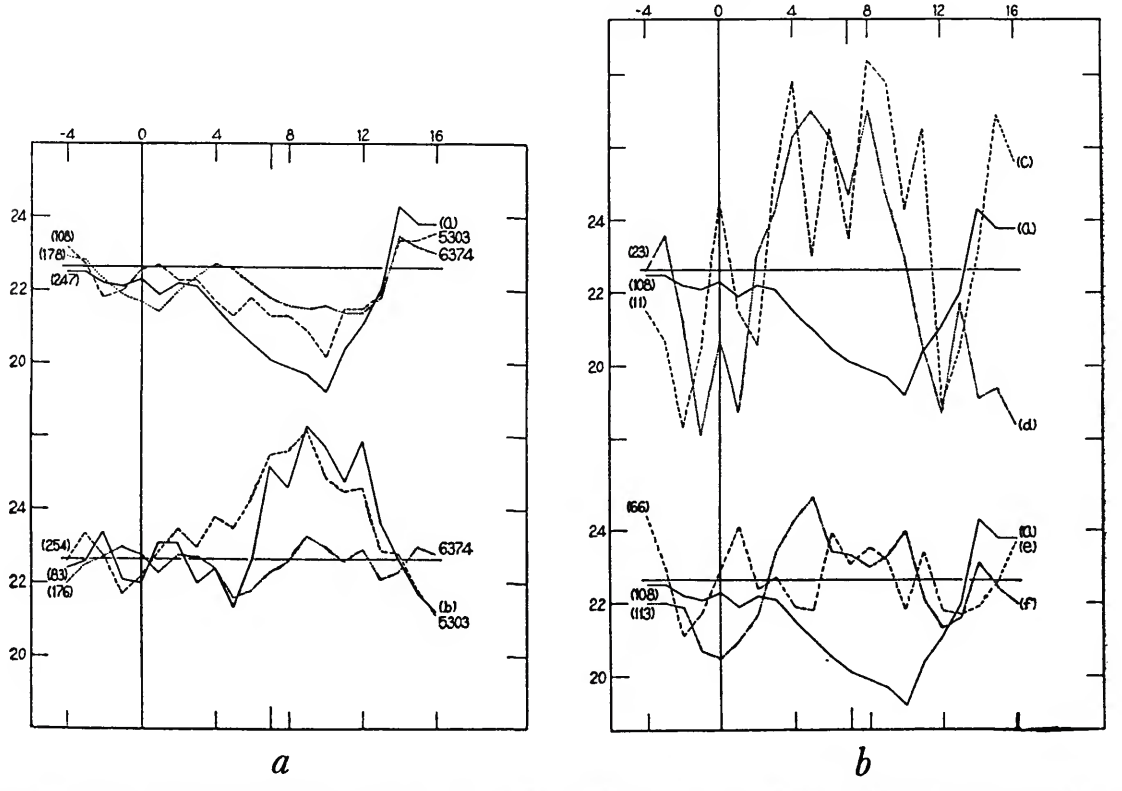

FIGURE 5.—Mean *Kp* following ELP of various combinations of red and green line intensities. *a*, *Kp* after ELP of regions with the two lines in agreement: line (a), strong 5303 intensities (20 percent) and strong 6374 intensities (30 percent), 108 cases; line (b), weak 5303 intensities (20 percent) and weak 6374 intensities (30 percent), 83 cases; results for each line alone included for comparison. *b*, *Kp* after ELP of regions having one line strong, the other not strong: curve (c), strong 5303 (20 percent) and weak 6374 (30 percent) intensities, 11 cases; curve (d), strong 6374 (30 percent) and weak 5303 (20 percent) intensities, 23 cases; curve (e), strong 5303 (20 percent) and not-strong 6374 (lower 70 percent) intensities, 66 cases; curve (f), strong 6374 (30 percent) and not-strong 5303 (lower 80 percent) intensities, 111 cases. (Curve (a) is reproduced from figure 5*a* for comparison.)

(in this period) storm-inhibiting active centers. Thus the curves of figure 5*a* may have special interest.

The top curves of figure 5*b* show the mean *Kp*'s following ELP of coronal centers in which one line is strong and the other weak. The curve when both lines are strong is included for comparison. The results are surprising. When the green line is strong and the red line weak, *Kp* is above the mean on days 3–11; when the red line is strong and the green line weak, *Kp* is above the mean on days 2–10; whereas when both lines are strong *Kp* is below the mean on days 4–12. While these differences appear to be statistically significant, we should keep in mind that the sample sizes are small. The bottom curves of figure 5*b* show the mean *Kp*'s following ELP of coronal centers in which one line is strong and the other line is not strong. While neither curve (e) nor (f) deviates significantly from the mean *Kp*, each appears to differ significantly from the case of both lines strong.

The bottom curve of figure 5*a* shows that no improvement over green line alone is obtained for the case of both lines weak. This result is perhaps to be expected since the weak red line alone shows no relation to *Kp*.

The interpretation of the results shown in figure 5*a*, and *b*, is not at present clear. However, the curves do indicate that the red as well as the green line should be considered in future studies of the relations between geomagnetism and coronal intensity, and that some improvement in predicting the geomagnetic effects of an active center might result from attention to the relative intensities of the two lines.

The yellow line, λ5694.—The rare appearance of the yellow line in the coronal spectrum appears to indicate a center of unusual activity. Waldmeier (1945), Roberts (1952), and Dolder (1952) have pointed out the frequent association between 5694 emission and small, highly active and sharply curved prominences of the sunspot type. They find evidence also for a close association between 5694 emission and solar flares (especially Dolder, 1952).

A search of the CRPL Bulletins revealed that the yellow line was observed at Sacramento Peak and/or Climax on 22 occasions between February 1950 and December 1952, 12 times on the east limb and 10 times on the west limb. We omitted three cases occurring in relatively high latitudes in 1953. Figure 6 shows the mean *Kp*'s associated with regions of yellow line emission. The mean *Kp* for the period covered by the 22 appearances of the yellow line is 22.65. Because of the small samples the curves are very irregular and the standard errors are large. Most of the fluctuations are not common to the east and the west limb curves and therefore should not be considered significant. However, each curve does show a maximum in *Kp* around CMP

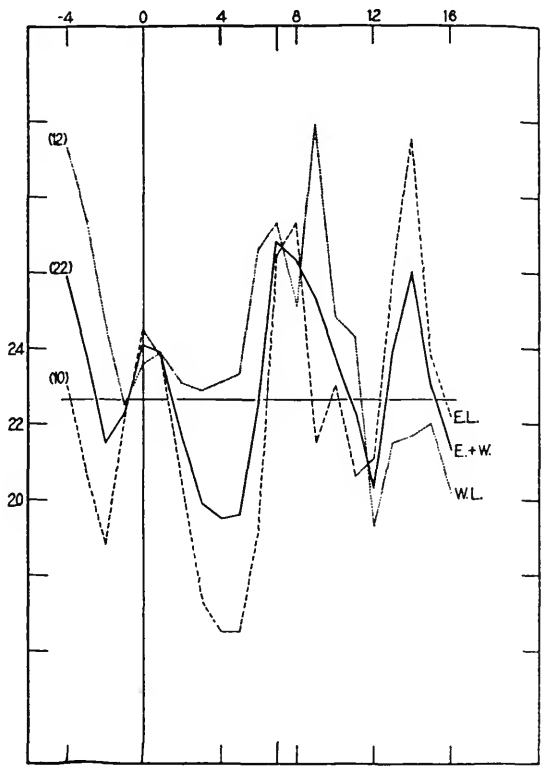

FIGURE 6.—Mean *Kp* following ELP of regions of yellow-line emission. The solid curve shows combined results for east and west limb observations; the broken curves show the results for east and west limb appearances separately.

of the region emitting the 5694 radiation. The individual maxima occur on days ELP +8 and WLP −5, while the maximum of the composite curve occurs on day 7. This maximum does not attain two standard errors from the mean.

To investigate further the relation between *Kp* and 5694, we determined the frequencies of $Kp > 30$, 20–30, and < 20 on days −2 through +4 around CMP of yellow-line regions, shown in table 1.

TABLE 1.—*Frequencies of* Kp *around CMP of yellow-line regions*

Kp\CMP	−2	−1	0	+1	+2	+3	+4
$Kp>30$	3	3	10	10	6	7	6
$30\geq Kp\geq 20$	8	9	5	8	11	5	7
$Kp<20$	11	10	7	4	5	10	9
$\%Kp>30$	14	14	45	45	27	32	27

A chi-square test indicates that the deviations of these frequencies from the expected values are not quite statistically significant; that is, they provide insufficient evidence to reject a hypothesis of independence between Kp and 5694. The last row of table 1 shows the percent of $Kp>30$; the individual values may be compared with a mean frequency of 24 percent for the three years in which the yellow line emissions occur.

While none of the yellow-line results can be declared statistically significant, the above tests do not take account of the location of the deviations from the mean or expected values, i. e., of the fact that the rise in frequency of strong Kp occurs when the yellow line region is on the central meridian. Moreover, yellow line emission appears to be relatively short-lived. Only two of the regions in our sample showed 5694 on both ELP and WLP; (in seven cases coronal observations were obtained on only one limb). Therefore, probably not all of the regions were emitting 5694 radiation when they crossed the central meridian. Certainly the changes in the frequency distribution of strong Kp are in the direction and the position to be expected if yellow line regions tend to produce geomagnetic storms. The results are also in general accord with recent findings by Denisse and Simon (1954) for yellow line regions in the period 1946–52. From the present small sample, however, we can draw no definite conclusions.

Green line intensity around zero-days defined by large Kp.—In order to obtain a picture of the average distribution of 5303 intensity as a function of longitude on the face of the sun at the time of geomagnetic storms, we prepared an inverse deck of IBM cards containing east limb intensities for days CMP −7 through +9 (ELP −14 through +2), and west limb intensities for CMP −9 through +7 (WLP −2 through +14). Using these cards we first calculated the average intensity of 5303 around zero days defined by the maximum 20 percent of the Kp's. Examination of the results for the 45 months revealed that the 5303 intensity tended to have a minimum on the central meridian of the sun 2–4 days before the occurrence of geomagnetic storms. This minimum appeared in each of the four time periods.

To determine whether sporadic and recurrent geomagnetic storms appeared to be associated with different patterns of coronal intensity we selected, from the lists published regularly in the Journal of Geophysical Research, those storms observed to have a sudden commencement (sc) at ten or more observatories. We omitted six storms that appeared clearly to be members of prominent M-sequences. For the remaining 38 storms we computed the pattern of 5303 intensity, shown by line (a) in figure 7. The average intensity was determined from six-month averages weighted by the number of sc-storms occurring in that six-month period. As figure 7 shows, nonrecurrent sc-storms apparently tend to be associated with above-average intensity of 5303 emission around the central meridian of the sun, but no clear time lag can be determined from our graph. The width of the maximum may perhaps arise from the tendency of sporadic storms to be associated with flares; the flares presumably occur in C-regions which need not be at the central meridian of the sun.

We also selected nine of the more prominent recurrence sequences, which gave 58 M-storm epochs, with the zero day defined by the onset

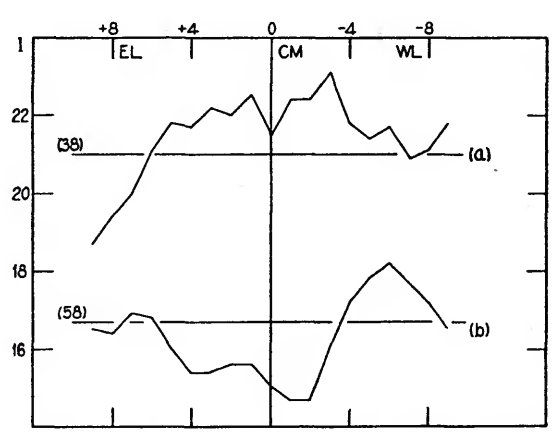

FIGURE 7.—Mean pattern of 5303 intensity at various positions on the solar disk: at times of sporadic sc-storms, line (a); of M-sequence storms, line (b).

of the storm. Figure 7, line (b), shows the resulting average distribution of 5303 intensity on the sun. M-type storms tend to be preceded by a minimum in 5303 intensity on the central meridian of the sun 1–2 days before the onset of the storm. The intensity of 5303 crossing the central meridian is below average from 3 days before to 5 days after the onset of the storm. Since each storm is represented only once, the time lag here should be rather precisely defined. The intensity is above its mean 4–9 days before the onset of the storms and drops quite sharply, a drop that corresponds to the relatively sharp if not "sudden" onset of the storm. Indeed the shape of the curve, inverted, resembles an M-storm profile.

We conclude that in the period covered by this investigation, nonrecurrent sc-storms tend to be associated with bright or at least moderately bright 5303 emission and not with weak 5303 areas. However, more C-regions appear to inhibit storms than to produce them. On the other hand, M-regions seem to be associated with regions of weak 5303 corona, with a lag of 1–2 days between CMP of the weak coronal region and the onset of the storm.

Heliographic latitude of the earth.—In the introduction, we mentioned the well-known tendency of aurorae and geomagnetic storms, especially the recurrent storms, to be most intense around March and September. No satisfactory explanation of these seasonal effects has been given, but most attempts associate the maxima in geomagnetic disturbance either with the equinoxes (i. e., with the geographic latitude of the sun), or with the heliographic latitude of the earth. Following the terminology of Bartels (1932) we may call these explanations equinoctial and axial, respectively. In this paper we consider primarily the axial hypothesis, since it is the more susceptible to investigation with our data and, we believe, is the more plausible.

Because the plane of the earth's orbit is inclined 7.2° to the solar equator, the heliographic latitude of the earth varies from 7.2° north of the solar equator about September 7, to 7.2° south of the solar equator about March 5. Thus we see a maximum area of the sun's northern hemisphere in September and a maximum area of the southern hemisphere in March, at approximately the times of greatest geomagnetic activity. The geomagnetic activity tends to be at a minimum around the times when the earth is crossing the heliographic equator. Apparently solar corpuscles intercept the earth more readily when the earth is farthest removed from the equatorial plane of the sun. On the other hand, the geomagnetic maxima and minima appear to lag behind and to fall closer to the equinoxes and solstices than to the axial parameters (Bartels, 1932).

The usual axial explanation is based on the fact that spots occur most frequently in heliographic latitudes 10–15° while the equatorial belt contains few spots. If the corpuscular streams start from the spot belts and leave the solar surface in a radial direction, corpuscles from the northern and southern belts are most likely to intercept the earth in September and March respectively. However, as we shall discuss later, a relation with the latitude of maximum spottedness is not the only possibility for an axial explanation.

The March and September maxima in geomagnetic activity have not been adequately investigated. Bartels (1932) studied the relation between facular area in the northern and southern hemispheres and geomagnetism. His results offered no support to an axial interpretation. Since he used only monthly means of facular areas and of the geomagnetic index, however, his results are not necessarily significant. The effect of the heliographic latitude of the earth in relation to active centers on the sun has not, so far as we are aware, been studied on a daily basis. We made an exploratory study of the problem from two directions.

Active centers or C-regions.—We had recorded, on the original IBM cards, the latitude of the brightest single 5303 intensity for the day. The value of this latitude we took to indicate whether the associated C-region was located in the northern or in the southern solar hemisphere. When two C-regions occurred simultaneously, one on either side of the equator, we disregarded the region with the weaker maximum; days with maxima of equal intensity in north and south were omitted.

We designated as "favorable" (f) those C-regions on the same side of the solar equator as the earth, and as "unfavorable" (u) those

C-regions on the opposite side of the solar equator from the earth. Using approximately the 20 percent highest intensities in each time interval to indicate C-regions, we subdivided the data into the following groups:

1f.	(South)	1 Feb. 1950– 6 Jun. 1950,
		8 Dec. 1950– 6 Jun. 1951.
1u.	(North)	1 Feb. 1950– 6 Jun. 1950,
		8 Dec. 1950– 6 Jun. 1951.
2f.	(North)	7 Jun. 1950– 7 Dec. 1950,
		7 Jun. 1951– 7 Dec. 1951.
2u.	(South)	7 Jun. 1950– 7 Dec. 1950,
		7 Jun. 1951– 7 Dec. 1951.
3f.	(South)	8 Dec. 1951– 6 Jun. 1952,
		8 Dec. 1952– 6 Jun. 1953.
3u.	(North)	8 Dec. 1951– 6 Jun. 1952,
		8 Dec. 1952– 6 Jun. 1953.
4f.	(North)	7 Jun. 1952– 7 Dec. 1952,
		7 Jun. 1953–15 Oct. 1953.
4u.	(South)	7 Jun. 1952– 7 Dec. 1952,
		7 Jun. 1953–15 Oct. 1953.

For each group we computed the *Kp*'s for days −4 through +16 around ELP of the C-regions. We computed also the over-all *Kp*'s for the favorable C-regions (1f+2f+3f +4f, 72 cases) and for the unfavorable C-regions (1u+2u+3u+4u, 118 cases). Figure 8 shows the results and reveals a conspicuous difference between the *Kp* curves following ELP of favorably and of unfavorably located C-regions. The unfavorable curve shows only irregular fluctuations without any significant deviations from the mean, but the favorable curve shows a clear and fairly symmetric minimum on day 10. This minimum is similar

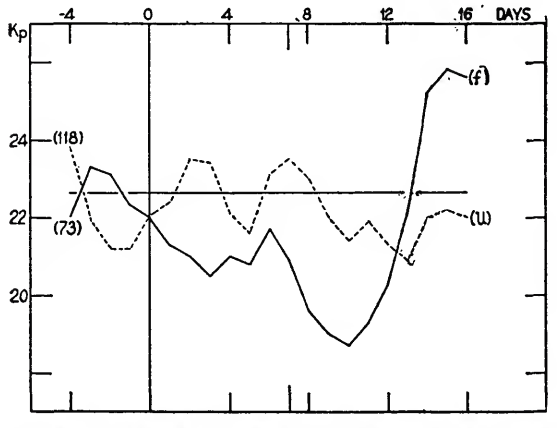

FIGURE 8.—Mean *Kp* following ELP of favorably (solid line) and unfavorably (broken line) located regions of bright green-line emission.

to others previously shown except that it is deeper than any other, including that shown when both green and red lines were strong. The *Kp* values on days 8 through 11 are two or more standard errors below the mean. We suggest comparison with figures 1*a*, 2, 4, and 5*a*.

Figure 9*a* shows the four separate curves, as 3-day running means, for the four groups of favorable C-regions; similarly, figure 9*b* shows the curves for the four groups of unfavorable C-regions. These groups of curves may be compared with figures 1*c* and 1*d* with respect to homogeneity, but it should be remembered that the 45 months have been subdivided differently in the two cases so that individual curves are not directly comparable.

In each of the four curves for the favorable C-regions (figure 9*a*) *Kp* is below the mean of its respective period on days 9–11. Figure 9*a* shows a greater homogeneity for the four periods after CMP of the C-regions, and declines in *Kp* of greater magnitude than appear in figure 1*c* where heliographic latitude is not considered. Since figures 9*a* and 9*b* do not involve any interpolated values of the intensity of 5303, they should be less influenced by autocorrelation; therefore, a variation in *Kp* in figure 9*a* should possess greater significance than a variation of equal amplitude in the curves of figure 1*c*. The four curves for the unfavorably located C-regions show very little homogeneity.

We conclude that, at least in the period covered by this investigation, C-regions on the same side of the solar equator as the earth have a greater influence on *Kp* than do C-regions on the opposite side of the solar equator. ELP of such favorably located C-regions tends to be followed by a decline in *Kp* with a minimum on day 10, or three days after CMP; whereas ELP of the unfavorable C-regions shows much less, if any, relation to subsequent *Kp* values. These relationships tend rather strongly to support an axial explanation of the seasonal variation in geomagnetic activity. Certainly such results would appear inexplicable by any equinoctial hypothesis.

M-regions.—From the evidence presented earlier we tentatively concluded that M-regions are associated with CMP of areas in the active

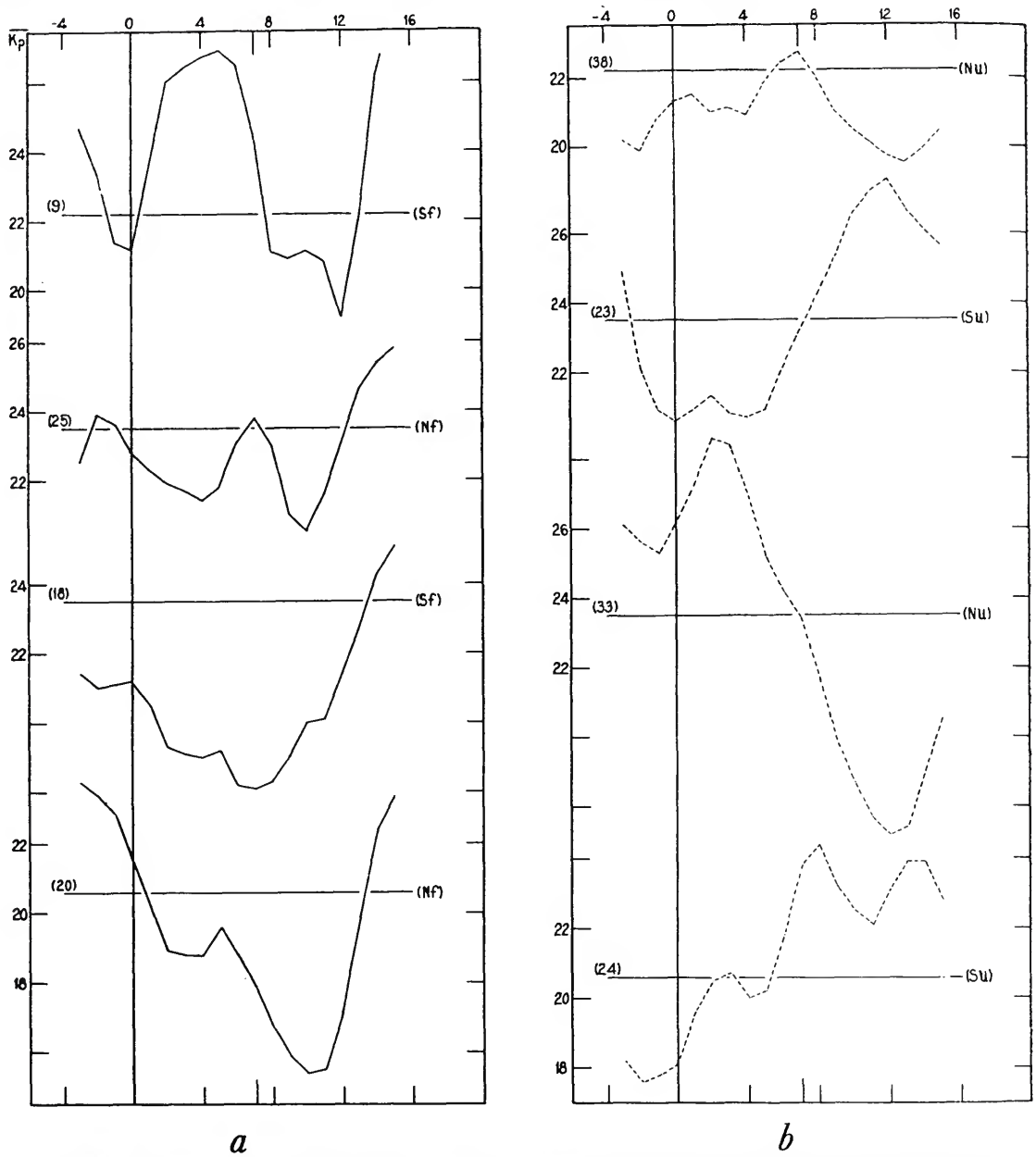

FIGURE 9.—Mean Kp following ELP, for individual time periods, of: *a*, favorable C-regions; *b*, unfavorable C-regions.

zones where the 5303 emission is unusually weak. The data recorded on our IBM cards were not the most suitable for fully exploring this hypothesis if an axial explanation of the semiannual period in geomagnetism is correct. Instead we should need separate intensities for the northern and southern hemispheres. Therefore, to investigate in a preliminary way the effect of heliographic latitude of the earth on M-storms, we calculated the average intensity of 5303 crossing the central meridian, for 5–25°N and for 5–25°S separately, for five days before and three days after the onset of each of the 58 M-storms comprising our nine M-se-

quences. Both east and west limb observations of the 5303 intensity were used. For each M-region we determined the average intensity distribution for each of the nine days, in the favorable and the unfavorable solar hemisphere separately. Inspection of this data (see Bell and Glazer, 1954a, for details) showed that the onset of most of the larger recurrent storms appeared to be associated with a region of weak 5303 intensity in the favorable hemisphere 1–3 days west of the central meridian.

This evidence appeared to indicate that the heliographic latitude of the earth possessed an importance to geomagnetic conditions not previously realized, and suggested that further exploration of the problem by use of separate intensity indices for the northern and the southern solar hemispheres might be fruitful. Such an approach would permit a more adequate study of the effect of the relative heliographic latitude of earth and of strong and/or weak coronal regions than had been possible with our single intensity index. The results are presented in Part II of this paper.

Summary of Part I.—The principal results and conclusions so far reached from a study of 1950–53 data are, in order of their apparent significance, as follows:

CMP of regions of weak 5303 corona tends to be followed 1–3 days later by above-average *Kp* index or by disturbed geomagnetic conditions. This tendency appears clearly in each of the four time periods and is the best established and most clearly significant of our conclusions. Conversely, the onset of magnetic storms of the recurrent type tends to be associated with regions of weak 5303 corona that have passed the central meridian 1–2 days previously. Investigation of individual M-sequences suggests that M-storms may be associated with weak 5303 intensities located on the same side of the solar equator as the earth, and that the semiannual period in geomagnetic activity can best be explained by some sort of axial hypothesis.

CMP of regions of strong 5303 corona tends to be followed 1–4 days later by diminished *Kp*, although the four time-period curves less clearly support this conclusion. The weakening in *Kp* (9–11) appears to be more pronounced if both coronal lines (5303 and 6374) are strong than if only one is strong. The weakening is also greater and more consistently present following CMP of C-regions in the favorable solar hemisphere than after CMP of C-regions in the unfavorable hemisphere. This result again suggests that the heliographic latitude of the earth may be a significant factor in geomagnetic conditions.

CMP of some C-regions appears to be associated with sporadic geomagnetic storms, particularly those C-regions having yellow line emission, and perhaps those having one coronal line strong and the other weak. These conclusions are least well established from our work.

These results suggest that geomagnetic conditions are influenced by corpuscles from two entirely different solar sources. The apparent association between some C-regions and some magnetic storms may be explained most obviously by assuming that some active solar centers, characterized by frequent flares, enhanced radio noise, and 5694 emission, eject corpuscles at high velocities and produce storms directly. These corpuscles we shall hereafter refer to as "active-center corpuscles." The apparent association between M-storms and the weakest 5303 regions, on the other hand, seems to imply some general source of corpuscles, perhaps arising, as Denisse has suggested, by evaporation from the corona over wide areas. The escape of these, which we shall hereafter call "the general solar corpuscles," is apparently inhibited by the presence of active centers.

Further discussion will be postponed until after the presentation of the evidence in the following sections.

Part II. Separate intensity indices for northern and for southern solar hemispheres

The investigation reported in this section covers a period of 47 months, from Jan. 1, 1950, through Dec. 7, 1953. As in Part I, the daily sums of *Kp* are used as the measure of geomagnetic activity. As measures of the 5303 intensity, however, separate daily indices are employed for the northern and the southern solar hemispheres. For the northern index, we have taken the mean of the three highest east-limb intensities north of the equator, while for the southern index we took the mean of the three

highest values south of the equator. Equatorial intensities themselves did not enter into either index. These intensity indices were corrected for plate threshold by the method described previously (Glazer and Bell, 1954). By interpolating between observations we obtained an east-limb index for the north and one for the south for each day; similarly, we obtained a pair of west-limb indices.

For the 6374 line we used as daily indices the mean of the two highest intensities for each solar quadrant. These red line indices were corrected to plate threshold five by the formulae

$$I_c' = I_c + 0.48\,(T_c - 5) \qquad (6)$$
$$I_c' = I_c + 0.43\,(T_c - 5),$$

and slight correction was made of the Climax (I_c) values to the Sac Peak (I_s) scale. We attempted no interpolations for 6374, but did use both Climax and Sac Peak intensities. The intensities of both coronal lines, and values of Kp for days ELP -4 through $+19$ were punched on standard IBM cards.

We divided the data into eight time periods, four with the northern solar hemisphere favorable and four with the southern solar hemisphere favorable. Each period began and ended with the earth's crossing of the solar equator. The periods are as follows:

Spring: Sf, Nu

1 Jan. 1950 – 6 June 1950
8 Dec. 1950 – 6 June 1951
8 Dec. 1951 – 6 June 1952
8 Dec. 1952 – 6 June 1953

Fall: Nf, Su

7 June 1950 – 7 Dec. 1950
7 June 1951 – 7 Dec. 1951
7 June 1952 – 7 Dec. 1952
7 June 1953 – 7 Dec. 1953

Since for each period there was a favorable (f) and an unfavorable (u) hemisphere index, we had 16 groups of data to work with. As before, relative intensities within each group rather than absolute values define the zero days of strong and weak coronal intensity.

The green line.—We computed mean Kp values for days -4 through $+19$ around zero days defined by ELP of the 10 percent, 20–10 percent, and 30–20 percent of the strongest (H) and of the weakest (L) 5303 intensities within each of the eight favorable and the eight unfavorable groups. We first combined these 16 results into four groups, Sf (south favorable), Su, Nf, Nu, and then further combined them into the two groups: f=Nf+Sf, u=Nu+Su. Using west-limb indices we made similar calculations for days -18 through $+5$ around zero days defined by WLP of strong and of weak corona.

Figure 10*a* shows the composite results for bright corona for the entire 47 months. In figure 10*a* and in all subsequent figures, favorable (f) hemisphere curves appear as solid lines, while the unfavorable (u) hemisphere results appear as broken lines. The average value of Kp for the period is 22.4. The dotted lines indicate a distance of two standard errors from the mean. The standard errors (σ') have been increased by about 35 percent over ordinary standard errors to take account of the autocorrelation among the Kp's as discussed in Part I.

Line (a) in figure 10*a* shows that bright corona (10H) on the east limb in the favorable solar hemisphere is followed on days 8–11 by a $Kp \geq 2\sigma'$ below the mean. Bright (10H) corona on the east limb in the unfavorable hemisphere, on the other hand, is followed by no significant deviations from the mean Kp. The minimum in the favorable curve occurs for Kp (10), and lies about 3.5 standard errors (σ') below the mean. This minimum in Kp is substantially deeper and of greater statistical significance than that in figure 1*a* where we took no account of the relative heliographic latitude of earth and bright coronal center. Note also the small rise at Kp (6–7) and a moderate maximum at Kp (14).

Corresponding to figure 10*a*, figure 10*b* shows the Kp's associated with bright 5303 for the spring half-years (Sf, Nu), while figure 10*c* shows those for the autumn half-years (Nf, Su). Figure 11*a–c* shows the average values of Kp preceding WLP of bright 5303 intensities in the favorable and the unfavorable hemispheres.

Since the corona can be observed only at the limbs of the sun, seven days before or seven days after CMP, the intensity of the corona at central meridian passage is necessarily somewhat uncertain. In an effort to minimize the uncertainty we have made a further set of calculations based on simultaneous consideration of the east-limb index and the west-limb index 14 days later. Figure 12*a–c* exhibits the aver-

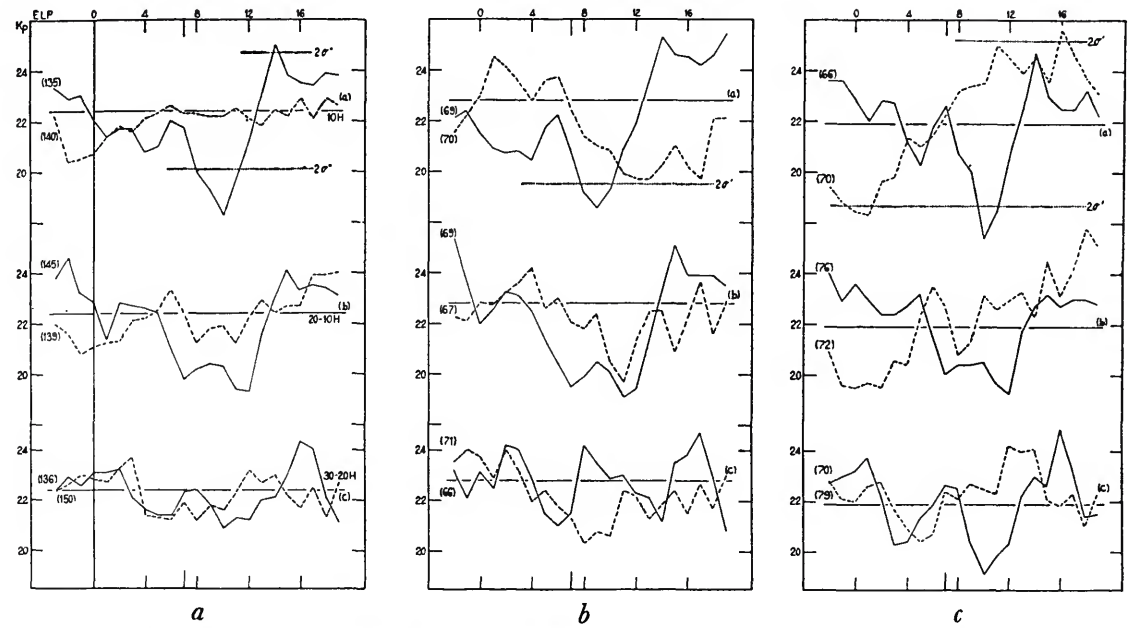

FIGURE 10.—Mean Kp following ELP of strong 5303 intensities in the favorable (solid line) and unfavorable (broken line) hemispheres; line (a) represents the 10 percent strongest intensities (10H), line (b) the 20H—10H, and line (c) the 30H—20H. *a*, Composite results for the 4-year period; *b*, spring half-years; *c*, autumn half-years.

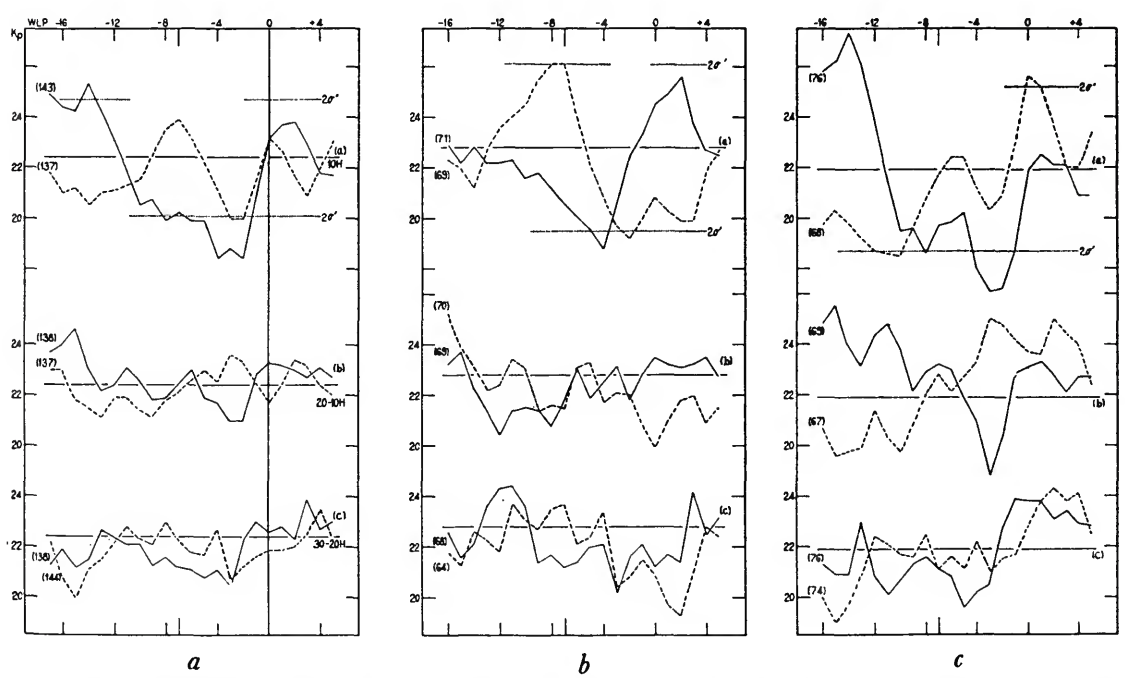

FIGURE 11.—Mean Kp preceding WLP of strong 5303 intensities in the favorable (solid line) and unfavorable (broken line) hemispheres; line (a) represents the 10 percent strongest intensities (10H), line (b) the 20H—10H, and line (c) the 30H—20H. *a*, Composite results for the 4-year period; *b*, spring half-years; *c*, autumn half-years.

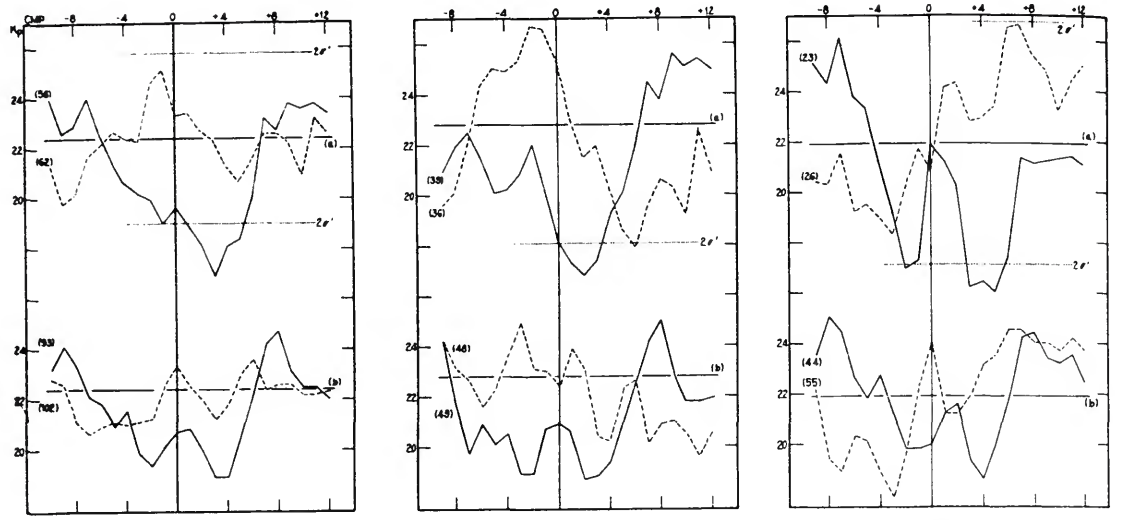

FIGURE 12.—Mean *Kp* associated with CMP of regions bright in 5303 intensity at both limb passages, in favorable (solid line) and unfavorable (broken line) hemispheres; line (a) represents regions with the 10 percent strongest intensities (10H) at ELP and at WLP; line (b) represents 20H (E and W) minus 10H (E and W). *a*, Composite results for the 4-year period; *b*, spring half-years; *c*, autumn half-years.

age values of *Kp* associated with CMP of regions that appeared bright in 5303 at ELP and bright also at WLP 14 days later. We can feel more confident that these regions were actually strong at CMP than we can of the regions used in figures 10 and 11. Note that the minima in the favorable curve around *Kp* (10) are deeper; because of the reduced sample size, however, they have no greater statistical significance than those shown in figures 10 and 11.

Since the regular appearance of any effect in independent samples forms an important test of the significance of any superposed epoch result, in figure 13*a*, *b*, we give the 10H results for the individual half-years. A greater number of days are plotted in connection with east-limb corona because only east-limb observations can be of practical use to forecasters. The others are of interest, however, in any attempt to understand the physical significance of the results.

Inspection of figures 10–13 indicates that CMP of bright corona located in the favorable solar hemisphere appears to be associated with the following *Kp* tendencies, listed in order of apparent significance:

The minimum in *Kp* around three days after CMP of Hf corona is the most conspicuous effect and occurs with convincing uniformity and regularity. The minimum exceeds $2\sigma'$ on all nine of the 10Hf curves of figures 10–12, and occurs in 30 out of 32 of the curves in figure 13*a*, *b*. The improvement in regularity compared with that in figure 1*c* is striking.

Kp tends to be somewhat above the mean around day 14 in most but not all of the Hf curves. Whether this reflects a tendency of corpuscles to concentrate at the edge of a region of deficiency, or a tendency of the magnetic field of the earth to react more strongly to an average supply of corpuscles after a dearth, cannot be decided without more understanding of the mechanism of geomagnetic storms. However, because of the general tendency of *Kp* to rise rapidly and decline more slowly, we incline to the second explanation.

A small rise in *Kp* is often but not always present around CMP of bright regions, days 6–8. As stated in Part I, we ascribe this rise to the storm-producing active centers, which in this phase of the solar cycle are substantially fewer than the number of inhibiting centers.

In the unfavorable hemisphere curves we see

no systematic trends. In the spring (Nu) *Kp* tends to be below the mean after CMP, whereas in the fall (Su) *Kp* tends to be above the mean after CMP of bright corona. Because of this inconsistency we conclude that our data do not indicate any systematic relation between Hu 5303 and *Kp*.

It is possible that such minima as do occasionally appear may result from the chance occurrence of days common to both the favorable and the unfavorable samples. This possibility is especially likely in the spring of 1953. The Nu curve shows a marked minimum in *Kp* around CMP; in this period, however, the only major active centers, N and S, lie within a few degrees of longitude of one another, so that bright Nu corona would inevitably appear to "produce" a minimum in *Kp* even though the Sf bright regions were the actual cause of the minimum. Investigating this possibility further, we found that for ELP of 10H, 22 (31 percent) Nu were included in Sf samples while only 8 (11 percent) Su were included in Nf samples. Of the eight periods, only two, 1950 (spring half) with nine cases and 1953 (spring half) with seven cases, had more than four days common to both favorable and unfavorable samples. In view of Becker's (1953) findings with paired sunspots, it is of interest to note that the depth of minima in *Kp* following CMP of strong favorable corona shows no apparent relation to the number of paired coronal maxima entering the sample.

Kp conditions that appear to be associated with CMP of faint 5303 corona are exhibited in detail in figures 14–17. Figure 14*a–c* shows the average values of *Kp* following ELP of faint (L) 5303 intensities in the favorable and unfavorable solar hemispheres. The top curve of figure 14*a* shows that faint corona on the east limb in the favorable solar hemisphere is followed on days 8–12 by a $Kp \geq 2\sigma'$ above the mean. The maximum occurs for *Kp* (9), which lies about 4.5 standard errors (σ') above the mean. This maximum in *Kp* is only slightly greater than that in figure 1*b*, where we took no account of favorable and unfavorable hemispheres. Although the improvement is only minor it appears entirely compatible with the existence of a hemisphere effect when we recall that a faint 5303 intensity defined by the index used in Part I necessarily indicated faint 5303 corona in both the favorable and unfavorable solar hemispheres. Moreover only a slight rise in *Kp* appears to follow CMP of faint 5303 regions located in the unfavorable solar hemisphere.

Figure 15*a–c* shows the average values of *Kp* preceding WLP of weak 5303 intensities from the favorable and the unfavorable west-limb indices. Here also we have attempted to minimize the uncertainty regarding the intensity of the 5303 line at central meridian by making a set of calculations based on simultaneous consideration of the east-limb index and the west-limb index 14 days later. Figure 16*a–c* shows the average values of *Kp* associated with CMP of regions that appeared faint in 5303 at ELP and faint also at WLP 14 days later. These are the regions that we can feel most certainly were actually faint at CMP. As in the case of the bright 5303 corona, the principal effect in *Kp*—but not its statistical significance—is enhanced by considering E and W indices simultaneously. The rise in *Kp* following CMP of unfavorable faint 5303 is also increased but continues to be less than for the favorable corona. Moreover, the two-standard-error bands in figure 16*a* and 16*c* apply only to the favorable curves; because the unfavorable samples are smaller, their standard errors would be larger.

Figure 17*a*, *b*, exhibits the 10L results for the individual half-years. The rise in *Kp* following CMP of faint 5303 corona in the favorable solar hemisphere appears with convincing regularity in the curves of figures 14–17. The one exception occurs in the spring of 1950 (top curves, figure 17*a*); this period is also distinguished from the other seven by an absence of any clear recurrent-storm sequences. Therefore the failure of the relation in the spring of 1950 can be readily understood in the light of our previous finding (figure 7) that only recurrent or M-type storms are associated with regions of faint 5303 corona. For this reason it might appear justifiable to remove 1950 Sf from the composite spring curves; when this is done the maximum in figure 16*b* rises to 30.6 (at day 10) with a mean of 23.7, as contrasted with the values shown of 27.6 and 22.8. Other curves would be similarly improved and the apparent inferiority of the Sf curves relative to Nf would be largely eliminated. If this explanation of the failure in 1950 Sf is correct, we should expect the relation of figures 14–17 to hold only at times of M-region activity; that is, primarily on the declining side of the solar activity cycle.

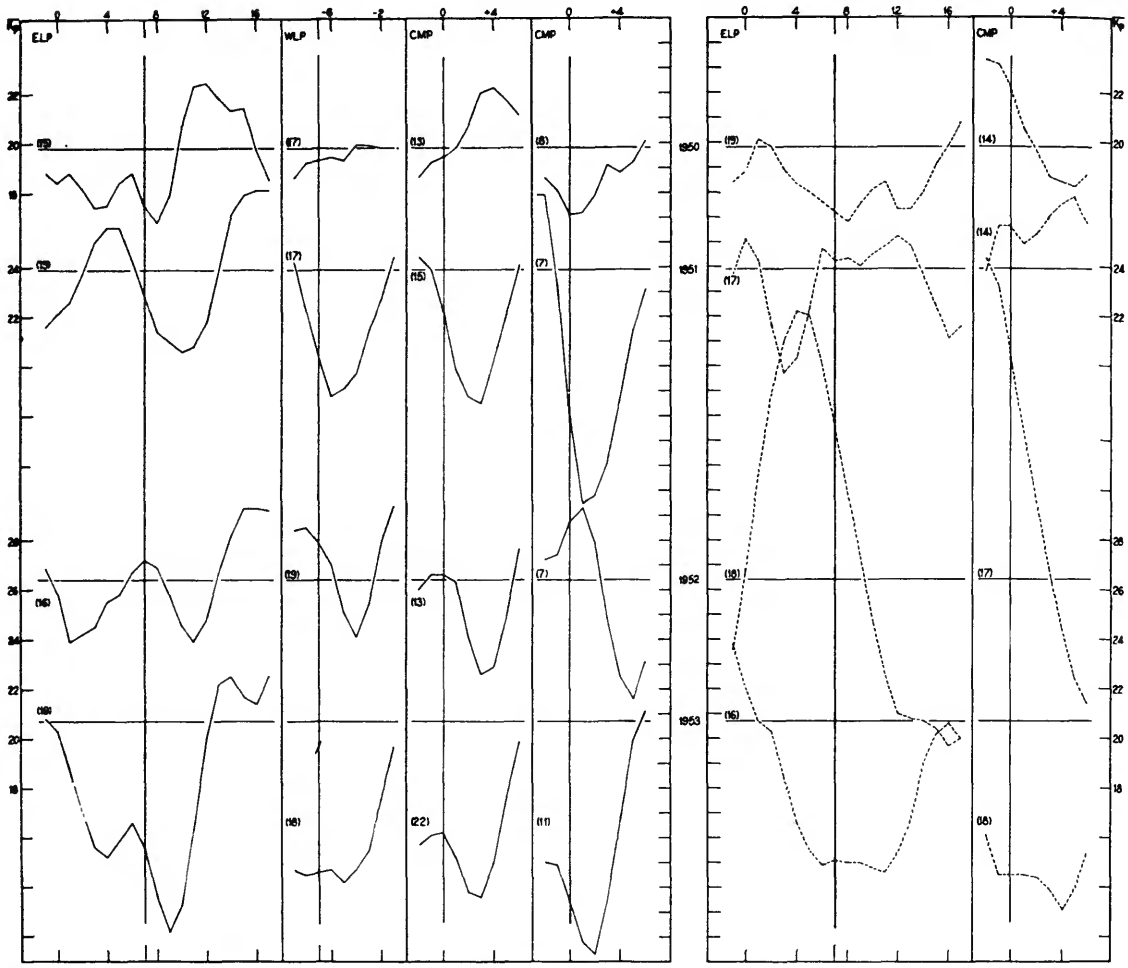

FIGURE 13.—Mean *Kp* associated with various circumstances of bright 5303 intensities for individual half-years. Columns from left to right are 3-day running means of *Kp* associated with: ELP of the 10 percent strongest intensities in the favorable hemisphere (10Hf); WLP of 10Hf; 10Hf at ELP or WLP, with 20Hf at the other limb; 10Hf at both ELP and WLP; ELP of the 10 percent strongest in the unfavorable hemisphere (10Hu); and 10Hu at ELP or WLP, with 20Hu at the other limb. *a*, Spring half-years; *b* (on facing page), autumn half-years.

While the unfavorable curves do show some tendency to a rise in *Kp* after CMP of faint 5303, this rise is always less than in the corresponding favorable curve; moreover the tendency is only irregularly present in the eight half-years. We therefore conclude that there is no clear relation between *Kp* and weak 5303 corona in the unfavorable solar hemisphere.

Table 2 shows the number of cases common to the favorable and the unfavorable ELP samples in figures 13 and 17.

TABLE 2.—*Number of cases common to f and u samples.*

Figure	1950	1951	1952	1953
13*a*	9	4	2	7
13*b*	2	2	4	0
17*a*	2	9	3	1
17*b*	6	2	2	9

The possible effect on *Kp* of similar coronal conditions in both favorable and unfavorable solar hemispheres has a special interest because of the findings of Becker (1953) and of Becker and Denisse (1954). We have already mentioned that we computed *Kp* following ELP of

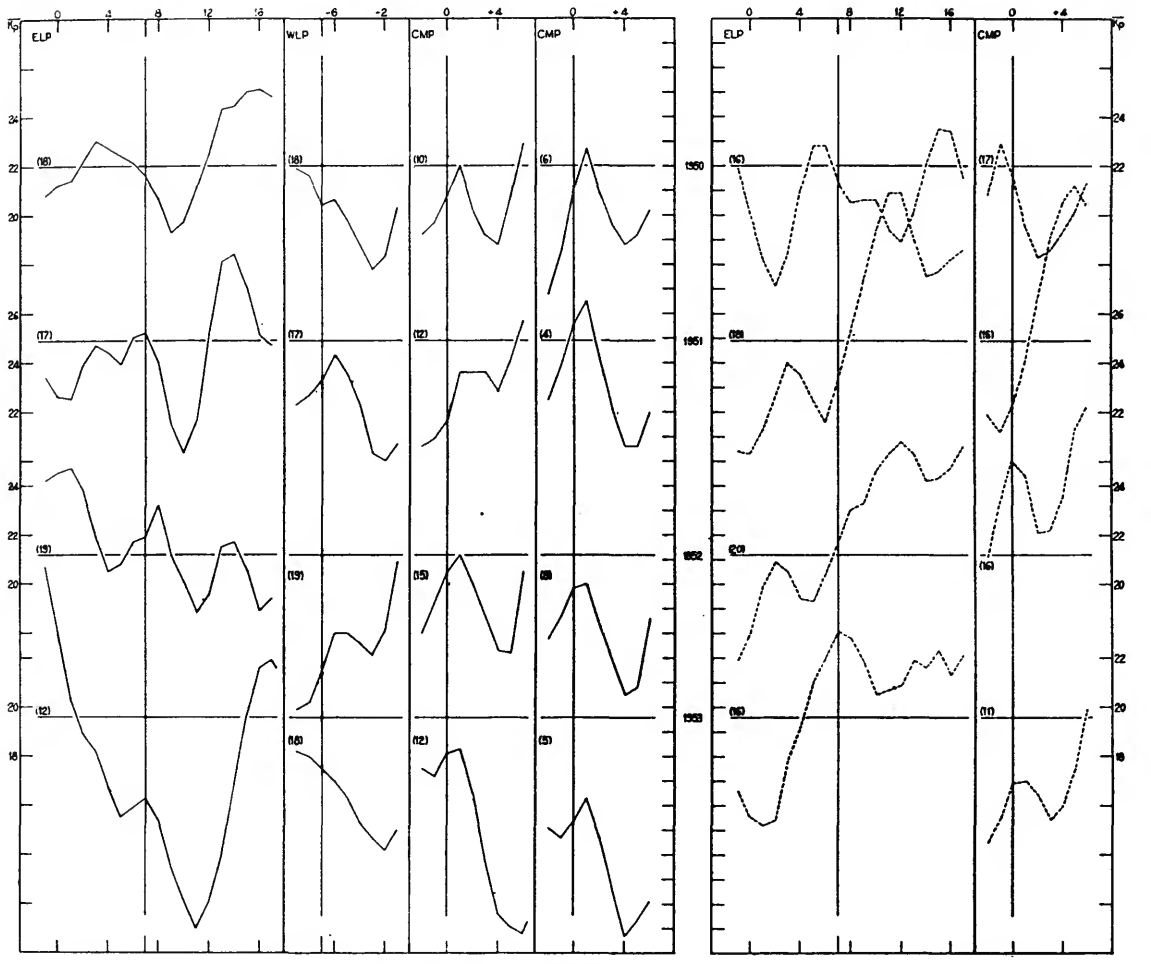

FIGURE 13*b*.—See explanation on facing page.

regions having 10Hf and 10Hu simultaneously; this did not notably deepen the minimum in *Kp*, and because of the small sample sizes the curves were conspicuously irregular. To work with somewhat larger samples, Sf cards were divided into three groups: 30H, 40M, and 20L (note: 30–20L omitted). The *Kp's* computed from these groups form the top row of curves in figure 18*a*. Each of these three groups was divided into three parts (Nu 30H, 40M, 20L) and the associated *Kp*'s were computed for each combination of Sf-Nu, as shown in figure 18*a*. The first column shows the three Nu-groups independently. A similar treatment of Nf, Su indices produced the results shown in figure 18*b*, which indicate that, insofar as *Kp* depends on 5303 intensity during the four autumn seasons covered by our study, *Kp* depended mainly on the Nf intensity and not perceptibly on the Su. No statistically significant differences appear among the curves in any given column; and the curves change along the rows in the manner to be expected under conditions of Nf dominance. In figure 18*a*, on the other hand, the situation is less clear, and there does appear some indication that Sf is more effective in giving the "expected" *Kp* results when paired with a similar Nu. The data appear to suggest that the northern solar hemisphere may have a more powerful "control" over *Kp* conditions than the southern; but in view of the short time

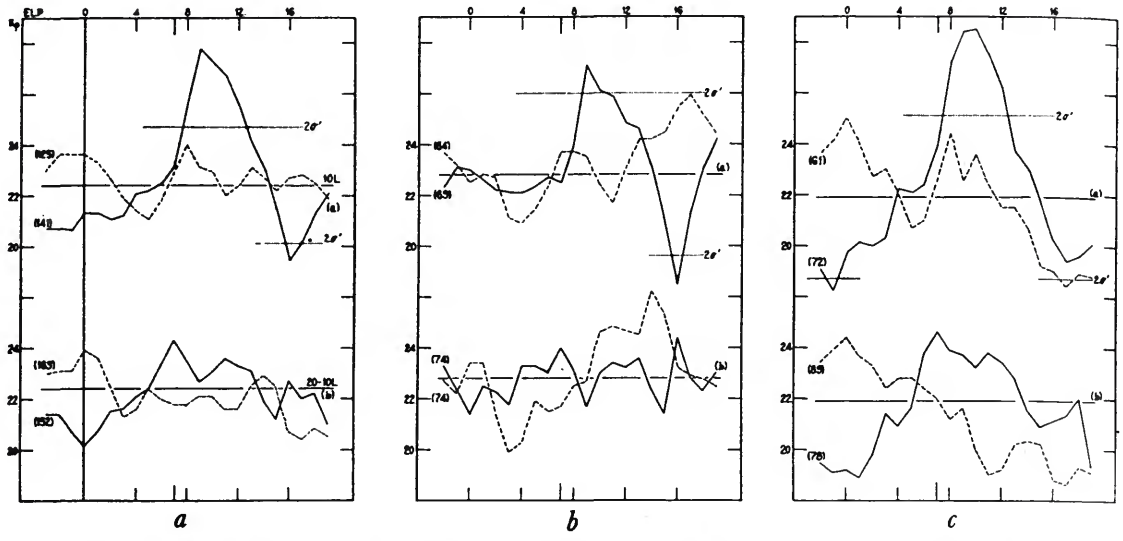

FIGURE 14.—Mean Kp following ELP of weak 5303 intensities in the favorable (solid line) and unfavorable (broken line) hemispheres; line (a) represents the 10 percent weakest intensities (10L); line (b) the 20L—10L. *a*, Composite results for the 4-year period; *b*, spring half-years; *c*, autumn half-years.

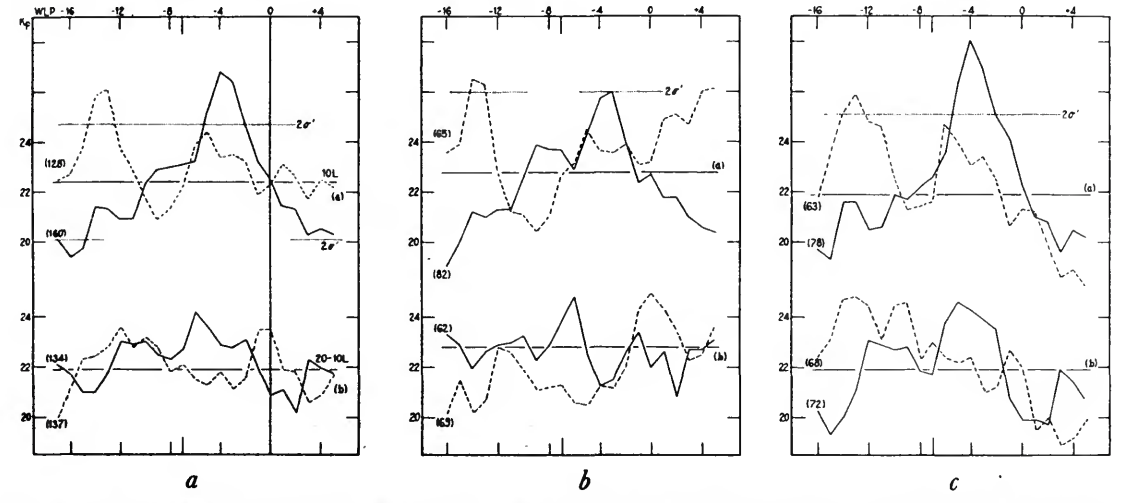

FIGURE 15.—Mean Kp preceding WLP of weak 5303 intensities in the favorable (solid line) and unfavorable (broken line) hemispheres; line (a) represents the 10 percent weakest intensities (10L), and line (b) the 20L—10L. *a*, Composite results for the 4-year period; *b*, spring half-years; *c*, autumn half-years.

covered, we would not propose that such an inherently unlikely suggestion be taken too seriously. Nor indeed should the apparent effect be regarded as real without further observational study.

As in Part I, we computed the frequency distribution of Kp associated with CMP of various conditions in the 5303 corona. Here we used the sum of the east-limb and west-limb indices as the measure of 5303 intensity. We omitted the spring of 1950 from these calculations in order to obtain samples more homogeneous with respect to M-region activity, as mentioned above. Figure 19*a*, *b* shows the fractions of strong corona and the fractions of weak corona in the favorable and unfavorable solar hemispheres separately, each associated with $Kp>30$ and with $Kp\leq 12$. The broken

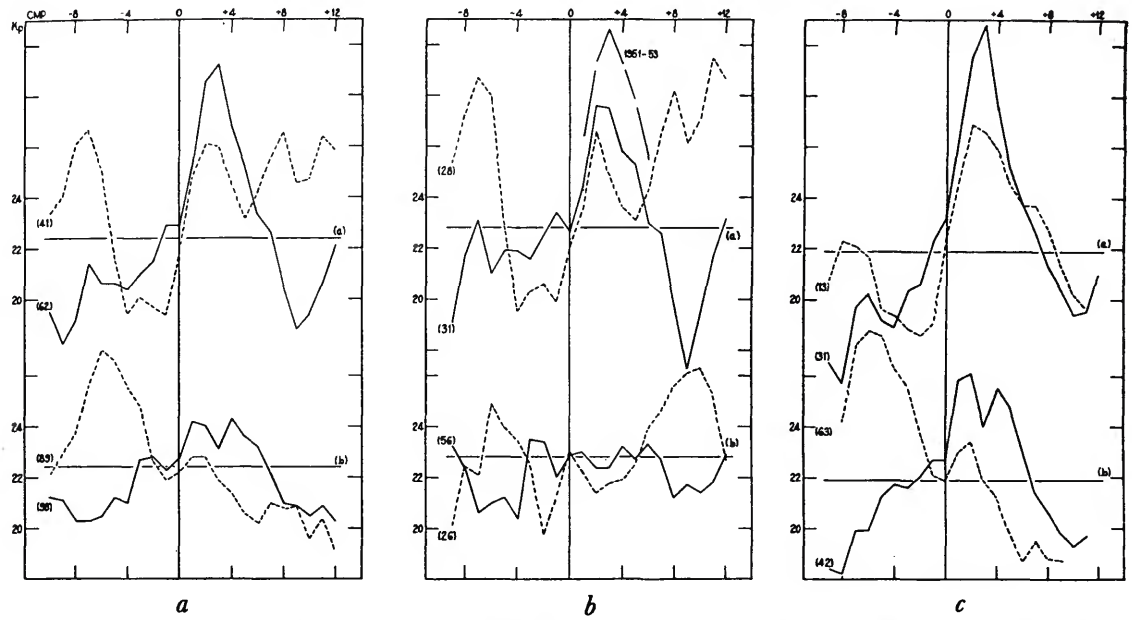

FIGURE 16.—Mean Kp associated with CMP of regions weak in 5303 at both limb passages, in favorable (solid line) and unfavorable (broken line) hemispheres; line (a) represents regions with the 10 percent weakest intensities (10L) at ELP and at WLP; line (b) represents 20L (E and W) minus 10L (E and W). *a*, Composite results for the 4-year period; *b*, spring half-years; c, autumn half-years.

line indicates the "expected fraction" of strong and weak intensities of 5303 that should be followed by high (or low) Kp if the 5303 intensity and Kp were completely independent. The results agree well with those found by the previous method, and serve further to assure us that they do not arise from domination of the curves by a small number of extreme values.

The coefficient of correlation between Kp and east-limb 5303 intensity in the favorable and the unfavorable solar hemispheres was computed by the procedure described in Part I. Figure 20 shows the resulting correlograms and may be compared with figure 3. Around Kp (10) we have indicated the correlations resulting when 1950-Sf is removed. The largest correlations occur in the favorable curves, on day 10, and amount to −0.26 for Nf, −0.20 for Sf (1951–53), and −0.23 for the composite f (omitting 1950-Sf), with about 720, 550, and 1270 cases, respectively. Very similar curves are obtained if we correlate Kp with the sum of the east and west indices; each coefficient at Kp (10) is increased by about 0.01 over the value obtained from east-limb intensities alone.

Figure 21 illustrates the behavior of mean Kp's associated with the entire range of intensity percentiles for the more significant groups of days. We calculated the average Kp associated with the percentiles 0–10 (low), 10–20, 20–50, 50–70, 70–85, and 85–100 (high) of 5303 intensities using days (4, 5, 6), (9, 10, 11), and (14, 15, 16).

The graphs for days (4, 5, 6) reveal no notable trends, as one would expect from the low correlations shown in figure 20; those for days (14, 15, 16) show a slight rise in mean Kp with increasing intensity of 5303. For days (9, 10, 11) the averages of Kp might appear to be more closely related to the intensity in the favorable hemisphere than the correlations of only about −0.2 would suggest. However one should bear in mind two facts. First, the scatter of the points around the respective mean values is not shown; and the standard errors of the groups of Kp's, while almost equal for each intensity interval (homoscedastic), are not very much less than the standard deviation of all Kp's regardless of 5303 intensity. Also if one examines the Kp's associated with the low intensities, the sharp drop (nonlinear)

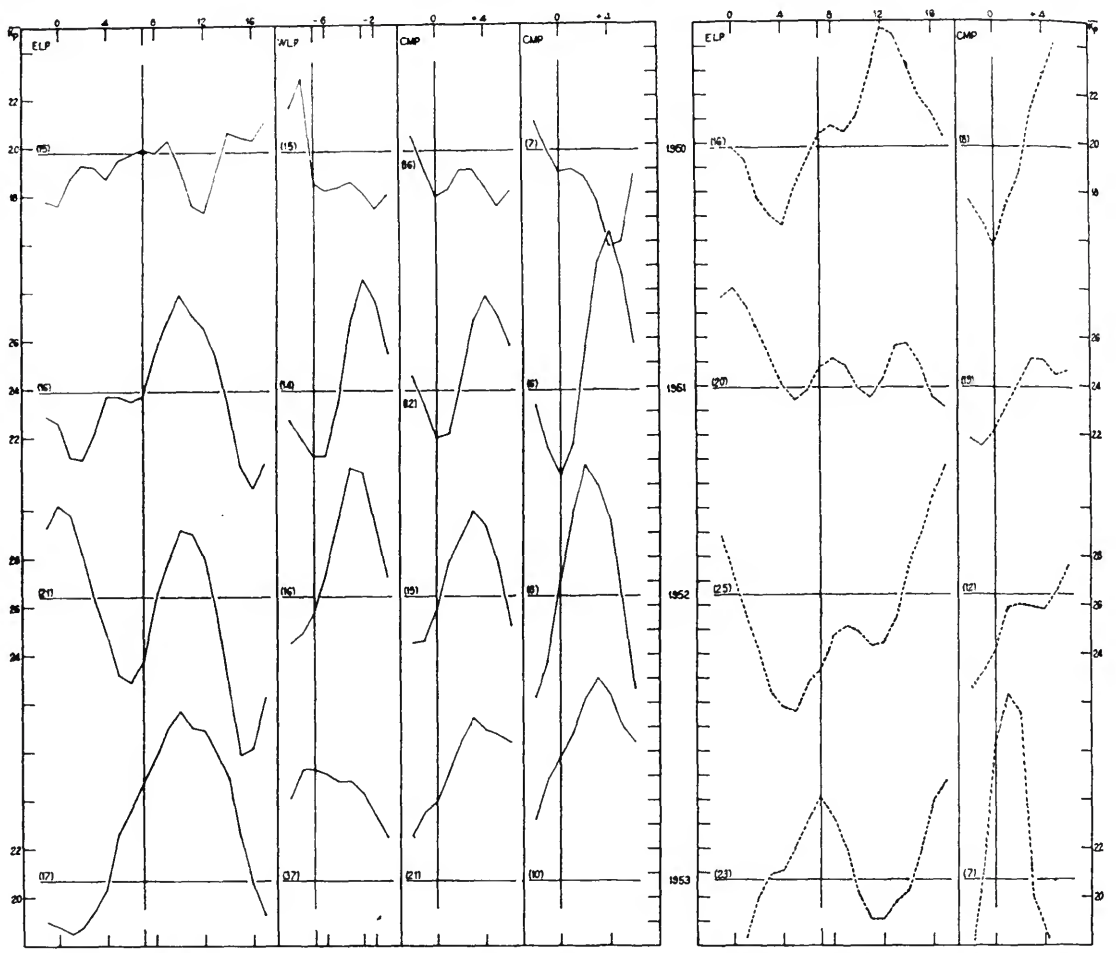

FIGURE 17.—Mean *Kp* associated with various circumstances of faint 5303 intensities for individual half-years. The columns from left to right are 3-day running means of *Kp* associated with: ELP of the 10 percent weakest intensities in the favorable hemisphere (10Lf); WLP of 10Lf; 10Lf at ELP or WLP, with 20Lf at the other limb; 10Lf at both ELP and WLP; ELP of the 10 percent weakest in the unfavorable hemisphere (10Lu); and 10Lu at ELP or at WLP, with 20Lu at the other limb. *a*, Spring half-years; *b* (on facing page), autumn half-years.

in mean *Kp* from the 10L to the next decile would tend to decrease the coefficient of linear correlation. In any case the results for *Kp* (9, 10, 11) agree with those previously obtained: *Kp* extremes are inversely associated with coronal extremes, whereas intermediate intensities are at most very slightly related to *Kp*.

These results are purely statistical in nature and no physical connection can be established between two phenomena by statistical means alone. On the other hand, figures 10–17 do, we believe, show several trends which might be expected if a physical connection did exist between *Kp* and the intensity of the 5303 corona in the favorable solar hemisphere:

1. Minima and maxima in *Kp* are, in every sample, more pronounced following CMP of favorable regions than of unfavorable regions.

2. In each of the figures 10–12, the 10 percent highest indices show the greatest negative *Kp* effect; these minima at *Kp*(10) are always deeper than those of 20H–10H, the second decile. Similarly, in each of the figures 14–16,

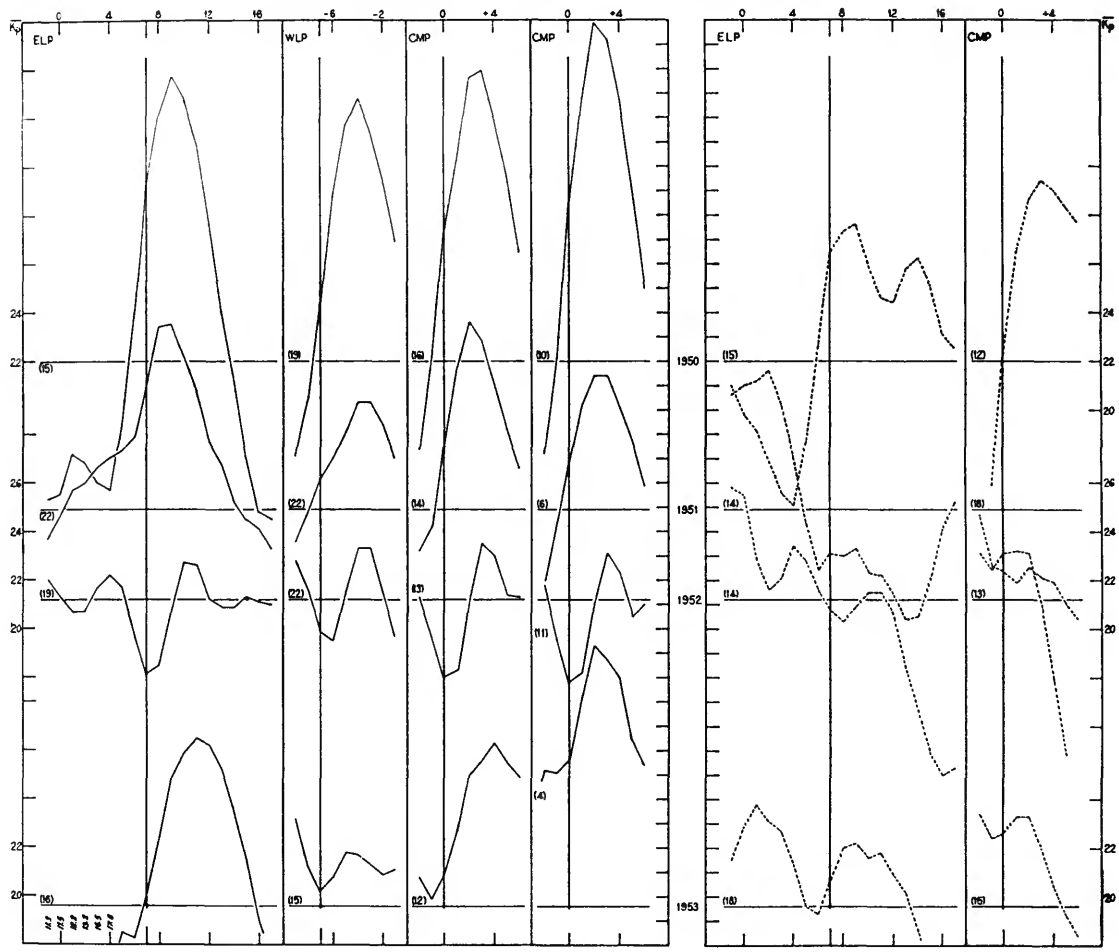

FIGURE 17*b*.—See explanation on facing page.

the 10 percent faintest 5303 show the greatest positive effect; these maxima at *Kp*(9–10) are always higher than those of the second decile.

3. The deepest *Kp* minima result when we employ both east and west indices to select coronal regions most certainly bright at central meridian. Similarly, the strongest *Kp* maxima result when we use both indices to select regions most certainly weak in 5303 at central meridian.

4. The principal *Kp* variations occur at a reasonable time interval, 2–4 days, after central meridian passage of the apparently associated coronal region.

Hemisphere versus angular distance.—The above results lead to a further important question: Is the contrast between favorable and unfavorable solar hemispheres, in regard to the apparent effect of 5303 intensity on *Kp*, merely a hemisphere effect in which the solar equator acts as some sort of barrier to the movement of solar corpuscles? Or is the angular distance between the earth and the bright coronal region significant?

To explore this question we used the latitude of the maximum intensity as an indicator of the position of the solar center. (Dr. Yü has informed us that Sacramento Peak line intensities contain a zero point error of about 5° in position angle; in determining latitudes of intensity maxima for Sacramento Peak 5303 we have therefore assumed the solar equator to lie at the solar position angles published as 95° and

422953—57——3

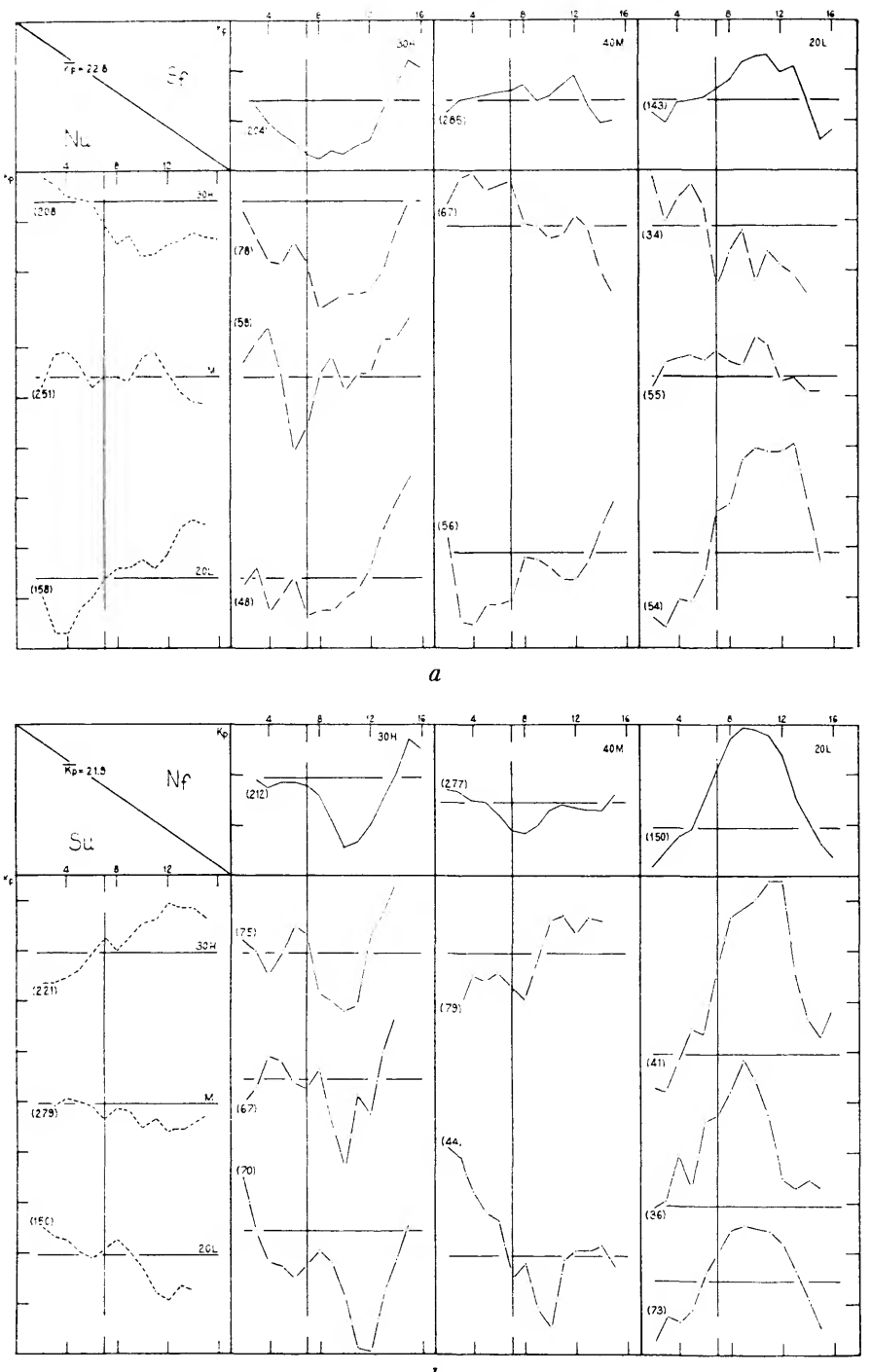

FIGURE 18.—Mean *Kp* following ELP of various combinations of 5303 intensities in the favorable and unfavorable hemispheres; curves in top row are for favorable hemisphere alone; those in left column are for unfavorable alone. *a*, Spring half-years; *b*, autumn half-years.

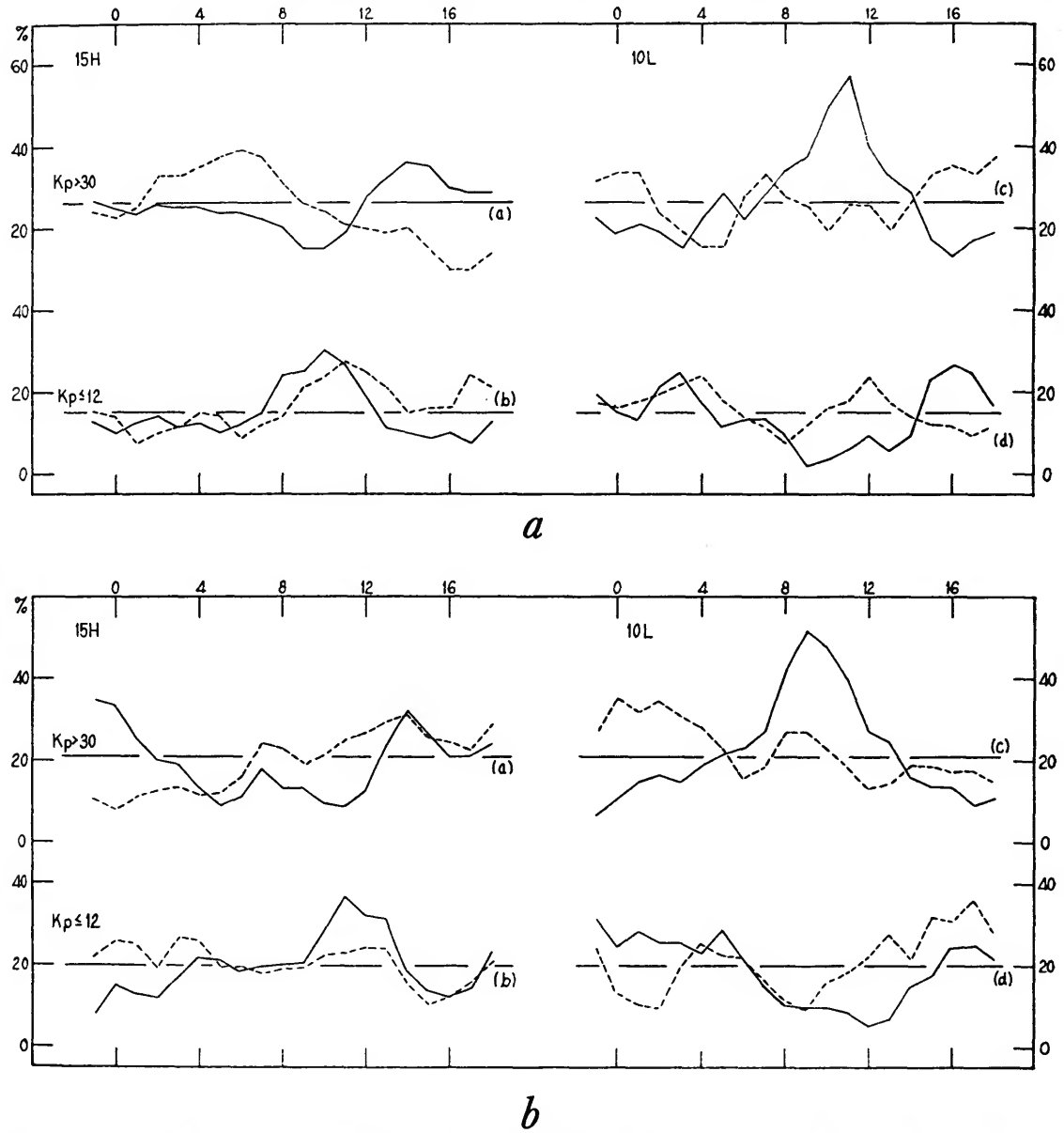

FIGURE 19.—Fractions of strong and weak 5303 intensities in the favorable and unfavorable hemispheres, associated with high and low Kp's. Curves at left show fractions of strong corona (15H) associated with $Kp>30$, top line, and $Kp\leq 12$, bottom line. Curves at right show fractions of weak corona (10L) associated with $Kp>30$, top line, and $Kp\leq 12$, bottom line. *a*, Spring half-years; *b*, autumn half-years.

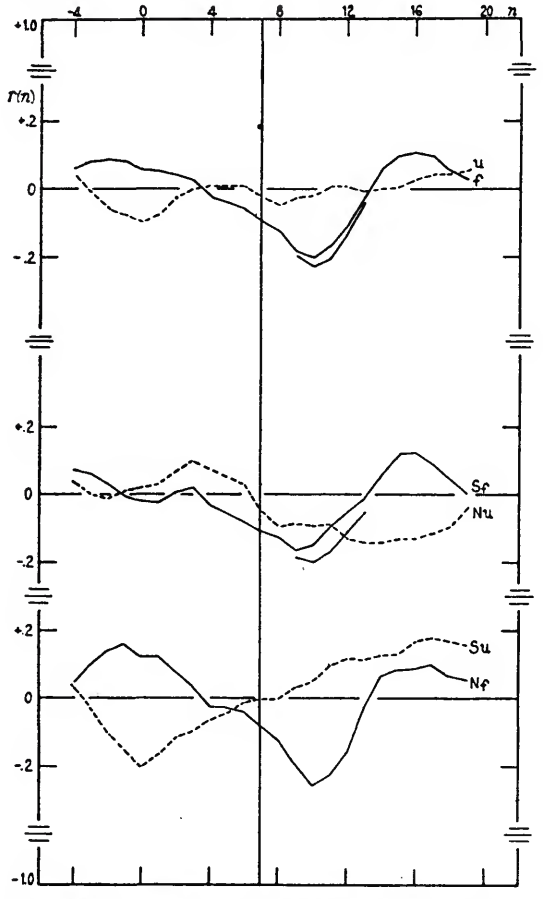

FIGURE 20.—Coefficients of correlation between 5303 intensity and *Kp*, with lags in *Kp* of −4 to +19 days after coronal ELP in favorable (solid line) and unfavorable (broken line) hemispheres, for the 4-year period (top), the spring half-years (middle), and the autumn half-years (bottom).

275°.) The days of 5303 intensity 20H, favorable and unfavorable separately, were divided into groups according to the location of the maximal intensity at 5°, 10°, 15°, 20°, ≥25°, from the solar equator. Those that had no maximum on the relevant side of the equator formed a further group, "O." For each latitude group the associated *Kp* values were computed in the usual way. Since we did not interpolate latitudes of maximal intensity, only days with an actual observation at Sac Peak or Climax are included. Therefore the east-limb and west-limb results here are based on completely independent observations, as is not altogether true when interpolated values are used.

Figure 22*a–c* shows the results from east-limb indices, while those from west-limb indices appear in figure 23*a–c*. The curves are the average *Kp*'s associated with 20H indices centered at 5° intervals of solar latitude. Some of the 25-degree curves are lacking, due to the very small size of the sample. The mean line for each curve has been computed from the mean *Kp*'s for the 8 half-years, weighted by the number of cases occurring in each half-year.

In these figures the average latitude of the earth may be taken as 3–4° f. Accordingly, if the *Kp*-minima around day 10 depend on the angular distance between the earth and coronal center, we should expect the largest dip in *Kp* at 5° f, with the effect diminishing about equally at increasing angular distances above and below this position. On the other hand, if the hemisphere effect arises from some sort of equatorial barrier, we should expect no systematic trends within the f-group, nor within the u-group, but only a difference between the two groups. The evidence appears to favor the second alternative.

More exactly, of course, the position of the earth varies by about 7° over a half-year. The latitude range covered by the solar centers (5–25°) is much greater than 7°, however, so that unless this procedure were to give evidence in favor of the angular-distance hypothesis, no more detailed attention to the position of the earth would appear worthwhile. Actually the figures provide no indication that the angular distance between the earth and the maximum 5303 intensity plays a significant role in the magnitude of the associated *Kp*-dip. Coronal maxima at 5°f appear no more favorable than those at 20° or 25°f; and maxima at 5°u appear, if anything, more unfavorable than those at 20° or 25°u. Analogous calculations for 10H and for 30H gave results very similar to those shown for 20H. It is relevant further to note that one of the first really bright 5303 centers of the new cycle, located at 35°Nf, appeared to be associated with the very low *Kp* observed on Oct. 12, 1954. We conclude that the relative location of the solar equator, rather than the angular distance between solar region and earth, is the significant factor in the hemisphere effect.

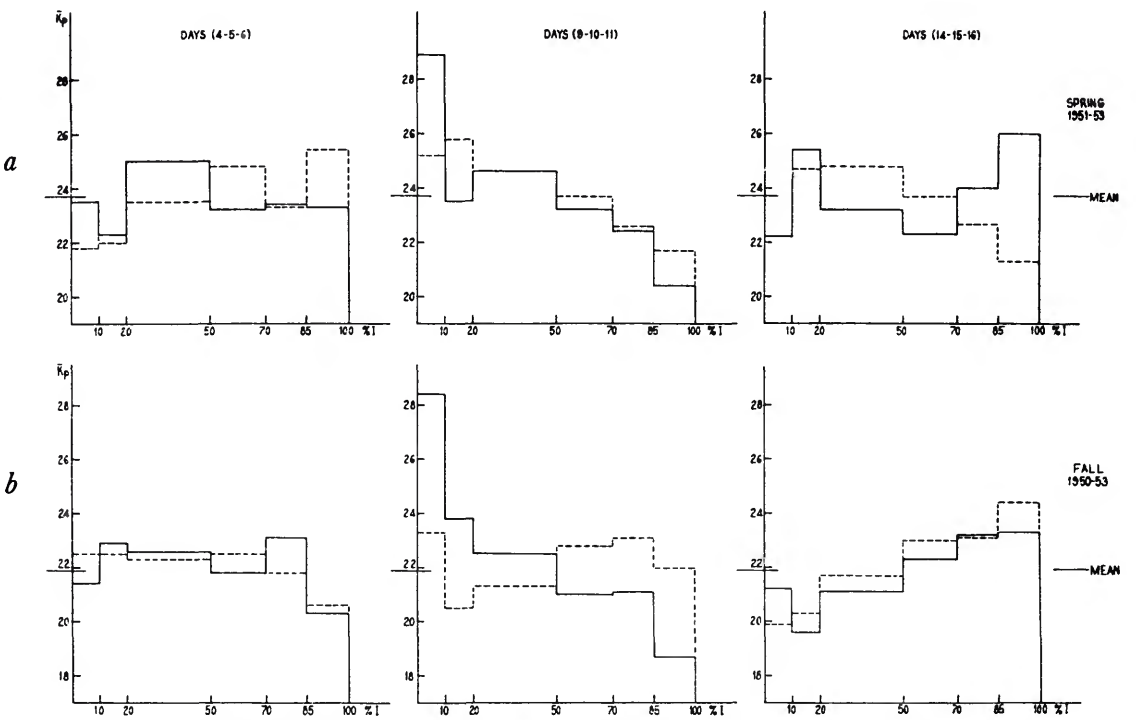

FIGURE 21.—Average *Kp* associated with various percentiles of 5303 intensity for selected groups of days after ELP, for favorable (solid line) and unfavorable (broken line) hemispheres. *a*, Spring half-years, 1951–53; *b*, autumn half-years, 1950–53.

Those days possessing indices in the 20H group, but lacking any maximum in the hemisphere under consideration, remain for comment. In defining the "O" group, we did not distinguish between days having the maximum located at the equator and those having it in the other hemisphere, but the latter condition is the more common. The *Kp*'s associated with these "O" groups tended to have a minimum around days 9–12, with no significant difference appearing between the favorable and the unfavorable groups. If the unfavorable index is high but has no maximum, we may reasonably infer an even higher index in the favorable hemisphere. Therefore a *Kp* minimum apparently associated with an Hu "O" index is easily reconciled with the hemisphere effect.

We also subdivided the 10L deciles of favorable and of unfavorable indices into two groups according to whether the hemisphere in question possessed a maximum in 5303. In the 10L group of course any such maximum would be very small, only 1–2 units above the surrounding intensities. Between these two groups of the 10L indices we found no significant difference in associated *Kp*'s. Both favorable groups clearly showed the expected maxima at *Kp* (9–10), in contrast to small or negligible maxima for the unfavorable groups.

Although the relative location of the solar equator rather than angular distance between earth and solar centers appears to be the significant factor in the hemisphere effect, inspection of a number of individual recurrence sequences reveals most often a gradual weakening of storm intensity rather than a sudden termination of the series at the time the earth crosses the solar equator. We shall therefore consider next not the angular distance between earth and solar centers but rather the angular distance of the earth from the solar equator. To investigate the effect of the angular distance between the earth and solar equator we divided each half-year into three parts: (a) the middle group of about 75 days when the heliographic latitude was greater than ~5.8°; (b) a group covering approximately the second solar rotation from the crossing of the equator, when the latitude of the earth was between 3.0 and 5.8°; and (c) the 27 days at the ends of the period when the latitude of the earth was less than ~3.0°. The periods were extended to overlap one another by 2 days on either end. Obviously no more detailed subdivision of the earth's heliographic latitude is practical since

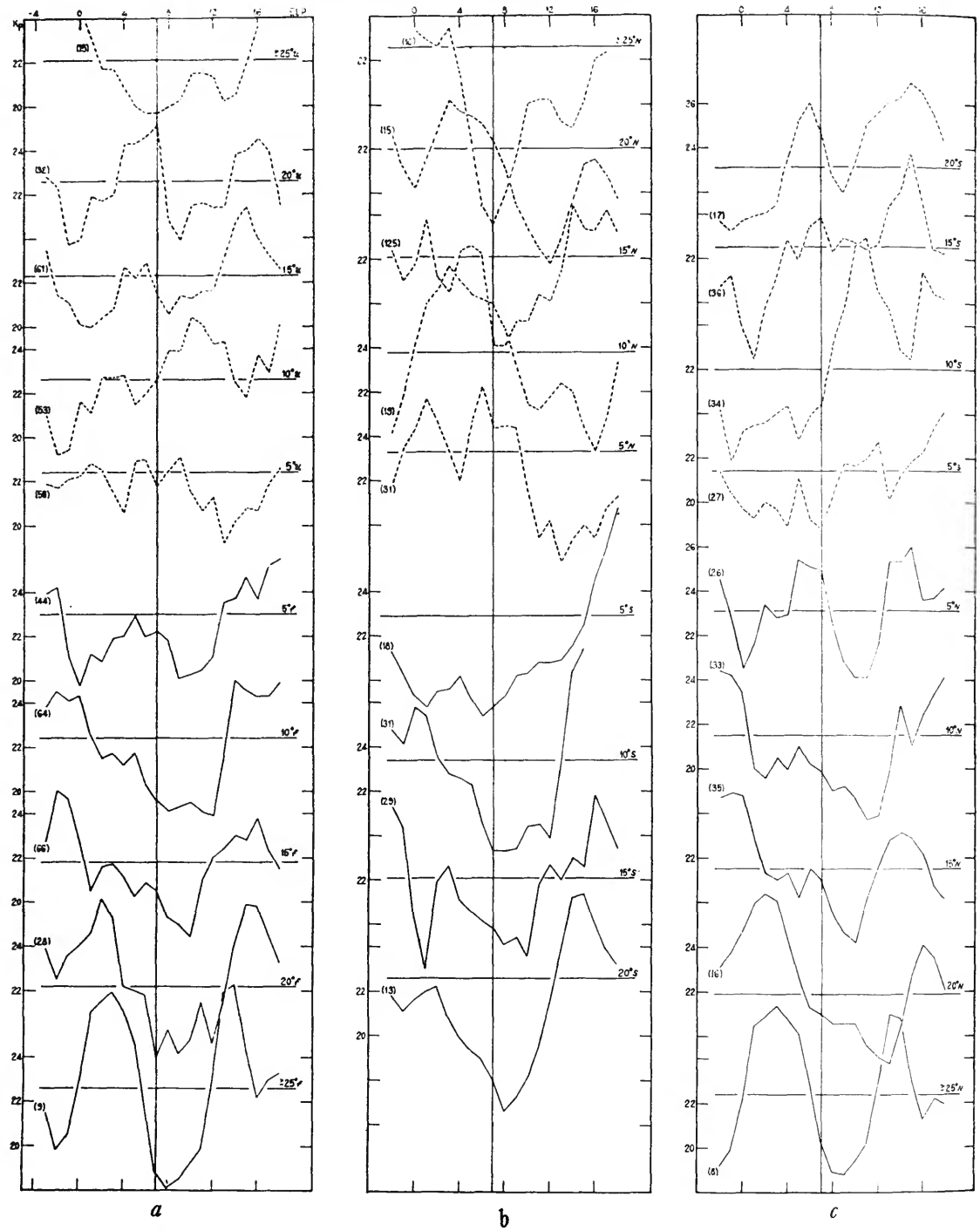

FIGURE 22.—Mean *Kp* following ELP of bright 5303 with maximal intensity occurring at various favorable (solid line) and unfavorable (broken line) heliographic latitudes, at 5° intervals from 25°u to 25°f; for samples less than 20 the curves are 3-day running means. *a*, Composite for the 4-year period; *b*, spring half-years; *c*, autumn half-years.

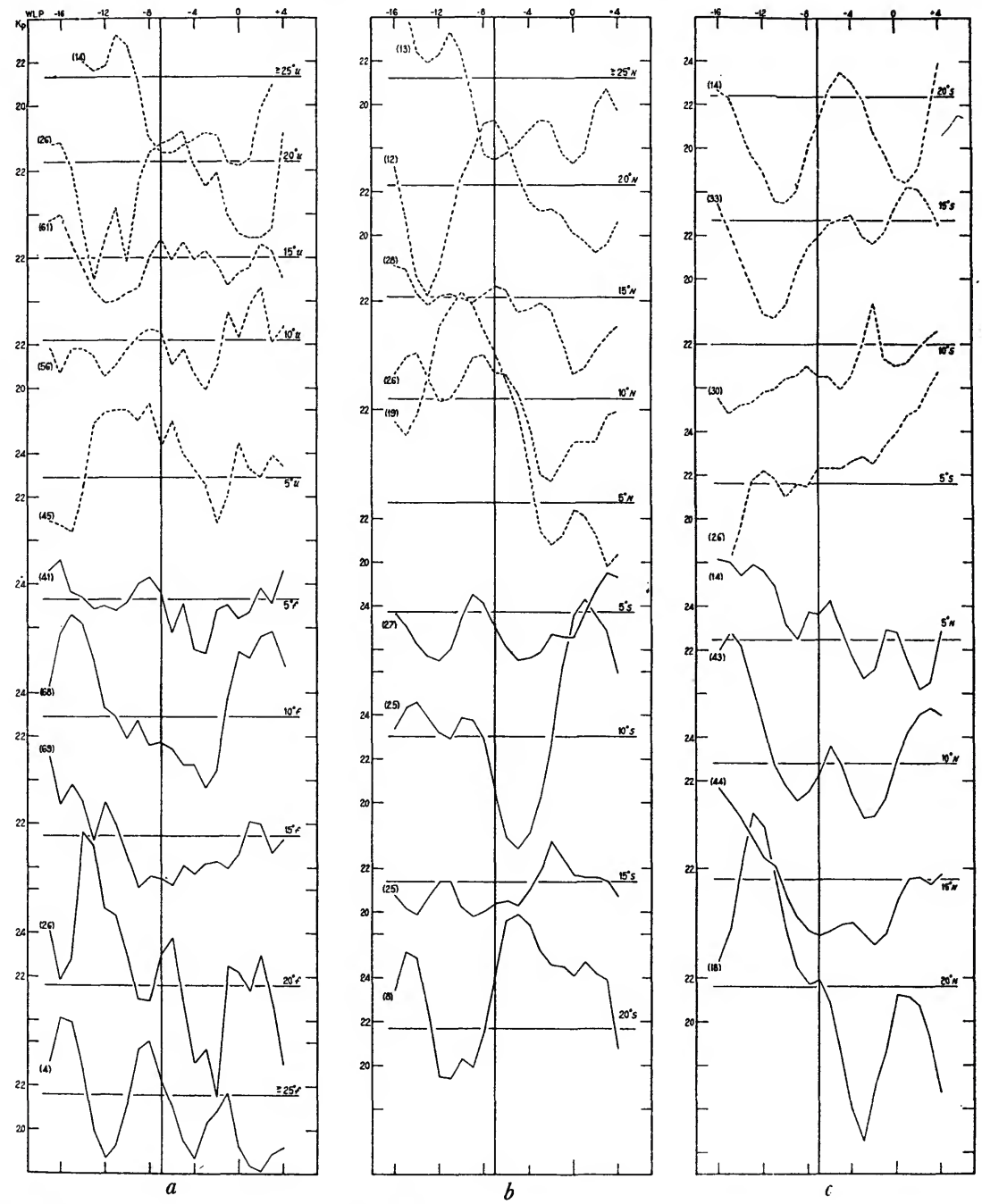

FIGURE 23.—Mean Kp preceding WLP of bright 5303 with maximal intensity occurring at various favorable (solid line) and unfavorable (broken line) heliographic latitudes. *a*, Composite results for the 4-year period; *b*, spring half-years; *c*, autumn half-years.

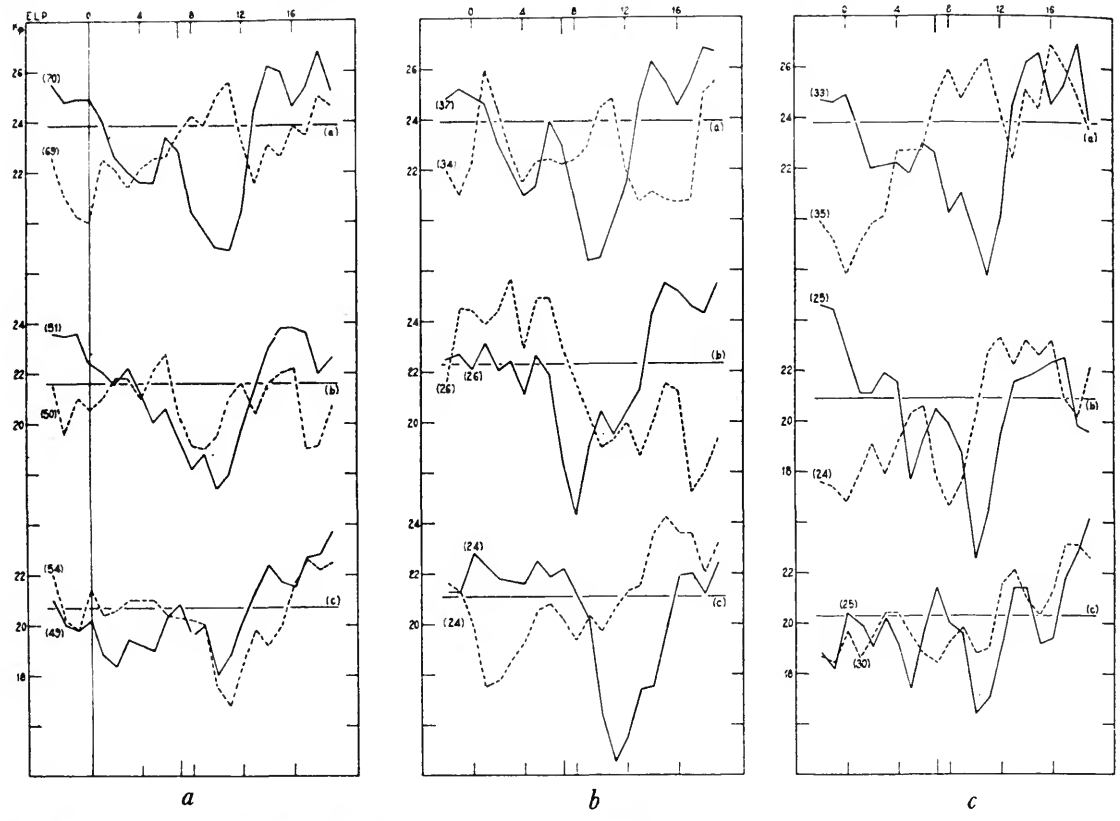

FIGURE 24.—Effect of angular distance of earth from solar equator; mean *Kp* following ELP of bright 5303 corona when the heliographic latitude of the earth is: $\geq 5.8°$, line (a); ~ 3.0 to $5.8°$, line (b); and $\leq 3.0°$, line (c). *a*, Composite for the 4-year period; *b*, spring half-years; *c*, autumn half-years.

each period should cover at least a full solar rotation. We must give every M-region a chance to appear in each curve if we are to gain an accurate impression of their waxing and waning with the change in the earth's heliographic latitude. Group (a) may be designated "most favorable" or "most unfavorable," with (b) "moderately" and (c) "slightly" favorable or unfavorable.

From each of the above groups we selected the 10H and 10L 5303 intensities, for zero days. The associated average *Kp*'s appear in figure 24*a–c* for the 10H, and in figure 25*a–c* for the 10L groups. To trace a sequence for the southern hemisphere from most favorable to most unfavorable, one proceeds in order from top to bottom in the figure for the spring half-years; then from bottom to top in the figure for the autumn half-years; and conversely for the northern hemisphere. As we should expect, from the well-known March and September maxima in geomagnetic and auroral activity, the means for the (a) curves are higher than the corresponding (b) means, and the (c) means are lowest of all. Also the favorable versus unfavorable differences are much more pronounced in the (a) curves than in those of (b) or (c); and the expected maxima and minima in *Kp* are largest in the favorable (a) curves.

From figure 24*a–c* we see that no hemisphere effect for the bright 5303 corona appears to exist while the earth is within 3° of the solar equator; that the effect begins to appear between 3° and 5.8°, and is conspicuous above 5.8°. The corpuscle-inhibiting power of an active center would thus appear to extend about 4–6° into the other solar hemisphere.

Figure 25*a–c*, for the faint corona, is especially interesting, and shows clearly what

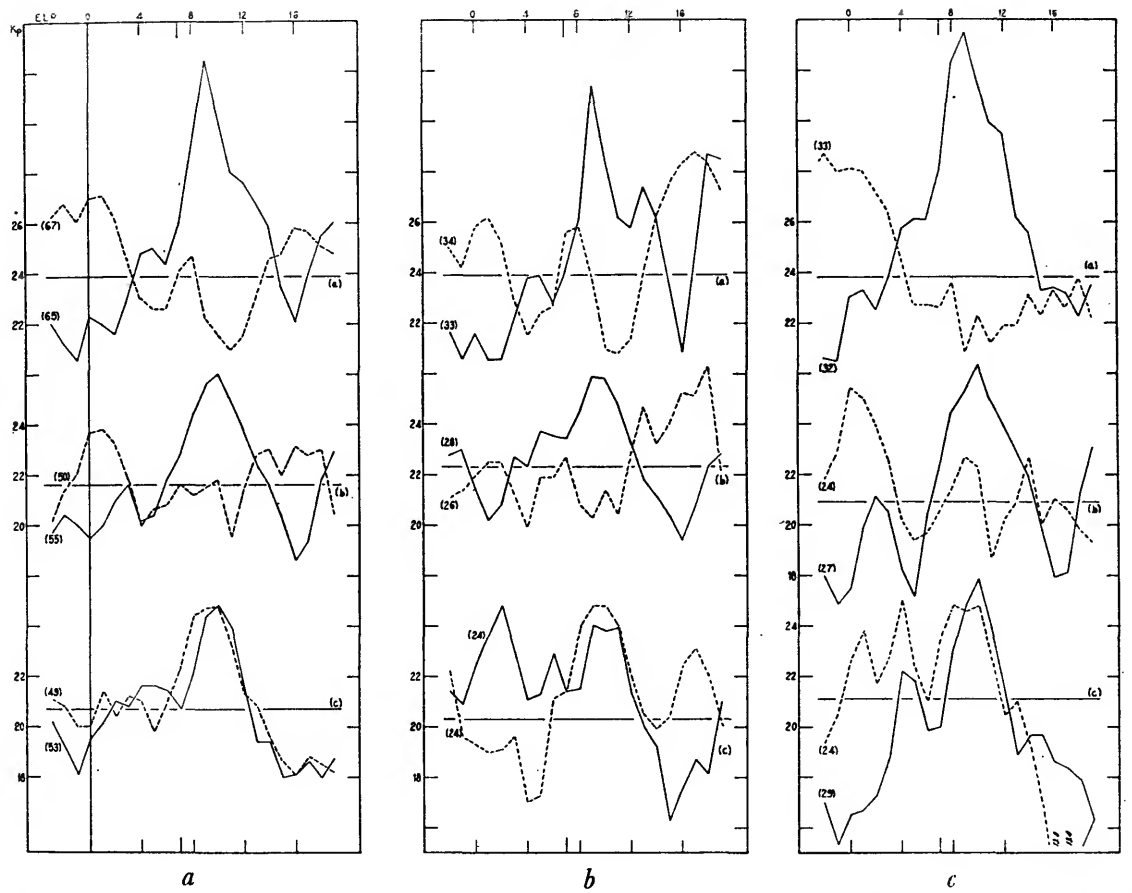

FIGURE 25.—Effect of angular distance of earth from solar equator; mean Kp following ELP of faint 5303 corona when the heliographic latitude of the earth is: $\geq 5.8°$, line (a); ≤ 3.0 to $5.8°$, line (b); and $\leq 3.0°$, line (c). *a*, Composite for the 4-year period; *b*, spring half-years; *c*, autumn half-years.

appears to be a waxing and waning of the geomagnetically-disturbing power of M-regions as the heliographic latitude of the earth varies from most favorable through the equator to most unfavorable. Within 3° of the solar equator the two hemispheres appear to act equally; around days 9–11 the favorable and unfavorable (c) curves are closely parallel and of equal height. In the interval of the second rotation, 3–5.8°, however, the predominance of the favorable hemisphere becomes clearly visible in both spring and fall. The most unfavorable curves (a) tend to lie below the means for days 8–12, while the most favorable ones are showing the largest peaks. We suggest that the progressive nature of the variations in Kp, especially in the case of the weak corona, provides particularly convincing support for the reality of a hemisphere effect and an axial explanation of the seasonal variation in Kp.

We shall defer comment until Part III on the Kp maxima that do appear, well away from CMP, in the most unfavorable curves. However, we note here that they appear to arise from the relative spacing in longitude of the principal northern and southern solar M-regions.

It should be emphasized that the hemisphere effects in the relation between Kp and the intensity of 5303 coronal emission, discussed so far in this paper, arise from the apparent behavior of the general solar corpuscles. Our results suggest that the general corpuscles,

422953—57——4

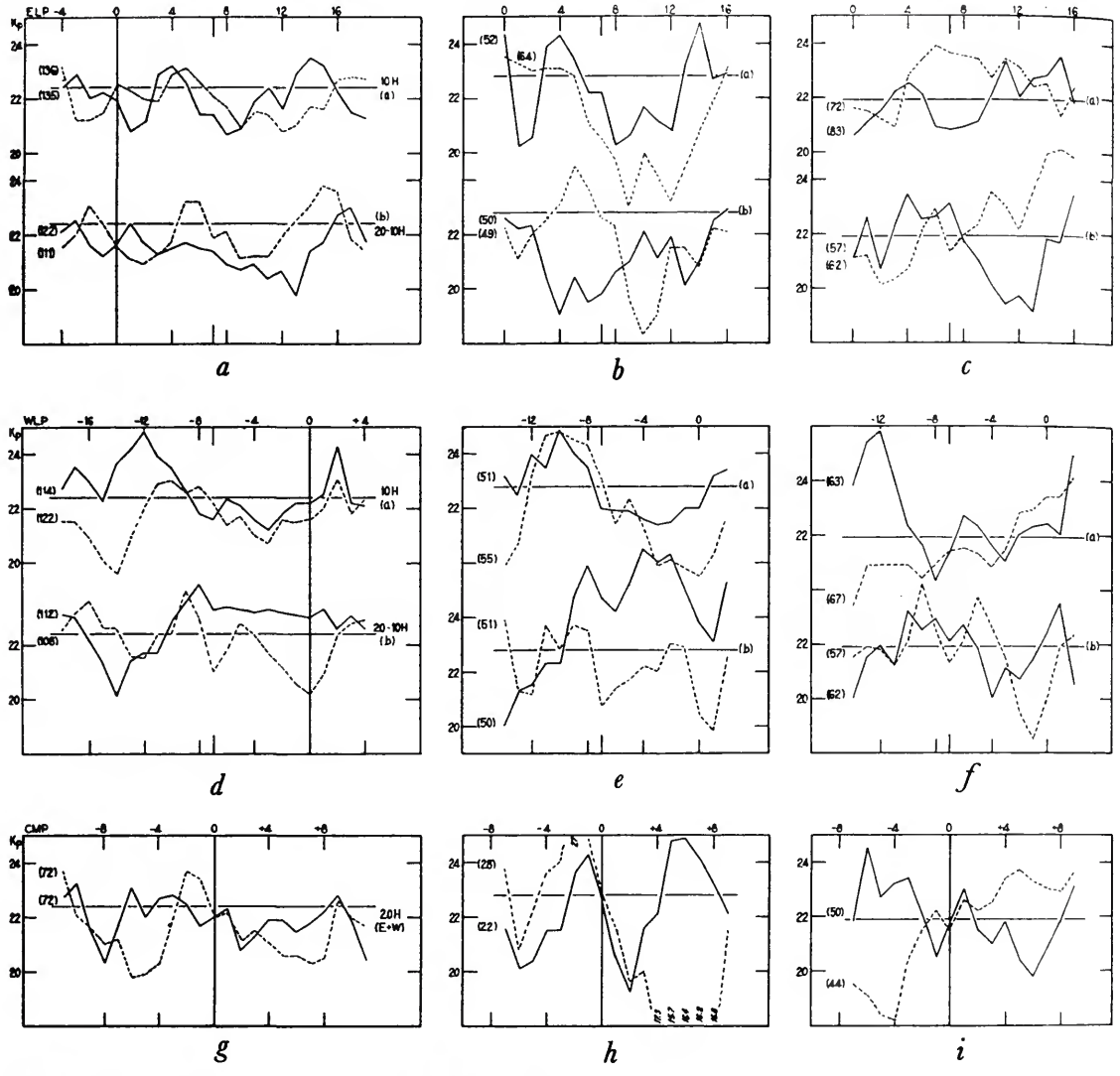

FIGURE 26.—Mean Kp associated with strong 6374 intensities in favorable (solid line) and unfavorable (broken line) hemispheres. *a–c*: Mean Kp following ELP of the 10 percent strongest (10H), line (a); of the 20H −10H, line (b). *a*, Composite for the 4-year period; *b*, spring half-years; *c*, autumn half-years. *d–f*: Mean Kp preceding WLP of bright 6374 corona (10H), line (a); and 20H −10H, line (b). *d*, Composite for 4-year period; *e*, spring half-years; *f*, autumn half-years. *g–i*: Mean Kp associated with CMP of regions of bright 6374 corona (20H) at ELP and at WLP 14 days later. *g*, Composite for 4-year period; *h*, spring half-years; *i*, autumn half-years.

whatever their exact source, encounter at the solar equator some sort of (presumably magnetic) barrier to their free movement. Of those originating in one solar hemisphere, only a minor portion appear able to cross more than about 3° beyond the solar equator and to affect the earth on the other side. Further, a bright coronal center apparently inhibits the escape of general corpuscles only 3–5° beyond its own hemisphere. However, we have no evidence as yet bearing on the presence or absence of a hemisphere effect in the behavior of the corpuscles that appear to be emitted from the relatively rare (in the 1950–53 period) storm-producing active centers.

The red line.—Using the indices of red line

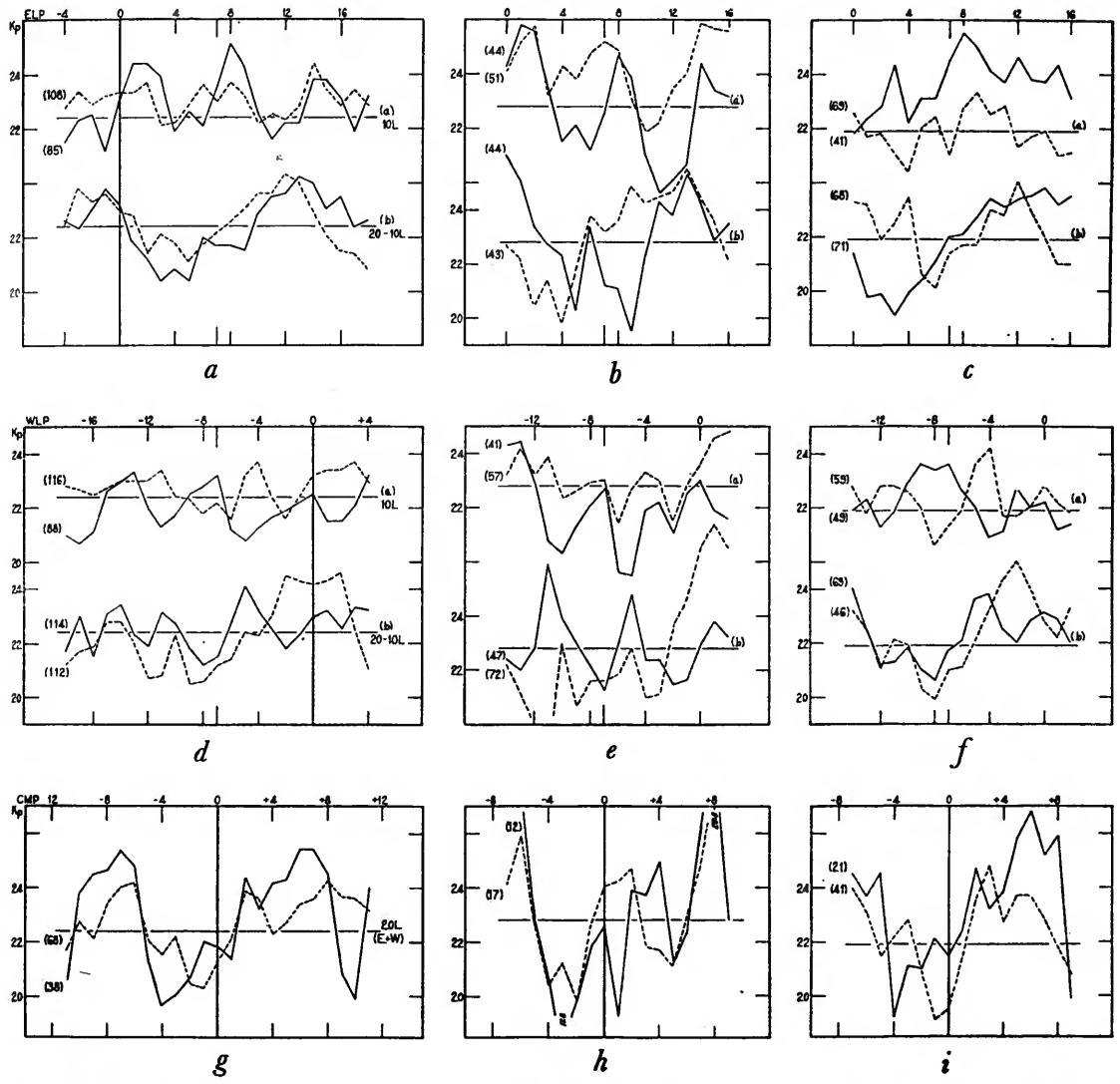

FIGURE 27.—Mean Kp associated with weak 6374 intensities in favorable (solid line) and unfavorable (broken line) hemispheres. *a–c*: Mean Kp following ELP of the 10 percent weakest (10L), line (a); of the 20L —10L, line (b). *a*, Composite for the 4-year period; *b*, spring half-years; *c*, autumn half-years. *d–f*: Mean Kp preceding WLP of weak 6374 corona (10L), line (a); of 20L —10L, line (b). *d*, Composite for the 4-year period; *e*, spring half-years; *f*, autumn half-years. *g–i*: Mean Kp associated with CMP of regions of weak 6374 corona (20L) at ELP and at WLP 14 days later. *g*, Composite for 4-year period; *h*, spring half-years; *i*, autumn half-years.

intensity, we computed mean Kp values associated with ELP of the 10 percent, 20–10 percent and 30–20 percent of the brightest and of the faintest 6374 intensities within each of the favorable and unfavorable groups. We made similar calculations from the WLP indices and computed the mean Kp's associated with CMP of regions having the red index 20H, and 20L, at both ELP and WLP 14 days later. The principal red-line results are shown in figure 26*a–i* and in figure 27*a–i*.

These figures show immediately that Kp appears to be much less closely related to red line intensity than to green line intensity. Indeed, if we had no preconception derived from the green line results it is doubtful that

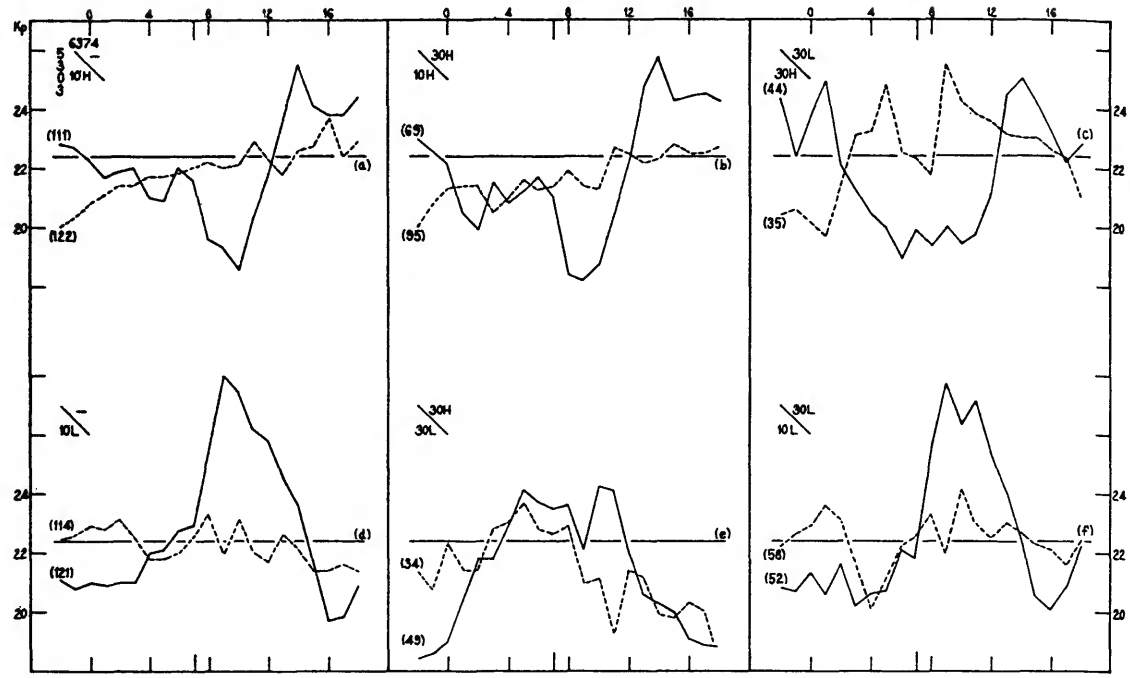

FIGURE 28.—Mean *Kp* associated with ELP of various combinations of 5303 and 6374 intensities in favorable (solid line) and unfavorable (broken line) hemispheres. Bright 5303 (10H) taken independently of 6374, curve (a); both lines bright, 5303 (10H) and 6374 (30H), curve (b); 5303 bright (30H) and 6374 faint (30L), curve (c); faint 5303 (10L) taken independently of 6374, curve (d); 5303 faint (30L) and 6374 bright (30H), curve (e); both lines faint, 5303 (10L) and 6374 (30L), curve (f).

we should see any relation between *Kp* and 6374 intensity. Certainly there are no clearly regular and systematic effects present in the various samples, either the favorable or the unfavorable. Some of the samples do show effects similar to but less conspicuous than the green line results, but these are not present in all cases. No hemisphere effect is distinguishable. But since any 6374-*Kp* relation is slight, this particular absence need not overly concern us.

This contrast between red line and green line results may have special interest in the light of certain results obtained by Athay and Roberts (1955) from observations of the 1952 eclipse. They measured the intensities of the 5303 (Fe XIV), 6374 (Fe X) and 7892 (Fe XI) lines, and of the continuum at 15 points around the limb. They found that the continuum intensity showed a substantially higher correlation with the intensity of 5303 ($r=0.87$) than with those of 6374 (0.41) or 7892 (0.54). This close relation between 5303 and continuum occurs primarily in the low and middle solar latitudes and appears to break down at high latitudes. As Athay and Roberts point out, the continuum, arising mainly from electron scattering, is very insensitive to changes in temperature as long as the temperature is high enough to completely ionize hydrogen. At coronal temperatures, therefore, changes in the brightness of the continuum should arise primarily from changes in the electron density. Their results indicate the brightness of 5303 to be substantially better than 6374 as an indicator of the coronal electron density, at least in lower and middle solar latitudes (presumably because the corona there is near the optimum temperature for Fe XIV).

We accordingly suggest that the difference between the red and the green line results may indicate that *Kp*, insofar as its variations arise from the behavior of general solar corpuscles, is closely related to the particle density in the corona of the favorable solar hemisphere at CMP. A high particle density in the CM-f

corona would appear to be associated with a reduced density of general solar corpuscles in the vicinity of the earth; whereas a low particle density in the CM-f corona appears to be associated with an above-average density of general solar corpuscles in the vicinity of the earth.

Red and green lines, simultaneously.—We have made a number of calculations of mean *Kp*'s associated with various combinations of red and green line indices, in the favorable and unfavorable solar hemispheres. Figure 28 shows an example of the results. Curves (a) and (d) have no interpolated values of the 5303 index and may be compared with those of figures 12 and 16 where interpolated values are used.

In figure 28 comparison of curve (a) with (b) and curve (d) with (f) indicates that the 5303 index alone gives results equally as good as those obtained when both indices are high (b) or both are low (f). When the two indices differ, one being high, the other low, the *Kp*'s tend to behave as previously found for the 5303 index alone. These results do not altogether agree with those shown in Part I, figure 5*a*, *b*, and may therefore be regarded with some reservations. However, using independent west-limb indices, we obtained results very similar to those shown in figure 28. We tend to feel, therefore, that figure 28 gives the more accurate picture and that some of the results of figure 5*a*, *b* may have arisen from neglect of the hemisphere separation.

The yellow line.—Because of the small sample size, we have made no hemisphere calculations for the yellow line cases. Of the 22 occurrences observed during the period under study, 5 appeared in the favorable hemisphere and 17 in the unfavorable. Therefore the *Kp* rise shown in figure 6 must be associated in large part with unfavorable 5694 regions, an inference confirmed by inspection of the individual cases. Our sample provides no evidence for any hemisphere effect in the *Kp*'s associated with yellow line regions. We therefore tentatively conclude that the motions of those storm-producing corpuscles apparently emitted by active centers are not significantly restricted by the equatorial barrier, which appears to act on the general solar corpuscles.

Part III. Inverse solutions for hemisphere effects

In order to study the average distribution of 5303 intensity as a function of distance from the solar central meridian at the time of geomagnetic storms, we prepared an inverse deck of IBM cards which contain *Kp* (0), and the sum of the east-limb 5303 index and the west-limb index 14 days later, for days CMP −8 through +9 (ELP −1 through +16), for the northern and for the southern solar hemispheres separately. We had two objectives: to investigate the coronal conditions associated with nonrecurrent sc-storms and with recurrent storms from the point of view of favorable and unfavorable solar hemispheres; and to study further the apparently distinctive coronal intensity pattern characterizing M-regions.

For Part I we compiled a list of 38 geomagnetic storms observed to have a sudden commencement (sc) at ten or more observatories. We excluded six storms with the requisite "sc" that were members of prominent recurrence sequences. The group of 38 does, however, contain several sc-storms that appear to recur although they are not members of the most striking sequences. Figure 29*a*, *b* shows the average favorable and unfavorable intensity patterns associated with onset of these 38 sc-storms, in spring and fall respectively. Day zero is the day of the "sc."

We also removed from the deck all high *Kp*'s that appeared to be part of one of the 38 sc-storms. The remaining high *Kp*'s thus belonged to storms without a widely observed "sc"; they may perhaps be considered to be of the M-region and "general corpuscle" type even if not all of them are clearly recurrent. The resulting average 5303 intensity distributions associated with zero day defined by $Kp \geq 32$ (except for the 38 sc-storms) are shown in figures 29*c*, *d*. Because the means of the north and of the south intensities are often quite different we did not superpose the favorable and unfavorable curves, but the scales were shifted vertically to bring the means of the two curves for a half-year on more or less the same line.

Figure 29*a–d* indicates a marked difference in the coronal patterns associated with the nonrecurrent and with the recurrent type of storms, particularly in the favorable solar hemisphere. The occurrence of nonrecurrent sc-storms appears to be associated with the presence of above-average coronal intensity around the central meridian of the sun although, as shown in figure 7, the time lag does not appear to be precisely defined. The curves give no clear evidence for the presence or absence of a hemisphere effect in the case of sc-storms. Such limited evidence as we possess would appear to contradict rather than to favor the

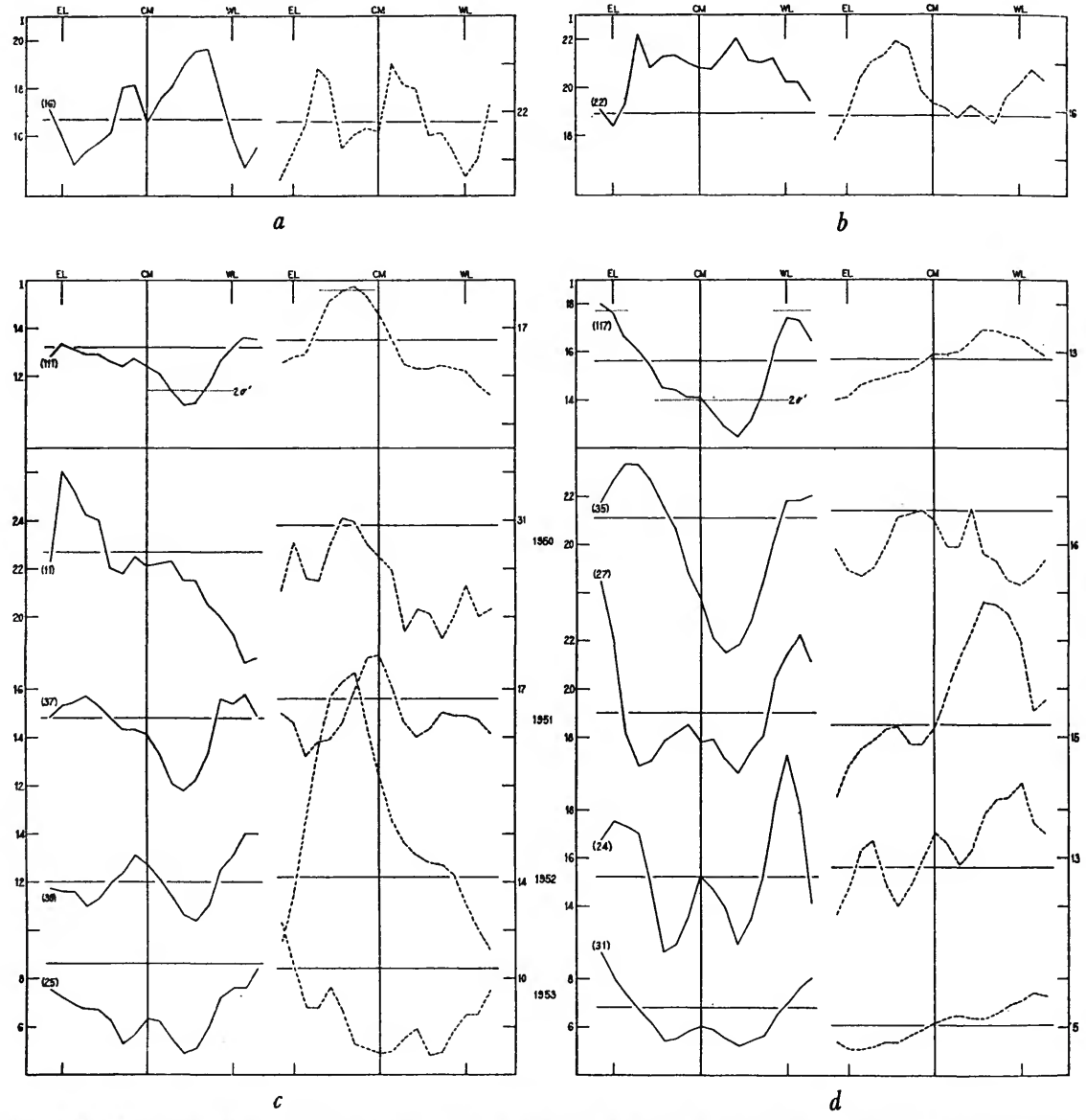

FIGURE 29.—*a, b:* Mean pattern of 5303 intensity in favorable (solid line) and unfavorable (broken line) hemispheres, associated with onset of geomagnetic storms of sc-type. *a*, Spring half-years; *b*, autumn half-years. *c, d:* Mean pattern of 5303 intensity in favorable and unfavorable hemispheres, when *Kp* is greater than 32 and not part of sc-storm; curves at top are composites of the 4 half-year curves below. *c*, Spring; *d*, autumn.

hypothesis of a hemisphere effect in such storms.

In the spring (figure 29*a*) both the favorable and unfavorable solar hemispheres show above-average intensity west of the central meridian at the time of the "sc," but the rise in the unfavorable curve occurs nearer to the expected time. In the fall only the favorable intensity is above average to the west of the central meridian but both are high on the eastern hemisphere at the time of the "sc." In this connection we note that during 1950–53 the north solar hemisphere may have had more highly active centers than the south; for example, of the 22 yellow line cases, 15 appeared in the north and only 7 in the south. Because of the small number of sc-storms during the years 1950–53, it is not practical to have more than two independent samples, and, since these do not agree, our results must remain inconclusive. Like the yellow line studies, however, figure 29*a*, *b*, provides no clear evidence for a hemisphere influence in the behavior of active center corpuscles.

Looking next at figure 29*c*,*d* we see that, as expected, the occurrence of M-region storms tends to be associated with the presence 2–4 days west of the central meridian of below-average 5303 intensity in the favorable solar hemisphere. This coronal minimum in the favorable hemisphere appears in seven of the eight periods; it is absent only in the spring of 1950, a period lacking clear recurrent sequences, as previously noted. Since all cases of $Kp \geq 32$ (except the 38 sc-storms) were used to define zero days in figure 29*c*,*d*, the time lag is not as precisely defined as when we use only the day of storm beginning. The 5303 intensities of the unfavorable solar hemisphere show no consistently recurring pattern.

M-regions.—The identification of Bartels' M-regions, the hypothetical solar sources of the corpuscles producing the long series of recurrent geomagnetic storms, has long been a perplexing problem. The results from Parts I and II indicate that, during the years 1950–53, M-regions were characterized by unusually weak emission in the 5303 coronal line in the favorable solar hemisphere. The weakness of 5303 appears to indicate a region of lower-than-average density in the corona. With figures 30–32 we may explore further some of the apparent properties of M-regions as indicated by the intensity of the 5303 emission. First, we have calculated the favorable and unfavorable intensity patterns associated with nine of the more prominent recurrence sequences in the 1950–53 period, with zero day defined by the onset of the storm. When originally selecting these sequences, we divided them into Class I and Class II, according to their impressiveness and the degree of certainty we felt in identifying them. Figure 30*a–d* shows the patterns of 5303 intensity associated with the nine sequences identified as follows:

Class I (figure 30*a*,*b*):

(a) 11 July, 7 Aug., 3 Sept., 1 Oct., 28 Oct., 25 Nov., 1950, Nf.
(b) 15 Dec., 10 Jan., 6 Feb., 3 Mar., 30 Mar., 28 Apr., 26 May, 1952, Sf.
(c) 1 July, 28 July, 24 Aug., 20 Sept., 17 Oct., 12 Nov., 8 Dec., 1951, Nf.
(d) 24 Feb., 23 Mar., 19 Apr., 15 May, 1953, Sf.
(e) 29 June, 26 July, 23 Aug., 19 Sept., 15 Oct., 12 Nov., 1953, Nf.

Class II (figure 30*c*, *d*):

(f) 7 Sept., 3 Oct., 30 Oct., 26 Nov., 1952, Nf.
(g) 12 Jan., 8 Feb., 6 Mar., 2 Apr., 1 May, 1951, Sf.
(h) 5 Jan., 1 Feb., 27 Feb., 24 Mar., 21 Apr., 18 May, 1952, Sf.
(i) 24 July, 19 Aug., 16 Sep., 14 Oct., 10 Nov., 6 Dec. 1950, Nf.

The dates listed were used in our calculations as "date of onset of storm" or zero days in figures 30*a–d*. They include the most prominent storms of each sequence, and may, but do not necessarily, include all of the lesser storms that appear to belong to some of the sequences. Also, the zero days used for each sequence in these calculations were confined to a 6-month interval within which a given solar hemisphere was favorable.

Each of the five recurrence sequences of Class I (figure 30*a*, *b*) shows a weak area in the 5303 corona in the favorable solar hemisphere 0–3 days west of central meridian at the time of storm onset. No pattern appears systematically in the unfavorable hemisphere corona. For Class II sequences the picture is less clear. Only sequence (f) shows an entirely satisfactory coronal pattern. Sequence (h) has a conspicuously weak 5303 region in the unfavorable solar hemisphere west of CM but no minimum at the expected position in the favorable hemisphere. We feel some doubt whether sequence (i) is altogether a true M-region sequence, arising from general corpuscles. It contains 3 sc-storms (included among the 38), and one of the few "great" storms (19 Aug.) of the four years under study.

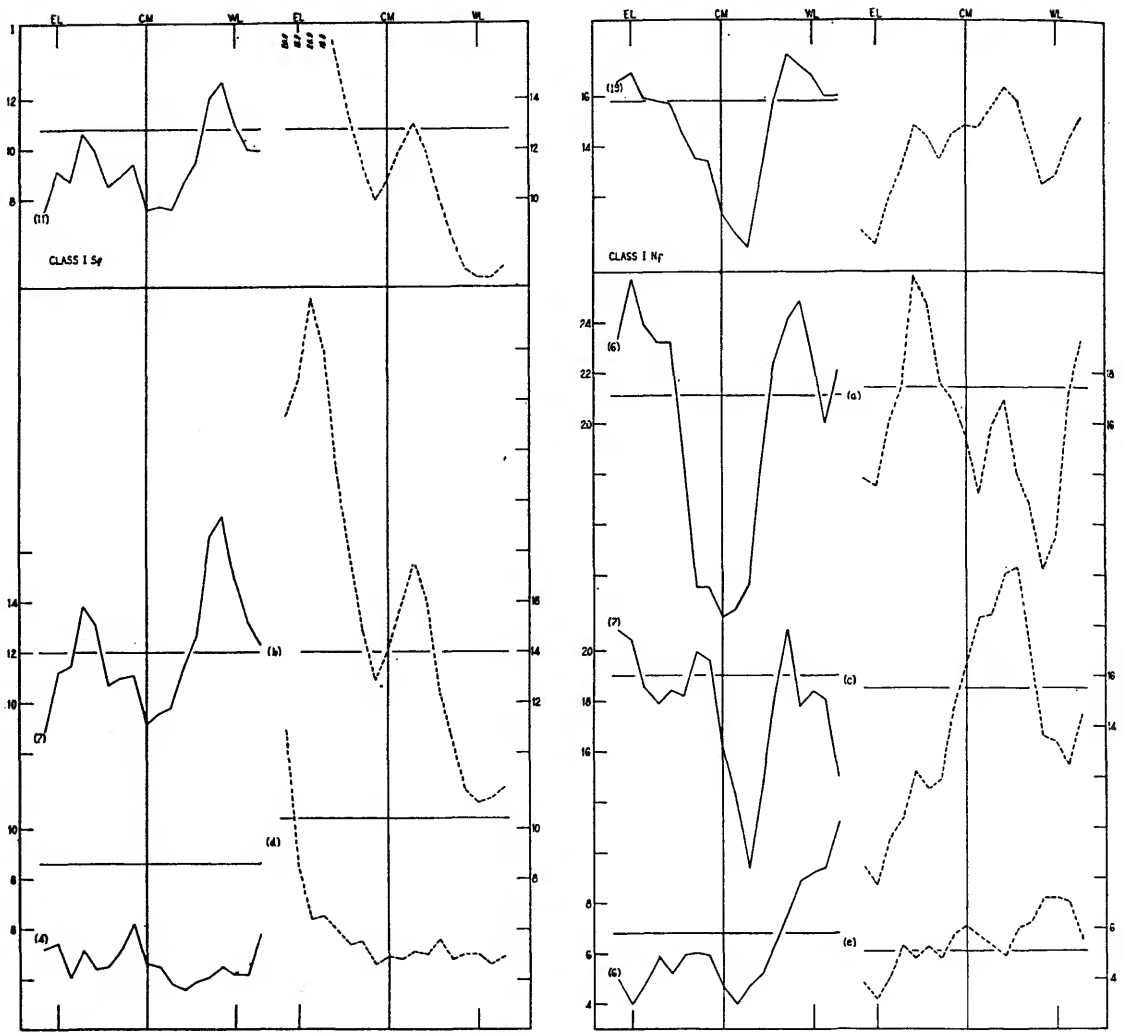

FIGURE 30.—Mean pattern of 5303 intensity in favorable (solid line) and unfavorable (broken line) hemispheres, associated with onset of storms in selected recurrence sequences; curves at top are composites of the individual M-regions below. *a*, Major recurrence sequences in spring half-years; *b*, in autumn half-years; *c*, recurrences of intermediate importance in spring half-years; *d*, in autumn half-years.

Sequences (a) and (b) have been discussed by others. Smyth (1952) found from Climax data that the intensity of 5303 showed a minimum on the east limb about eight days before the onset of the storms of sequence (a). Bruzek (1952) found a similar result from Wendelstein data, for this sequence as well as for two sequences in 1942–44. Both of these results are in good agreement with our findings. (Maxwell (1952) also has discussed this sequence.)

Trotter and Roberts (1952) and Müller (1953), discussing sequence (b), found evidence for the return of the eastern hemisphere effect of Shapley and Roberts. This sequence is responsible for the apparent eastern hemisphere effect showing in the 1952 unfavorable curve of figure 13*a*; the corresponding coronal peak is conspicuous in figure 30*a* (unfavorable curve).

Von Klüber (1952) has suggested a possible connection between sequence (b)—in particular

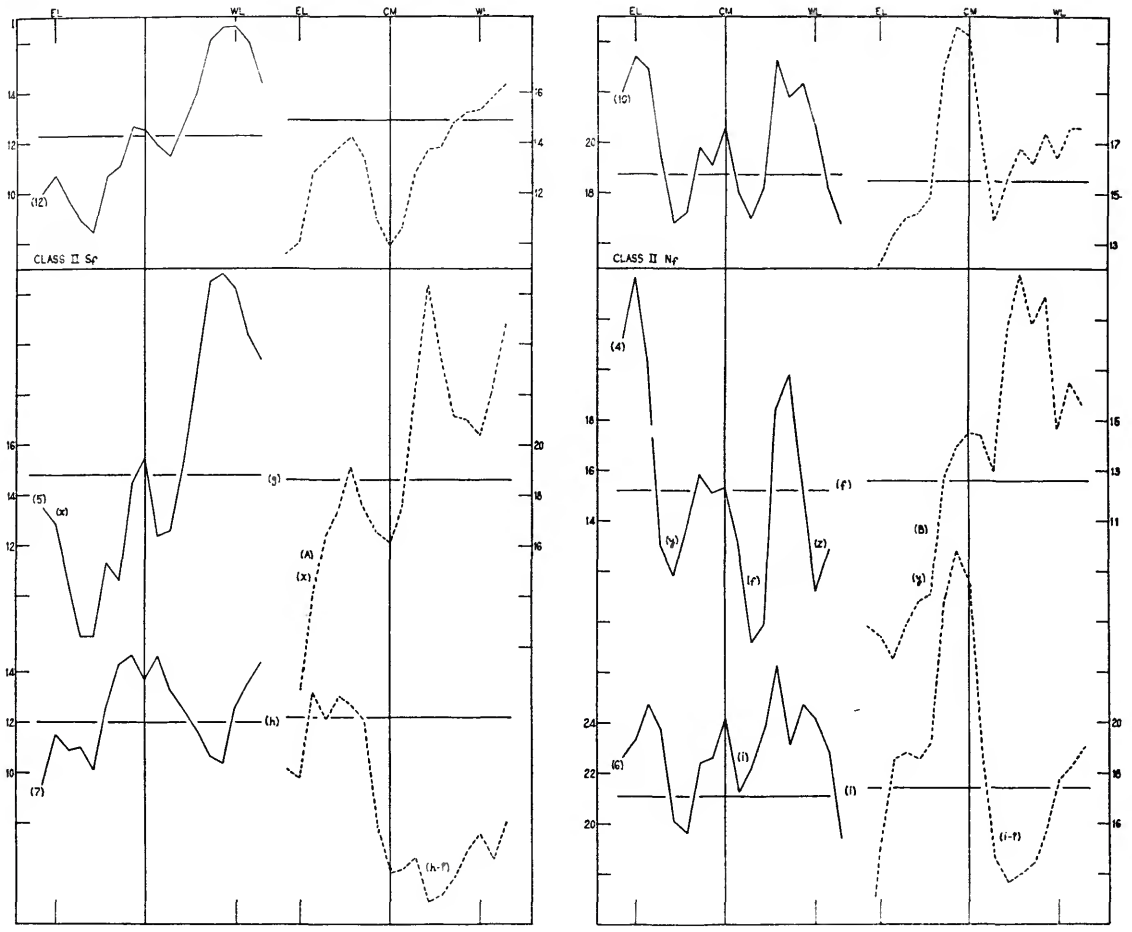

FIGURE 30*c*, *d*.—See explanation on facing page.

the storm commencing 3 March—and the CMP of the prominent white light coronal streamer observed at the 25 Feb. 1952 solar eclipse. More generally, Allen (1944), von Klüber (1952), and others have suggested that the white light streamers may be a manifestation of the corpuscular streams responsible for recurrent magnetic storms, and hence a property of M-regions. Since the white light corona has been observed to date only during total solar eclipses, there has been little opportunity to test this hypothesis.

Although its exact longitude is uncertain, the streamer of 25 Feb. 1952 could have passed the central meridian at a time appropriate for the storm of 3 March. However, the streamer is centered at about 20° N, whereas the southern solar hemisphere is favorable for this sequence of storms and contains a region of weak corona at the proper location. Inspection of eclipse photographs (see Biesbroeck, 1953, figs. 5, 6) indicates that the streamer, whatever its nature, was pointing in a direction very unfavorable for intercepting the earth in the spring. At most, the earth might pass near its edge, and even this looks doubtful. On the other hand, the storm sequence in question was one of the most impressive of the four years (see fig. 31*a*). We consider it improbable that one of the most impressive sequences of this cycle should arise from so unfavorably directed a streamer. What could we then expect from a favorably

located streamer? Therefore, and because of our other results, we doubt that any physical connection exists between the white light streamer of 25 Feb. 1952 and sequence (b). Also, since there is no streamer in a favorable location, we are inclined to reject Allen's original hypothesis that white light coronal streamers are a characteristic of M-regions.

On the other hand, according to the hypothesis that seems to be indicated by the relation of recurrent storms to green line weakness, we should expect a region of relatively low coronal density to exist somewhere on the SE limb at the time of the February 1952 eclipse. The results of Hepburn (1955) on the variation of electron density with position angle at this eclipse, appearing in the interval between the completion and the publication of our paper, now make possible a check on this expectation. It can be seen from her figure 10 that the electron density is indeed relatively low along the entire SE limb, and especially in the region 15–30° S. Because of our other results, we therefore suggest that this area of relatively low electron density, rather than the streamer at 20° N, may be the M-region associated with the geomagnetic storm of 3 March and with sequence (b).

Sequence (e) is the one the Babcocks (1955) have suggested may arise from a magnetic unipolar region that passes the solar central meridian 1–4 days before the onset of the storms of this sequence. As they point out, their observations cover too short a period to permit any definite conclusions from the observed coincidence. We do note, however, that the unipole was in the northern or favorable solar hemisphere. Also a second, less conspicuous, unipole, not followed by any geomagnetic storms, would appear to be a southern one, which could account for the apparent failure of this unipole as an M-region.

Figure 31*a*,*b* shows half-year averages of *Kp* over 27-day periods, with day zero corresponding to the zero days of Bartels' magnetic rotations (5 Jan. 1950, etc.). Note that the *Kp* scale is half that used in Parts I and II. The nine individual recurrence sequences stand out more or less clearly. Spring and fall are plotted separately to emphasize a characteristic of the present cycle first noticed by Bhargava and Naqvi (1954). (See also Naqvi and Bhargava, 1954.) They pointed out the two very long sequences of geomagnetic activity that appear clearly in our figure 31*a*,*b*. Their longest sequence, which maximizes in September, comprises our peaks labeled (a, c, f, e), connected by broken line (A); their second sequence, maximizing in March, shows as our peaks (b, d), connected by broken line (B). From the displacement of the successive annual peaks we estimate periods of 27.08 days for sequence A and of 27.1 days for B. Bhargava and Naqvi found the mean period between individual recurrences for each sequence to be 27.05 days.

Corresponding half-year averages of the coronal index appear in figure 32*a* for the southern hemisphere and figure 32*b* for the northern hemisphere. The time scale is displaced relative to that of figure 31*a*,*b* to correspond to a 3-day lag between coronal CMP and the expected associated *Kp*.

Several points of interest may be noted in figures 31 and 32. A region of weak 5303 corona (A) in the north (figure 32*b*) appears to extend, in approximately the same position, from mid-1950 through 1953. Only when the north solar hemisphere is favorable, however, does storm sequence A appear in a conspicuous manner. Similarly, a weak coronal region (B) in the south appears in approximately the same position from mid-1951 through 1953; but only in the spring when south is favorable does the magnetic-storm sequence B appear prominently. Note particularly that the areas of weak corona persist without significant change through their unfavorable periods, but that in each case the magnetic storm sequences weaken markedly or even disappear when the apparently associated solar hemisphere becomes unfavorable. The solar M-regions appear to persist substantially unchanged in coronal pattern and thus, by inference, in intrinsic character and influence on solar corpuscles; whereas the position of the earth varies between favorable and unfavorable for the interception of their corpuscles. The behavior of these sequences appears to demand an axial explanation for the March and September maxima in geomagnetic activity. Moreover, as Bhargava and Naqvi first suggested, rather than a semiannual period in geomagnetism, we should properly speak of two

annual periods overlapping and out of phase with each other by six months.

To compare the curves in figures 30*d* and 31*b* showing sequence (f), we have labeled two other *Kp* peaks, (y) and (z), which fit nicely into the coronal minima to either side of the (f) minimum. Magnetic peak (y) has a coronal minimum in the unfavorable hemisphere also, corresponding to M-region B; plots of the daily *Kp*-sum against time indicate that sequence (y) is stronger in January and May and weakest around March, so that it appears to be a part of sequence B. Similarly magnetic peaks (x) and (w) appear to be parts of sequence A, weakened when the earth passes into regions relatively unfavorable for the interception of corpuscles from M-region A.

With the two major M-regions, A and B, in mind, we suggest the reader look again at figures 14–16 and 25 in Part II. The locations of the *Kp* maxima associated with ELP of unfavorable weak corona can now be readily accounted for without postulating any actual relation between *Kp* and the very unfavorable weak corona. The unfavorable maxima in *Kp* occur in approximately the positions we should expect as a consequence of the relative locations of coronal regions A and B. Similarly the coronal curves (figure 32) for the first half of 1953 reveal why we should expect a minimum in *Kp* in figure 13*a* for 1953 unfavorable as well as favorable, and why the former should be less sharp than the latter.

In concluding this section let us return for a moment to examine quantitatively the principal characteristics of figures 24 and 25. For each of the curves we have computed *Kp* (8–12); from this quantity we subtracted the mean plotted $\overline{Kp}$. We thus define $\Delta Kp = Kp\,(8\text{–}12) - \overline{Kp}$. In figures 33*a* and 33*b* we have plotted ΔKp and *Kp* (8–12), respectively, against $(10 \sin \phi)^3$, where ϕ is the average heliographic latitude of the earth, taken as positive when favorable and negative when unfavorable. The quantity ΔKp shows a close linear relation with $(10 \sin \phi)^3$ and yields the regression equations and correlations

$$\Delta Kp(\mathrm{H}) = -1.98 - 1.40\ (10 \sin \phi)^3,\ r^2 = 0.94, \tag{7}$$
$$\Delta Kp(\mathrm{L}) = 2.08 + 2.22\ (10 \sin \phi)^3,\ r^2 = 0.91.$$

A $\sin^2 \phi$ relation gives about equally good correlation but requires an artificial introduction of negative $\sin^2 \phi$'s for the unfavorable latitudes. We suggest that the good fit of the above equations provides further significant support for the hemisphere effect in the relation between *Kp* and the intensity of 5303 emission, and for the hypothesis of a substantial axial contribution to the semiannual variation in *Kp* and in the aurorae.

The possibility of some additional contribution from equinoctial conditions in the earth's atmosphere is, however, suggested by the plot of *Kp* (8–12) against $(10 \sin \phi)^3$ (figure 33*b*). The linear relationship with $\sin^3 \phi$ shown by ΔKp is here distorted by the end points, all of which appear to lie too high. If we subtract the constant amount of 2.5 from each of the four end points, we then obtain the relations

$$Kp\,(8\text{–}12)\,(\mathrm{H}) = 19.2 - 1.37\ (10 \sin \phi)^3 \quad r^2 = 0.95, \tag{8}$$
$$Kp\,(8\text{–}12)\,(\mathrm{L}) = 23.2 + 2.23\ (10 \sin \phi)^3 \quad r^2 = 0.94.$$

These slopes are very close to those in the ΔKp equations. Note that in figure 33*b* the end points are plotted in their observed positions so that they deviate conspicuously from the regression lines.

We hope to explore these relations between *Kp* and $\sin \phi$ more fully in a later paper. However, we tentatively suggest that equations (7, 8) may represent the axial contribution while the 2.5 subtracted from each of the end points before we solved equation (8) may represent the equinoctial contribution to the semiannual variation in *Kp*.

Other periods: 1942–44, 1944–49.—While we feel that the results for 1950–53 are quite convincing, a word of caution is in order at this point. It should not be forgotten that, in any analysis which covers only four years, the possibility of coincidences between two series of phenomena, each with a 27-day recurrence period, can not be altogether ruled out. However, geomagnetic quiet following CMP of bright corona has now been found by a number of investigators covering the period 1942–46 and 1950–53. An apparent association of M-storms with coronal minima has also been

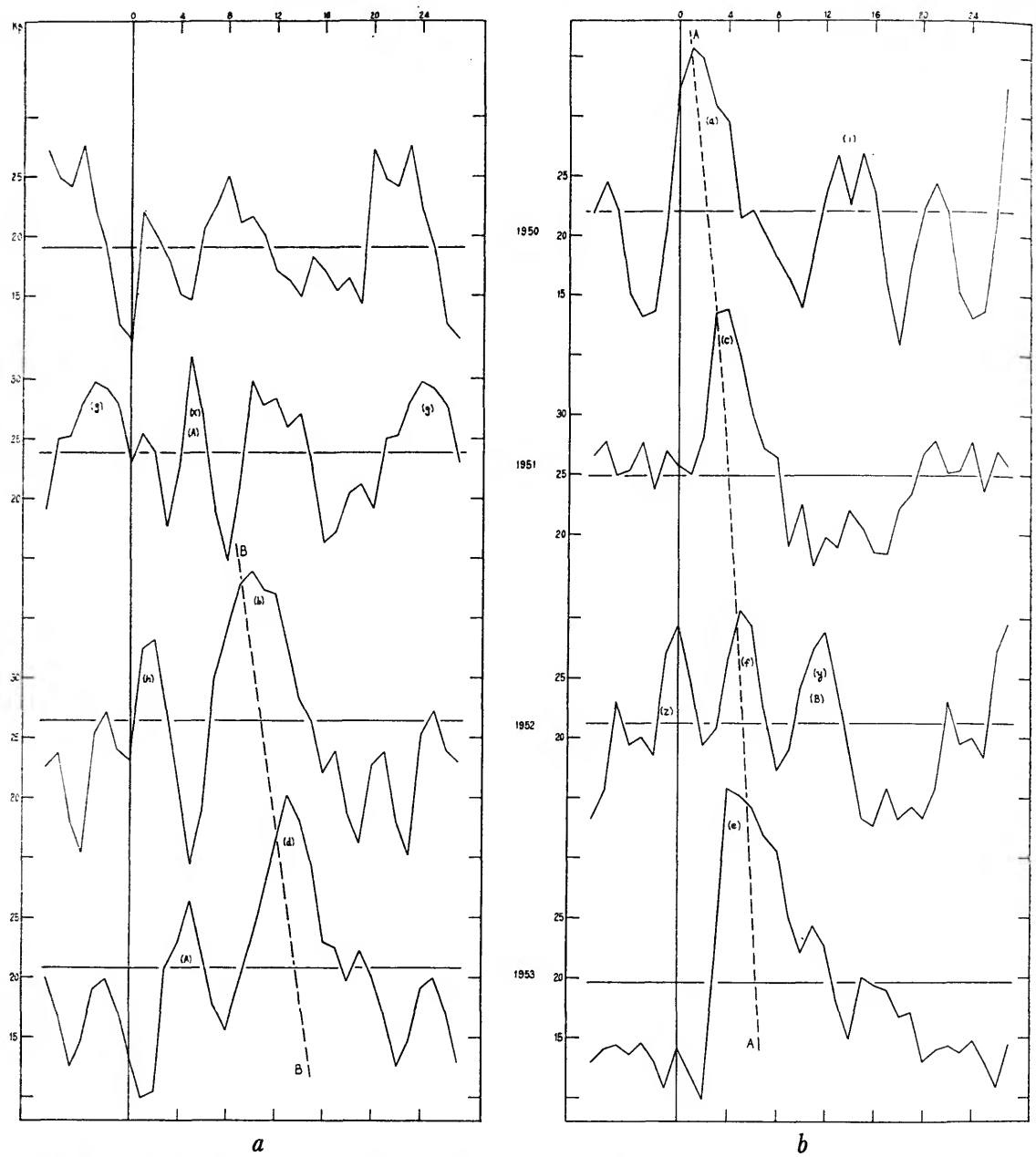

FIGURE 31.—Half-year averages of Kp over 27-day periods, showing major long-lived recurrence sequences, (A) and (B), with annual periods of intensity variation; small letters identify individual half-year sequences with those in figures 30*a–d* and 32*a*, *b*. *a*, Spring half-years; *b*, autumn half-years.

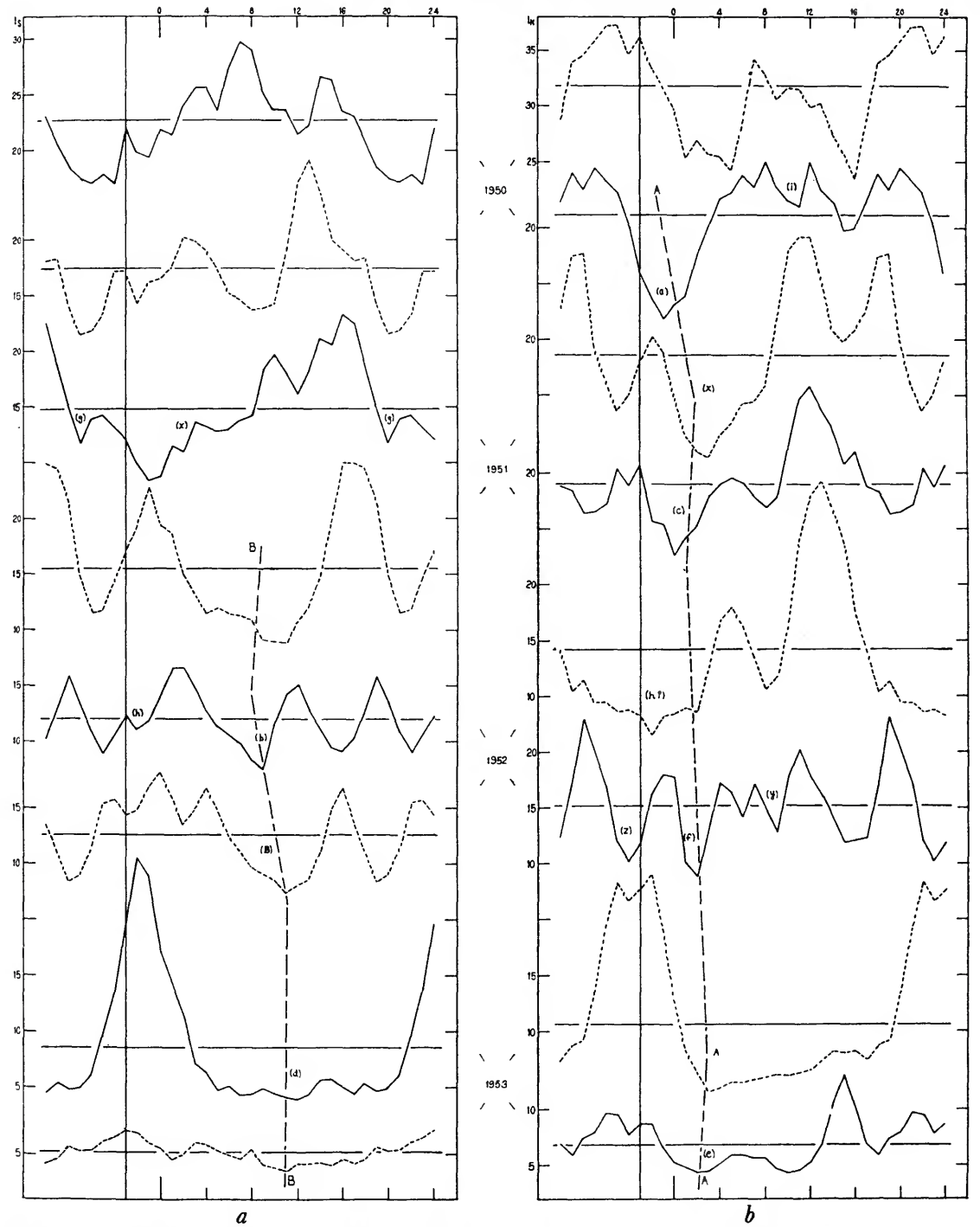

FIGURE 32.—Half-year averages of 5303 intensity over 27-day periods, showing long-lived regions of weak corona, (A) and (B), which correspond to storm sequences (A) and (B) in figure 31. The coronal curves are represented by a solid line when in the favorable, and by a broken line when in the unfavorable solar hemisphere. Small letters identify half-year coronal features associated with the K_P recurrence sequences in figure 31; the time-scale is displaced by 3 days relative to that of figure 31. *a*, Spring half-years; *b*, autumn half-years.

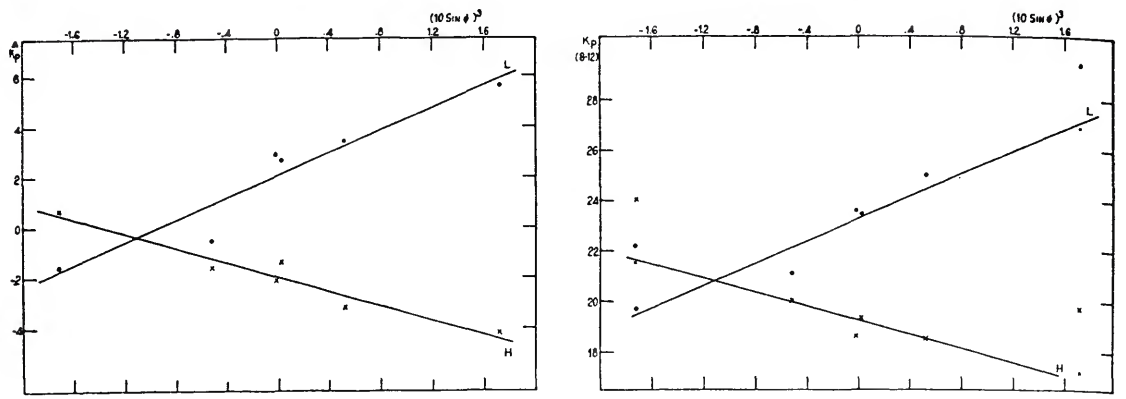

FIGURE 33.—Seasonal variations in Kp. *a*, Deviation from mean of Kp for days 8–12, after ELP of bright (x) and faint (•) 5303 corona, plotted against heliographic latitude of earth; favorable hemisphere taken positive, unfavorable taken negative. *b*, Kp for days 8–12, plotted in the same way.

found for 1943, by Bruzek (1952). On the other hand, the hemisphere effect has not been previously noted, and if we examine Bruzek's three M-regions we find that two of them (1943/b and 1950) have the coronal minimum in the favorable solar hemisphere, while for the third (1943/a) the principal part of the 5303 minimum lies in the unfavorable hemisphere but extends also about 20° into the favorable hemisphere.

To investigate this earlier period with our hemispheric index, we computed the indices for 5303 from Climax data from August 1942 (when Climax began observing) through 1949, for the northern and southern solar hemispheres separately. These indices were corrected for plate threshold. To date no interpolations have been attempted except for 1942–44. This earliest period has special interest here because of its correspondence, in phase of the solar cycle, to our 1950–53 period. For these two years, we therefore tried to fill in some of the gaps in Climax indices, at least approximately by reference to data from Arosa, Pic du Midi, and Wendelstein. Thus in the 1942–44 period the locations of the principal bright coronal regions seem reasonably well defined. The coronal minima, on the other hand, are less satisfactorily located. On a substantial number of days the 5303 corona was below the threshold of visibility at Climax, and in general, as Kiepenheuer (1947) has remarked regarding faint Wendelstein values, the weak values are more uncertain because of scattered light.

We divided the coronal data into three periods according to phase of the solar cycle—Aug. 1942–6 June, 1944 (declining phase); 7 June, 1944–7 Dec., 1946 (rising phase); 8 Dec., 1946–8 Dec., 1949 (maximum phase)—and performed the ordinary superposed epoch analyses, based on relative intensities within each half year. The results for the period from mid-1942 to mid-1944 are shown in figure 34*a–f*.

In figures 34*a–c* the "eastern hemisphere effect" found by Shapley and Roberts for this period appears conspicuously in each of the curves, favorable and unfavorable, which are remarkably parallel. The expected Kp minima around 9–11 days after ELP also appear, with no significant difference between favorable and unfavorable bright corona.

In figures 34*d–f*, CMP of faint corona is followed by above-average values of Kp, again without significant difference between favorable and unfavorable weak corona. In the autumn curves the unfavorable weak corona actually appears to give the better results. The curves of figure 34*f* are determined more by the autumn of 1943 than of 1942, and appear to be in accord with the results of Bruzek. The sequence he calls 1943/b appears as the small rise after CMP in

the favorable curve; while his sequence 1943/a, the principal sequence of the two years, appears as the rise in the favorable curve with its peak on day −2 and in the unfavorable curve with a peak on day 11. Bruzek found his sequence 1943/b associated with a weak coronal area which appears to lie primarily in the northern solar hemisphere; while the storms of his 1943/a sequence appeared to be associated with a southern weak region which, however, extended about 20° into the northern solar hemisphere.

Thus, while the results from the period 1942–44 are not clearly incompatible with a hemisphere effect, they provide no evidence in favor of such an effect. The final answer to this question must therefore wait, probably until the decline of the next solar cycle and the appearance of a new series of M-regions. For the present, the best evidence in support of a hemisphere effect is, we suggest, the waxing and waning with annual periods of the two long-lived M-sequences, A and B (figures 25, 31 and 32), while their respective coronal minima remain more or less constantly present throughout both favorable and unfavorable periods. It may be worth noting that 1950–53 was a period of more numerous M-sequences and higher average *Kp* than the corresponding phase of the previous cycle.

Our study of the rising and maximal phases of the past solar cycle, 1944–49, is only preliminary and we shall defer any detailed discussion. It seems fairly clear however, that the association between regions of weak corona and high *Kp* does not appear in any sytematic and convincing way in years of high solar activity. In these years even the "weak" corona is rather bright. Perhaps this relation appears only when the intensity of the "weak" corona falls below some particular level on an absolute scale.

The tendency to a *Kp* minimum following CMP of bright corona continues to appear in the 1944–46 period. In the maximum period we find a tendency, in the favorable curves at least, for the CMP of the

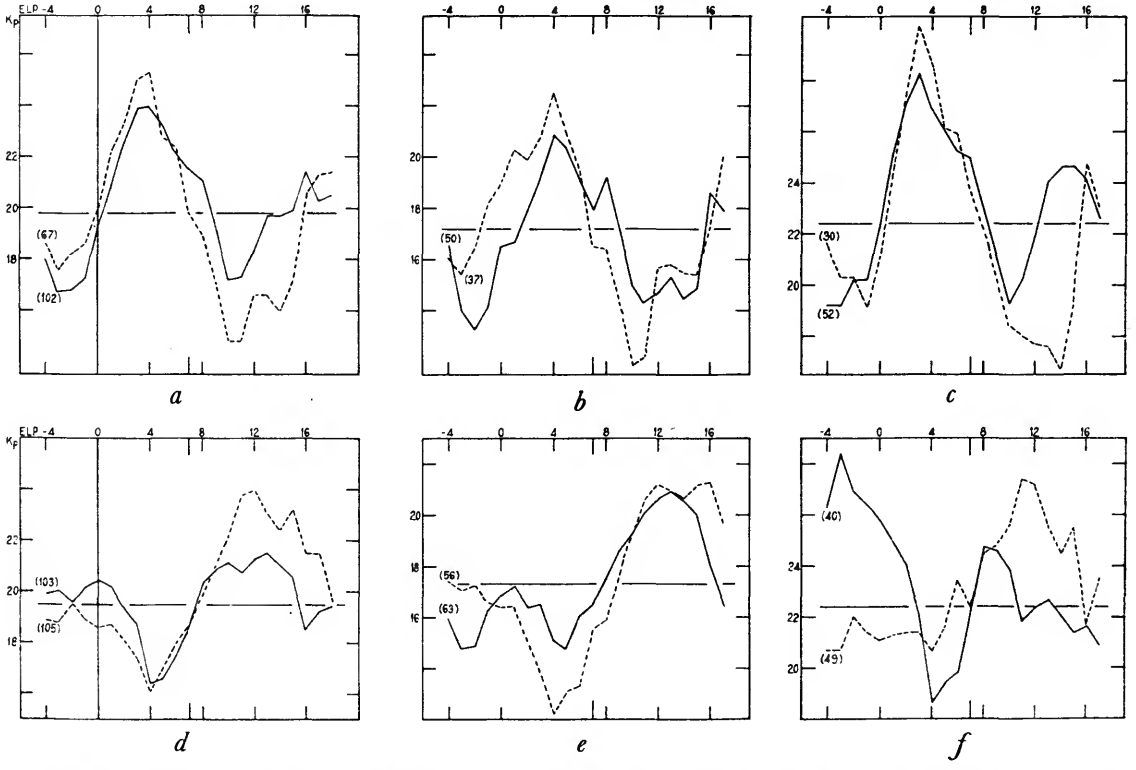

FIGURE 34.—Mean *Kp* following ELP of selected coronal intensities in favorable (solid line) and unfavorable (broken line) hemispheres for the period 1942–44. *a–c:* For bright 5303 corona: *a*, mean for 2-year period; *b*, spring half-years; *c*, autumn half-years. *d–f:* For faint 5303 corona: *d*, mean for 2-year period; *e*, spring half-years; *f*, autumn half-years.

top 10 percent of 5303 to be followed by enhanced Kp, while the 20-10H group shows a decrease in Kp. The tendency, which is merely suggestive and not present in every half-year period, should not, however, be surprising. Waldmeier (1939, 1942) found an association between bright 5303 corona and geomagnetic storms in 1939, nearer to sunspot maximum than most investigators have worked. Kiepenheuer (1947) found that CMP of "very strong" corona tended to be followed by high Kp, whereas moderately strong corona was followed by diminished Kp. Also the work of Denisse (1952, 1953) has made it clear that active centers can act on geomagnetism in two ways: some centers appear to inhibit geomagnetic activity while others appear to produce storms. It seems probable that in years of high solar activity we cannot hope to attain particularly reliable results from a simple 5303 coronal index, and that radio noise data and yellow-line observations will be important in separating the two types of coronal centers.

The yellow line.—Our previous results (Bell and Glazer, 1954a, and Part I of this paper) and those of Denisse and Simon (1954) have indicated that CMP of regions of yellow line emission tends to be followed by enhanced geomagnetic activity. To investigate further the possibility of a hemisphere effect in active-center corpuscles, we used the appearances of the yellow line, observed at Climax and Sac Peak, 1946–51, and listed by Dolder, Roberts, and Billings (1954). Figure 35*a–c* shows the average Kp's associated with CMP of these yellow line regions. The tendency for above-average Kp following CMP of yellow line regions appears to be about the same whether the region lies in the favorable or the unfavorable solar hemisphere. The peaks in the favorable curves occur at CMP+2, while those in the unfavorable curves appear at CMP +4, a difference in time lag which may have some significance since it appears in both spring and fall samples independently. Since the samples are small, however, any conclusions should be regarded as tentative.

In table 3 are given the percents of $Kp \geq 30$ and the percents of $Kp \geq 40$ associated with the favorable and with the unfavorable appearances of the yellow line.

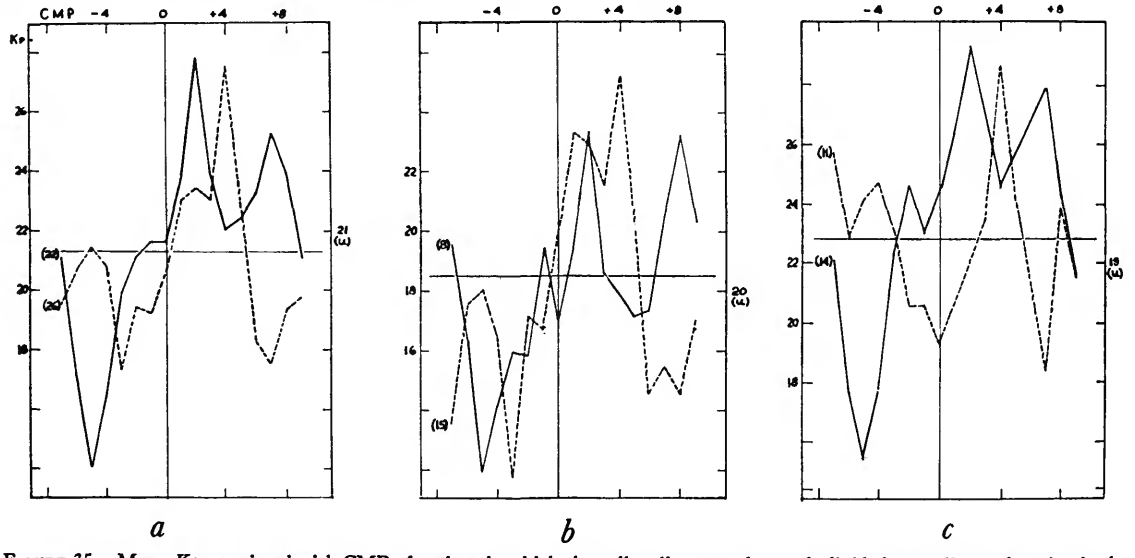

FIGURE 35.—Mean Kp associated with CMP of regions in which the yellow line was observed, divided according to location in the favorable (solid line) and unfavorable (broken line) hemisphere. *a*, For the period 1946–51; *b*, spring half-years; *c*, autumn half-years.

TABLE 3.—*Percents of high* Kp *associated with f and u yellow line.*

	Day	−6	−5	−4	−3	−2	−1	0	+1	+2	+3	+4	+5	+6	+7	+8
$\%Kp \geq 30$	f	9	5	5	23	23	14	18	32	50	27	27	27	36	41	23
	u	15	8	12	8	12	8	12	31	19	31	31	19	12	4	8
$\%Kp \geq 40$	f	4	0	0	4	9	0	9	4	9	14	18	9	9	4	9
	u	4	4	0	4	0	0	0	4	8	4	12	4	0	0	0

For the entire period, 18 percent of $Kp \geq 30$, and 4.7 percent of $Kp \geq 40$. For CMP (-5 through -1) the average percents of $Kp \geq 30$ are 14 and 9 for (f) and for (u) respectively, while for CMP ($+1$ through $+5$) we find 33 and 26 percent. The contrast between pre- and post-CMP days is nearly the same for each hemisphere. The difference between favorable and unfavorable results is not statistically significant and is actually less than similar numbers would show for the advantage of north (14, 37 percent) over south (8, 17 percent). See also figures 35*b* and 35*c*.

These yellow line results support a tentative conclusion that active-center corpuscles show no significant hemisphere effect.

Summary and interpretation

Since the present investigation, like others in this field, is statistical in nature, we emphasize that no physical connection between any solar and geomagnetic phenomena has been demonstrated. We have examined the relation between two sets of phenomena, each of which shows a recurrence period of 27 days. Therefore, whether or not any causal connection actually exists, an apparent relation might be found, particularly for any short time interval in which C-regions and M-regions are about equal in number.

While no physical connections have been or can be demonstrated by statistical procedures alone, the available evidence does suggest certain connections. The principal effects occur at a reasonable time lag after CMP of regions of bright and faint coronal intensities. The apparent *Kp* effects are greatest for the extreme (10H, 10L) deciles of green line intensity; they are enhanced when the coronal regions, bright or weak, are located with the greatest certainty by using east-limb and west-limb indices simultaneously. The homogeneity of the curves for the various samples is an important indicator of the likelihood that the relationship between coronal and geomagnetic conditions is real. Agreement of our results with those from other solar cycles should also be considered. Our principal conclusions, based primarily on study of the 1950–53 period, are summarized below.

Solar M-regions appear to be distinguished by unusual weakness of the green coronal-line emission. In contrast to the previously noted (Allen, 1944) characteristic absence of sunspots, this weakness in the coronal line often permits a fairly definite localization of the M-region in solar longitude. Because of the high correlation between green line and white light coronal intensities in spot-zone latitudes (Athay and Roberts, 1955), we infer that M-regions may be characterized by a relatively low coronal density. This inference receives direct support in the one instance where a test is available. We believe that M-regions should not be identified with white light coronal streamers. They may possess weak unipolar magnetic fields (Babcock and Babcock, 1955). We suggest that an M-region permits more or less continuous escape of general solar corpuscular radiation along its meridian of longitude as long as its green coronal emission remains weak.

The efficacy of an M-region in producing geomagnetic storms is greater, however, when the earth is on the same (favorable) side of the solar equator as the M-region. Other things being equal, the efficacy of an M-region appears greatest when the earth is around its maximum favorable heliographic latitude, and least when the earth is near its maximum unfavorable heliographic latitude.

When the earth is within about 3° of the solar equator, favorable and unfavorable M-regions seem to be about equally efficient, while beyond this distance the storm-producing power of an unfavorable region falls off markedly. This hemispheric tendency would appear sufficient to account for most of the semi-annual variation in *Kp* and in aurorae; however, the possibility of some additional contribution from equinoctial conditions in the earth's atmosphere should not be excluded.

While unusual weakness in the green coronal line indicates a condition peculiarly favorable for the escape of general solar corpuscles, the bright green line conversely appears to distinguish regions that inhibit the escape of general corpuscles. The inhibiting power of a bright C-region acts primarily on the corpuscles of its own solar hemisphere but shows no discernible relation to the heliographic latitude of maximal intensity or to the angular distance between earth and C-region. Relative to the mean level of activity, the inhibiting power

appears to vary systematically with the angular distance of the earth from the solar equator, being greatest when the earth is at maximum favorable and least at the most unfavorable heliographic latitude. This systematic variation arises as much from change in the general level of geomagnetic activity as from apparent variation in actual inhibiting power. Near the equator favorable and unfavorable C-regions inhibit about equally, while the inhibiting power of an unfavorable C-region tends to disappear as the earth moves more than about 5° beyond the solar equator.

We suggest that every bright coronal center tends to inhibit the escape of the general solar corpuscles arising along its meridian of longitude and on its side of the solar equator. However, CMP of some C-regions appears to be associated with nonrecurrent geomagnetic storms. These centers, by virtue of their more violent activity, appear able to eject streams of what we have called active-center corpuscles. These centers tend to be distinguished by yellow lin emission, large and/or frequent flares, and enhanced radio noise, and to be most important in years of high sunspot activity. We find no evidence for a hemisphere effect in this type of storm, although because of the small sample sizes this conclusion must be more tentative than some of the others.

It seems clear that geomagnetic storms may properly be divided into two categories, according to their origin from (1) the general solar corpuscles from M-regions, or (2) the active-center corpuscles from C-regions. This dichotomy based on source of corpuscles corresponds at least roughly to previous dichotomies based on the tendency to recurrence, sudden commencement, etc. However, we should be inclined to put into the "general corpuscle" category most, if not all, storms that cannot reasonably be associated with some solar feature or event, regardless of recurrence or "sc" properties.

It is generally agreed that *Kp* is a measure of the solar corpuscular radiation and that large *Kp* indicates a relatively high density of solar corpuscles in the vicinity of the earth. The evidence presented in this paper suggests that extremes of high or low coronal density tend to be inversely associated with the density of general solar corpuscles in the vicinity of the earth. CMP of a solar region of relatively high coronal density tends to be associated with a relatively low corpuscular density in the vicinity of earth; and, conversely, CMP of a solar region of unusually low coronal density tends to be associated with a relatively high corpuscle density around the earth.

These conditions may be most obviously interpreted by assuming that corpuscles arise—perhaps from solar spicules—more or less uniformly and constantly over the entire solar surface. M-regions occur, when the local force fields are favorable for the acceleration and escape of the corpuscles, as electrically neutral streams of ions and electrons. When the local force fields are not favorable, the corpuscles are trapped and C-regions of increased density are built up. The Babcocks (1955) have suggested that these two types of local force fields may be identified respectively with the weak unipolar and the bipolar magnetic regions they have observed on the solar surface.

The Babcocks have also pointed out that if unipolar regions in low latitudes are conducive to the escape of corpuscular streams, then the sun's polar regions, with their weak general fields, may be even more copious sources. They note that the lines of force of the general solar magnetic field, although distorted by the moving ionized clouds, should tend "to guide diffuse corpuscular streams ejected from the polar regions to the general vicinity of the equatorial plane."

Following this line of thought, we should like to suggest further that these high latitude regions may be the major source of general solar corpuscles that reach the vicinity of the earth. We would postulate that corpuscles, as electrically neutral streams of ionized gases, are regularly ejected from the high latitude regions of the sun. The paths taken in space by these polar corpuscles are determined primarily by the general and local magnetic fields of the sun. If unperturbed by local solar fields, the general field tends to direct the corpuscular streams into, or near to, the plane of the equator where they often are able to strike the earth. Local magnetic fields, in the spot zones, influence the paths of corpuscles along and near their meridian of longitude.

These magnetic centers tend to deflect the corpuscles from their normal paths, perhaps guiding a substantial portion into their own vicinity where these corpuscles add to the coronal density and become visible as enhanced brightness of the 5303 line and as Hα-filaments. For the most part, active centers guide into their own neighborhood corpuscles ejected from the high latitudes of their own hemisphere, although very large and powerful centers conceivably may influence the paths of corpuscles from the other pole. The density and energy of the ejected high-latitude corpuscles, as well as the pattern of the controlling magnetic field, probably varies during the 11-year cycle of solar activity.

This theory is strictly phenomenological, developed to explain our observational results. It does not specify any particular mechanism for ejecting the particles or accelerating them to the required velocities of 500–5000 km/sec. However, let us now consider more specifically how this "polar source" idea might apply to the various observational results.

M-storms, we postulate, occur when the polar corpuscles are deflected only by the general magnetic field of the sun. The center of the corpuscle stream from a given pole is not deflected as far as the equator. The earth therefore intercepts a greater density of corpuscles when it is near its maximal heliographic latitude and intercepts fewer corpuscles when it is near the plane of the solar equator. The 27-day recurrence in geomagnetic activity results simply from the recurrence in the spot zone of undisturbed regions, which are necessary to permit the corpuscle streams to escape to the vicinity of the earth. These undisturbed regions are thus characterized by weak 5303 emission precisely because they are unable to trap any high-latitude corpuscles with which to increase their density above that provided by their underlying surface.

A C-region, on the other hand, exists largely because its magnetic field has concentrated the corpuscles ejected on and near its meridian of longitude. The corpuscles, thus concentrated, appear as regions of higher density; they cannot escape and intercept the earth and *Kp* is diminished. The "polar source" theory seems to us to explain—more easily than a direct spot-zone theory—the apparent independence of inhibiting power and angular distance between earth and bright center. We further suggest that this picture of C-regions is compatible with photographs by Lyot of the edge of the sun in the light of 5303 and 6374 (see Kiepenheuer, 1953, p. 426). These photographs show that the emission-line corona possesses a marked filamentary structure, not radically different perhaps from that of the Hα prominences. General corpuscles from the unfavorable hemisphere do not normally cross the solar equator more than about 3–5° and are thus less significantly related to geomagnetic conditions.

Statistical procedures alone, of course, can merely suggest relationships between *Kp* and solar phenomena. The most accurate predictions of geomagnetic conditions cannot be obtained without theoretical understanding of the causal physical connection between solar and geomagnetic phenomena. At present, since no adequate theory exists to describe the dynamical behavior of an ionized gas stream in a magnetic field, we cannot definitely accept or reject either of the two possibilities discussed in this paper.

Acknowledgments

The work reported herein has been accomplished in part under the sponsorship of the Air Force Cambridge Research Center, Geophysics Research Directorate, through Contract AF19(604)–146 with Harvard University, and in part with the support of the Central Radio Propagation Laboratory (CRPL) of the National Bureau of Standards during a 3-month visit as a consultant by one of the authors (Bell).

A detailed account of the results of Part I previously appeared in Harvard Scientific Report No. 17 (Bell and Glazer, 1954a) and in brief summary elsewhere (1954b). For a summary of Parts II and III see Bell and Glazer (1956).

We wish to thank Hope I. Leighton, Rhoda McDuffie, Marion B. Wood, and William L. Taylor of CRPL for assistance in various phases of the numerical calculations. We are indebted to Dr. Walter O. Roberts, Director of the High Altitude Observatory of the University

of Colorado, for a number of stimulating and helpful discussions of solar-geomagnetic problems during our stay with CRPL.

Also, special thanks go to John E. Alman, Director, and Lloyd C. Peterson, Assistant Director, of the Office of Statistical and Research Services of Boston University, and to James E. Starkey, Director, and James C. Byrum, Assistant Director, of the IBM Service Department of the University of Colorado, for their generous cooperation and assistance in permitting the use of their IBM computing equipment.

Dana Wickware assisted in preparing the figures for publication.

References

ALLEN, C. W.
1944. Monthly Notices Roy. Astron. Soc., vol. 104, p. 13.

ATHAY, R. G. AND ROBERTS, W. O.
1955. Astrophys. Journ., vol. 121, p. 231.

BABCOCK, H. W., AND BABCOCK, H. D.
1955. Astrophys. Journ., vol. 121, p. 349.

BARTELS, J.
1932. Journ. Terr. Magn., vol. 37, p. 1.

BECKER, U.
1953. Zeitschr. Astrophys., vol. 32, p. 195.

BECKER, U., AND DENISSE, J. F.
1954. Journ. Atm. Terr. Phys., vol. 5, p. 70.

BELL, B., AND GLAZER, H.
1954a. Harvard Sci. Rep., No. 17.
1954b. Journ. Geophys. Res., vol. 59, p. 551.
1956. Journ. Geophys. Res., vol. 61, p. 179.

BENKOVA, N. P.
1942. Journ. Terr. Magn., vol. 47, p. 147.

BHARGAVA, B. N., AND NAQVI, A.
1954. Nature, vol. 173, p. 498.

BIESBROECK, G. VAN
1953. *In* Kuiper, ed., The sun, p. 601. University of Chicago Press.

BRUZEK, A.
1952. Zeitschr. Naturforsch., vol. 7a, p. 708.

CHERNOSKY, E. J.
1951. Trans. Amer. Geophys. Union, vol. 32, p. 861.

CHREE, C., AND STAGG, J. M.
1927. Philos. Trans. Roy. Soc. London, ser. A, vol. 227, p. 21.

DENISSE, J. F.
1952. Ann. Geophys., vol. 8, p. 155.
1953. Comptes Rendus Acad. Sci., Paris, vol. 236, p. 1856.

DENISSE, J. F., AND SIMON, P.
1954. Comptes Rendus Acad. Sci., Paris, vol. 238, p. 1775.

DENISSE, J. F., STEINBERG, J. L., AND ZISLER, S.
1951. Comptes Rendus Acad. Sci., Paris, vol. 232, p. 2290.

DOLDER, F. P.
1952. Technical Report, Office Naval Res.-High Altitude Obs.

DOLDER, F. P., ROBERTS, W. O., AND BILLINGS, D. E.
1954. Astrophys. Journ., vol. 119, p. 120.

GARTLEIN, C. W.
1950. Trans. Amer. Geophys. Union, vol. 31, p. 18.
1951. Nature, vol. 167, p. 277.

GLAZER, H., AND BELL, B.
1954. Harvard Sci. Rep., No. 18.

GRAVES, W. M. H., AND NEWTON, H. W.
1929. Monthly Notices Roy. Astron. Soc., vol. 89, p. 641.

HEPBURN, N.
1955. Astrophys. Journ., vol. 122, p. 445.

KIEPENHEUER, K. O.
1947. Astrophys. Journ., vol. 105, p. 408.
1953. *In* Kuiper, ed., The sun, p. 322. University of Chicago Press.

KLÜBER, H. VON
1952. Observatory, vol. 72, p. 207.

LINCOLN, J. V., AND SHAPLEY, A. H.
1948. Trans. Amer. Geophys. Union, vol. 29, p. 849.

MAUNDER, E. W.
1904. Monthly Notices Roy. Astron. Soc., vol. 65, p. 2.

MAXWELL, A.
1952. Observatory, vol. 72, p. 22.

MEINEL, A. B.
1951. Astrophys. Journ., vol. 113, p. 50.

MÜLLER, R.
1953. Observatory, vol. 73, p. 75.

NAQVI, A. M., AND BHARGAVA, B. N.
1954. Indian Journ. Meteorol. Geophys., Special No., vol. 5, p. 195.

NEWTON, H. W.
1943. Monthly Notices Roy. Astron. Soc., vol. 103, p. 244.
1944. Monthly Notices Roy. Astron. Soc., vol. 104, p. 4.
1949. Monthly Notices Roy. Astron. Soc., Geophys. Suppl., vol. 5, p. 321.

NEWTON, H. W., AND MILSOM. A. S.
1954. Journ. Geophys. Res., vol. 59, p. 203.

ROBERTS, W. O.
1952. Astrophys. Journ., vol. 115, p. 488.

ROBERTS, W. O., AND TROTTER, D. E.
1955. Journ. Atm. Terr. Phys., vol. 6, p. 282.

SHAPLEY, A. H.
1946. Journ. Terr. Magn., vol. 51, p. 247.
1947. Trans. Amer. Geophys. Union, vol. 28, p. 715.

SHAPLEY, A. H., AND ROBERTS, W. O.
1946. Astrophys. Journ., vol. 103, p. 257.
SMYTH, M. J.
1952. Observatory, vol. 72, p. 236.
THELLIER, E., AND THELLIER, O.
1948. Comptes Rendus Acad. Sci., Paris, vol. 227, p. 1044.
TROTTER, D. E., AND ROBERTS, W. O.
1952. High Altitude Obs.-Nat. Bur. Standards Report, No. 10.
WALDMEIER, M.
1939. Zeitschr. Astrophys., vol. 18, p. 241.
1942. Zeitschr. Astrophys., vol. 21, p. 275.
1945. Astron. Mitteil. Zürich, No. 146.
1946. Journ. Terr. Magn., vol. 51, p. 537.
1950. Zeitschr. Astrophys., vol. 27, p. 42.
WULF, O. R., AND NICHOLSON, S. B.
1948. Publ. Astron. Soc. Pacific, vol. 60, p. 37.
1950. Publ. Astron. Soc. Pacific, vol. 62, p. 202.

Abstract

This paper analyzes the relations between the intensity of the coronal emission lines and the geomagnetic activity index, *Kp*. The study emphasizes the years 1950–53, with brief reference to 1942–49, and begins with a general discussion of the problems of solar-geomagnetic relationships.

In Part I, the analyses employ a single daily index of intensity for each coronal line (λ5303 and λ6374). Solutions are carried out by the superposed epoch method for the average *Kp* around zero-days defined by east limb passage (ELP) of regions of strong and of weak coronal emission. Inverse solutions are made for the average 5303 intensity around zero-days defined by specified geomagnetic conditions. It is found important to distinguish between sporadic sc-type geomagnetic storms and recurrent storms, which appear to be associated with different types of 5303 intensity distribution. The concluding sections explore the possible influence of the heliographic latitude of the earth on the March and September maxima in geomagnetic activity. The concept of favorable and unfavorable solar hemispheres is introduced, and possible hemisphere effects for active centers and for M-regions are considered.

In Part II, the analyses employ, for each coronal line, separate intensity indices for the northern and for the southern solar hemispheres, and the hemisphere effects for the years 1950–53 are explored more fully. In solutions for *Kp* from specified coronal conditions, the effect of angular distance of the bright coronal region from the sun's equator and of the heliographic latitude of the earth on geomagnetic conditions is investigated.

Part III presents inverse solutions for the patterns of coronal conditions, in the favorable and in the unfavorable solar hemispheres, which are associated with various geomagnetic conditions. The distinction between recurrent and sc-type storms with respect to coronal intensity patterns is explored further, and the distribution of 5303 intensity associated with several individual recurrence sequences is studied. Two long-lived M-regions are found, each characterized by unusual weakness in the 5303 corona in one solar hemisphere and by an annual period of waxing and waning in its geomagnetic effectiveness. The relations between coronal and geomagnetic conditions for the years 1942–44 and 1944–49 are briefly discussed.

The principal conclusions are as follows:

The green line (λ5303) shows a closer relation to geomagnetic conditions than does the red line (λ6374).

ELP of regions of bright 5303 emission tends to be followed by a decrease in geomagnetic activity, with a minimum on day +10.

ELP of regions of unusually faint 5303 emission tends to be followed by geomagnetic disturbance, of the recurrent type, with a maximum on day +9.

Both the above tendencies are enhanced markedly if only coronal intensities in the favorable solar hemisphere are considered, i. e., intensities on the same side of the solar equator as the earth.

Bartels' M-regions are identified with areas of unusually weak emission in the 5303 corona in the favorable solar hemisphere.

An axial explanation is indicated for the major part of the March and September maxima in geomagnetic activity in years dominated by recurrent storms.

The relative location of the solar equator, rather than the angular distance between coronal region and earth, appears to be the major factor in the hemisphere effects on geomagnetic activity, which are negligible when the heliographic latitude of the earth is less than about 3°.

Finally, the hemisphere effect manifests itself in the recurrent or M-region storms and in the inhibiting power of C-regions but not in the sporadic sc-type of magnetic storms. The distinction between these two types of storms appears to depend on a difference in origin—the recurrent storms arising from general solar corpuscles, the sporadic from active-center corpuscles.

U. S. GOVERNMENT PRINTING OFFICE: 1957